

## NASA Technical Memorandum 104566, Vol. 23

# SeaWiFS Technical Report Series

**Stanford B. Hooker, Editor**  
*NASA Goddard Space Flight Center*  
*Greenbelt, Maryland*

**James G. Acker, Technical Editor**  
*Hughes STX*  
*Lanham, Maryland*

**Elaine R. Firestone, Technical Editor**  
*General Sciences Corporation*  
*Laurel, Maryland*

## Volume 23, SeaWiFS Prelaunch Radiometric Calibration and Spectral Characterization

**Robert A. Barnes**  
*ManTech, Inc.*  
*Wallops Island, Virginia*

**William L. Barnes**  
**Wayne E. Esaias**  
**Charles R. McClain**  
*Goddard Space Flight Center*  
*Greenbelt, Maryland*

**Alan W. Holmes**  
*Hughes Santa Barbara Research Center*  
*Santa Barbara, California*

**Tomas Svitek**  
*Orbital Sciences Corporation*  
*Dulles, Virginia*



National Aeronautics and  
Space Administration

**Goddard Space Flight Center**  
Greenbelt, Maryland 20771

This publication is available from the NASA Center for Aerospace Information,  
800 Elkridge Landing Road, Linthicum Heights, MD 21090-2934, (301) 621-0390.

## ABSTRACT

Based on the operating characteristics of the Sea-viewing Wide Field-of-view Sensor (SeaWiFS), calibration equations have been developed that allow conversion of the counts from the radiometer into Earth-exiting radiances. These radiances are the geophysical properties the instrument has been designed to measure. SeaWiFS uses bilinear gains to allow high sensitivity measurements of ocean-leaving radiances and low sensitivity measurements of radiances from clouds, which are much brighter than the ocean. The calculation of these bilinear gains is central to the calibration equations. Several other factors within these equations are also included. Among these are the spectral responses of the eight SeaWiFS bands. A band's spectral response includes the ability of the band to isolate a portion of the electromagnetic spectrum and the amount of light that lies outside of that region. The latter is termed *out-of-band response*. In the calibration procedure, some of the counts from the instrument are produced by radiance in the out-of-band region. The number of those counts for each band is a function of the spectral shape of the source. For the SeaWiFS calibration equations, the out-of-band responses are converted from those for the laboratory source into those for a source with the spectral shape of solar flux. The solar flux, unlike the laboratory calibration, approximates the spectral shape of the Earth-exiting radiance from the oceans. This conversion modifies the results from the laboratory radiometric calibration by 1–4%, depending on the band. These and other factors in the SeaWiFS calibration equations are presented here, both for users of the SeaWiFS data set and for researchers making ground-based radiance measurements in support of SeaWiFS.

---

## 1. INTRODUCTION

In addition to its role as an ocean color experiment, the Sea-viewing Wide Field-of-view Sensor (SeaWiFS) serves as a satellite procurement experiment for the National Aeronautics and Space Administration (NASA). In a standard procurement, NASA provides the instrument builder with a detailed specification for the design of the sensor. In this procedure, NASA also maintains detailed control over the construction of that instrument. The builder provides NASA with the satellite sensor on a cost-plus basis. NASA eventually obtains the specified instrument, but at a price. The price includes a substantial supervisory overhead by the agency, a substantial documentation overhead on the builder showing compliance with the detailed NASA specification, and often a substantial increase in the cost of the instrument as the specifications from NASA change during the construction of the instrument. This process is the price that must be paid for the construction of new satellite sensors which expand the definition of *state of the art*.

SeaWiFS does not break radically new ground in sensor design. The necessary improvements in the SeaWiFS measurements, over those of its predecessor—the Coastal Zone Color Scanner (CZCS)—are straightforward technically (Barnes and Holmes 1993 and Hooker et al. 1993). From NASA's point of view, SeaWiFS is considered an improved replacement instrument for its predecessor. Such an instrument does not require the financial and supervisory overheads of a standard NASA procurement. These overhead items have been replaced with a well defined and well scrubbed set of performance specifications.

For the SeaWiFS Project, NASA is procuring data, *not* a specific instrument. NASA has entered a contractual agreement with Orbital Sciences Corporation (OSC) to obtain, at a fixed price, an ocean color data set. SeaWiFS is a data buy. OSC has entered into an agreement with the Hughes/Santa Barbara Research Center (SBRC) to build, as a subcontractor, the satellite sensor required to provide this data set. In this arrangement, SBRC has the freedom to design an instrument to meet the predetermined set of performance specifications. The actual design of the instrument has been left to SBRC.

Based on SBRC's design of the SeaWiFS radiometer, it has been possible to develop a set of radiometric calibration equations for the sensor. These equations, and the philosophy behind them, are presented below. The equations are presented in a form that allow for their update as relative changes in the instrument's radiometric sensitivity are detected during on-orbit operation. In addition, the set of prelaunch radiometric calibration coefficients is presented.

This report also presents the spectral response of the eight SeaWiFS bands, using laboratory measurements from SBRC. On orbit, there is no method for determining spectral shifts in the instrument's response. The primary laboratory method of determining the spectral response of the SeaWiFS bands has been accomplished through measurements of individual parts in the instrument's optical train. In addition, system level response measurements have been made using a monochromatic light source. The system level measurements are used as a confirmation to the piece part measurements, since the system level apparatus does

not have the sensitivity to measure the out-of-band responses at wavelengths where the response is extremely small. The piece part results are presented here.

## 2. INSTRUMENT DESCRIPTION

SeaStar is being built by OSC and is currently scheduled to be placed into orbit by an OSC stretch-Pegasus booster in 1995. The SeaWiFS radiometer is shown mounted on the SeaStar satellite in Fig. 1. The instrument is located on the top spacecraft shelf between the three antennas. SeaWiFS is the only research instrument that will be carried by SeaStar. SeaWiFS consists of a scanner and an electronics module. The scanner, which contains the optics, detectors, preamplifiers, and scan mechanisms, is located on the nadir face of the instrument shelf. The electronics module, which contains signal conditioning, command and telemetry, and power supply components, is located directly opposite the scanner on the inside surface of the instrument shelf. The total weight of the instrument is about 110 pounds.

SeaWiFS is designed to measure Earth-exiting radiances. The sensor's instantaneous field-of-view (IFOV) is 1.6 by 1.6 mrad per pixel, with one scan covering  $+58.3^\circ$  about nadir. The SeaWiFS scanner can be tilted to  $+20$ ,  $0$ , or  $-20^\circ$  relative to nadir to minimize the number of glint contaminated measurements in the data set. Each pixel value is digitized to 10 bit accuracy, with a typical scene producing about 600 counts with about one count of noise.

The SeaWiFS scanner is illustrated in Fig. 2. Light first strikes the primary mirror, an off-axis parabola, and then is reflected from a second surface polarization scrambler and the half angle mirror before reaching the field stop. The half angle mirror removes the rotation of the image from the scan of the telescope. The mirror rotates at exactly half the rate of the telescope and polarization scrambler, and it uses alternating mirror sides on successive telescope scans. The field stop is actually 50% larger than the detectors, and it restricts stray light through the system. After the field stop, the light is collimated by another off-axis paraboloid and directed to the aft optics assembly. Dichroic beam splitters divert the light into four focal plane assemblies, each containing two spectral bands delineated by narrowband filters in close proximity to the detector. The optical paths in the aft optics assembly are shown in Fig. 3.

Attention in the design of SeaWiFS has been given to minimizing the sensitivity of the instrument to polarized light. This consideration is the principal reason for splitting the telescope into two sections, with each rotating at a different speed. This design minimizes the incidence angle of light on the mirrors. There are other possible instrument designs which reduce this mechanical complexity, but they require large incidence angles on one or more mirrors, producing unacceptable polarization variations, particularly in the blue. In addition, SeaWiFS uses a polarization scrambler (Fig. 2 and 3) to further reduce these

variations. The scrambler eliminates the need for individual compensators to remove residual polarization at each focal plane assembly. The scrambler consists of two optical wedges that act as a variable wave plate to convert incident polarized light into several cycles of circular, horizontal, and vertical polarized light across the instrument's aperture. The sensitivity of the output of SeaWiFS to polarized light is measured in the laboratory, using a source producing plane polarized light. The rotation of the polarized light through  $360^\circ$  produced changes of less than 0.5% in the eight SeaWiFS bands.

Two instrument bands, which have four detectors each, form a focal plane. The four detectors in each group are added using a time delay and integration (TDI) technique to improve signal-to-noise ratios (SNRs). The signal from each detector is amplified, processed through a selectable gain stage, and digitized with a 12 bit analog-to-digital converter (ADC). The four digital words from a band are then: delayed, summed to obtain the TDI advantage, truncated to 10 bits, and transmitted to the SeaStar satellite bus through the electronics module. A solar calibrator is mounted on the instrument so that, if desired, the optical system views a solar illuminated diffuser when passing over the South Pole. The entire spacecraft can be rotated to allow the instrument to view the nearly full moon, which is considered to be a stable calibration source for the purpose of monitoring the long-term repeatability of the SeaWiFS measurements (Woodward et al. 1993).

## 3. BILINEAR GAINS

Tests of the instrument at SBRC in the spring of 1993 revealed that SeaWiFS measurements would be contaminated by stray light from clouds in adjacent pixels on orbit. These tests also showed the stray light contamination to be roughly proportional to the brightness of the adjacent cloud. As part of the set of instrument improvements, SBRC has changed the sensor's electronics to allow on-orbit measurements of the radiances from clouds. These changes also maintain the sensitivity of the SeaWiFS measurements of the ocean as specified in the initial requirements for the instrument.

The new electronic configuration uses the four detector circuits in each SeaWiFS band to create bands with bi-linear gains. The response for SeaWiFS band 1,412 nm, is shown in Fig. 4. The channel has a high sensitivity, i.e., considerably less than 1 mW per count, over three-quarters of the band's dynamic range. Above this point, the channel's sensitivity is reduced, allowing the measurement of cloud radiances up to 60 mW (Fig. 4, top). For ocean measurements, the band will have the same response as before, except over a reduced number of counts (Fig. 4, bottom).

The operation of the four channels in a SeaWiFS band can be illustrated using the radiance levels for band 1. The values for this band are given in Tables 1-4. The

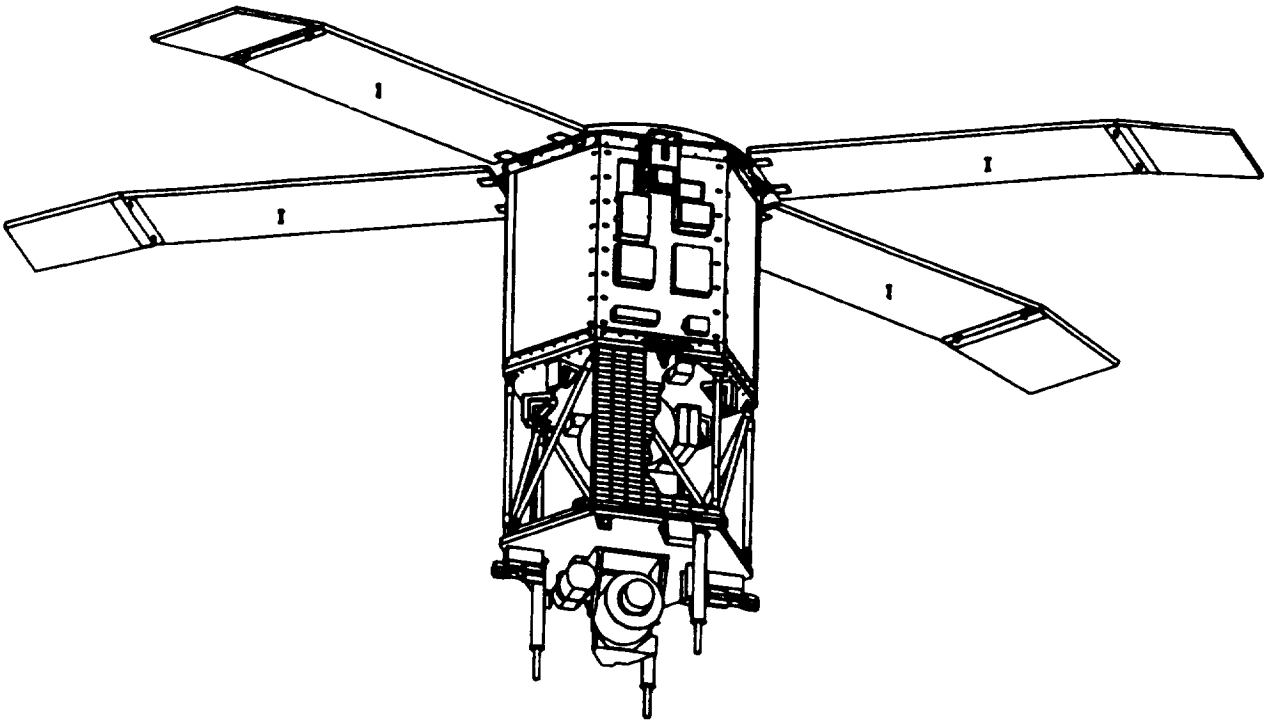


**Fig. 1.** The SeaStar spacecraft. The SeaWiFS instrument is mounted on the top payload shelf between the three antennas.

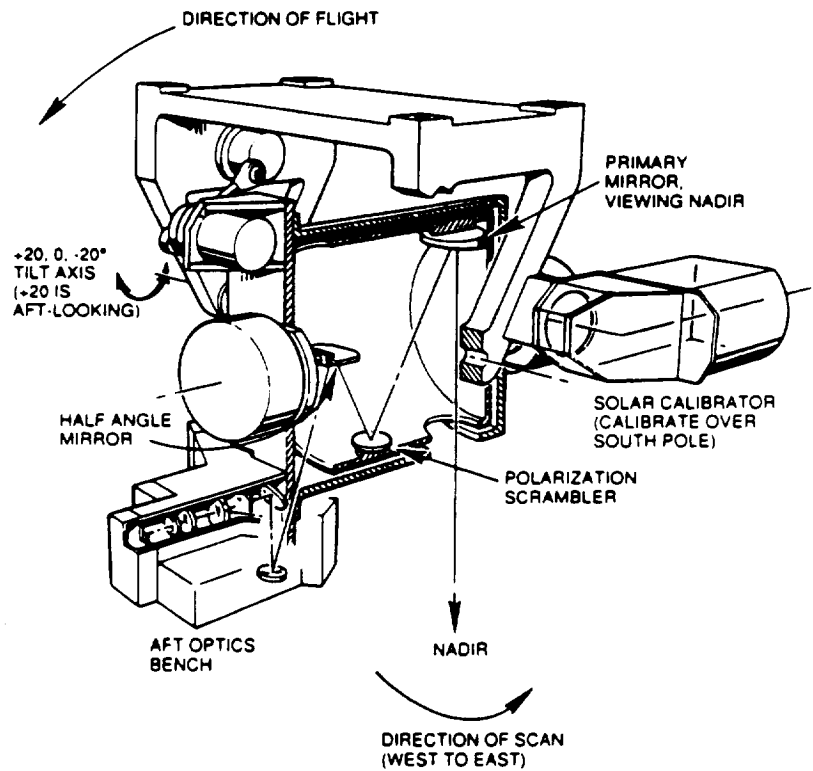


**Fig. 2.** The SeaWiFS scanner assembly. The scanner mounts to the payload shelf using the four mounting points at the top of the figure.

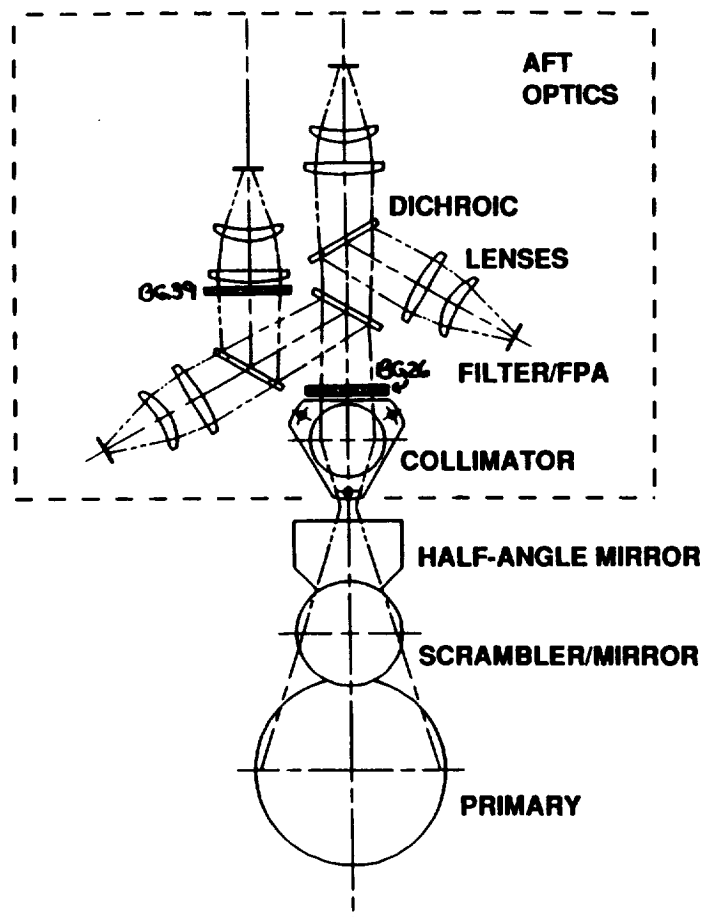


Fig. 3. The SeaWiFS aft optics assembly.

values are given for Science Gain 1, the standard gain for SeaWiFS ocean measurements. The values are given using the output from all four channels for this band. This is the standard detector configuration for the instrument. The input radiances, counts, and zero offsets (Table 1) come from measurements of the radiometric calibration of the instrument. With the zero offsets removed, the net counts, along with the sphere radiance, are used to calculate the sensitivity for each channel (Table 1). Channel 1, with low sensitivity, allows measurement of the high radiances from clouds. Channels 2, 3, and 4, with high sensitivities, allow measurements of the low radiances from oceans. These sensitivities, in mW of radiance per count, are fundamental to the calibration of SeaWiFS. They allow the conversion of the counts from the instrument into radiances at the instrument's optical input.

Tables 1-4 describe, in stepwise fashion, the determination of *knee* and *endpoint* locations for the bilinear gains

for SeaWiFS band 1. The calculations are made for Science Gain 1. Details of the stepwise calculation algorithm are given with the tables.

The SeaWiFS channels are digitized at 10 bits. The output from each channel range from 0-1,023 counts. When the zero offsets are removed, the saturation counts for the four channels in SeaWiFS band 1 range from 1,000-1,005 counts (Table 2). From these saturation counts and the sensitivities for the channels, it is possible to calculate the saturation radiances for each of the channels. These values are given in Table 2. For radiances greater than the saturation radiances, the output from the SeaWiFS channels will remain at their saturation count levels.

The saturation radiances in Table 2 give the three knee radiances and the maximum radiance for band 1 (gain 1). The minimum radiance is zero for zero counts, i.e., for zero counts after the removal of the offset. Using the saturation radiance levels and the sensitivities, it is possible to calcu-

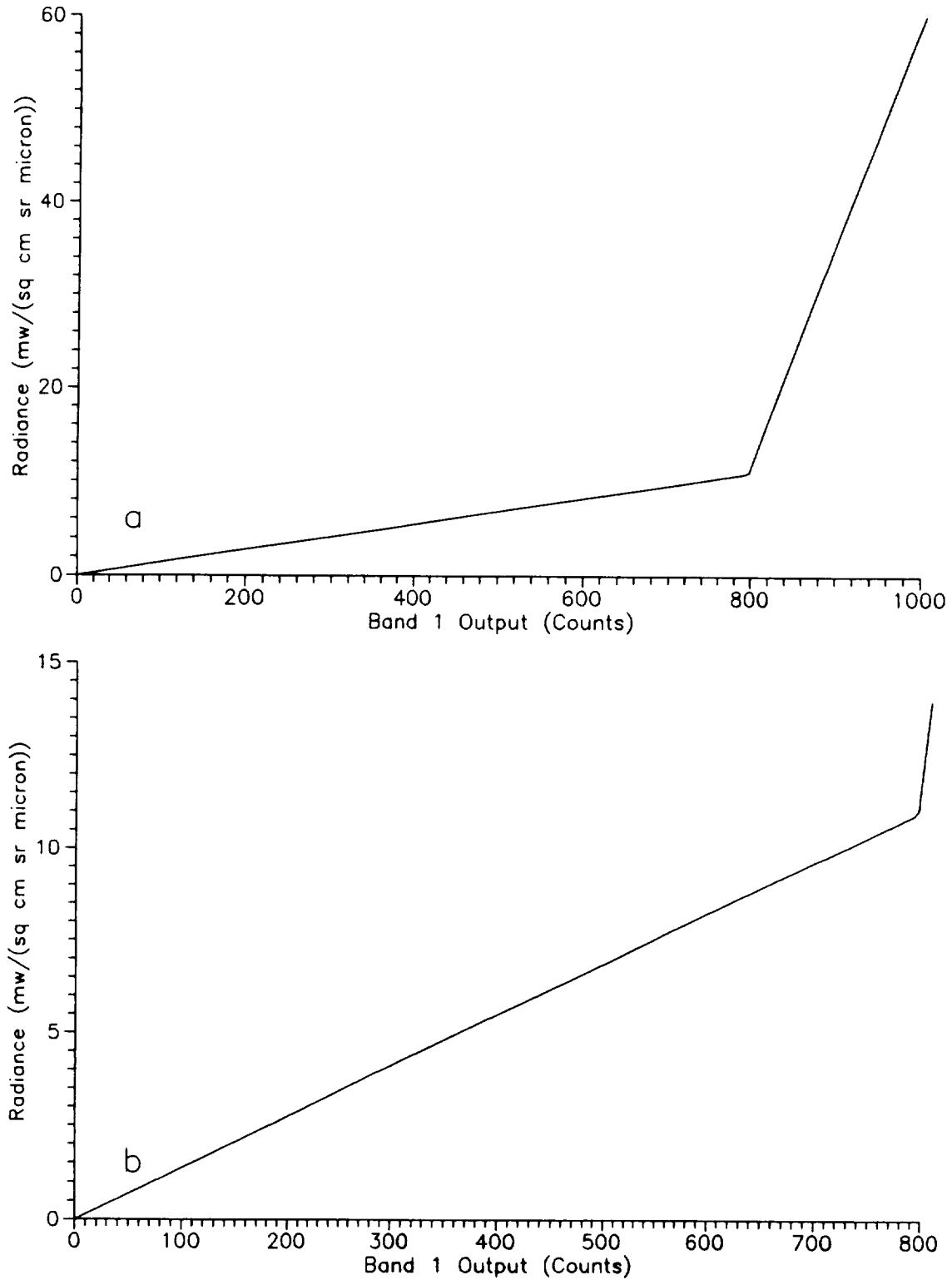


**Fig. 4.** Instrument response for SeaWiFS band 1 with a bilinear gain. The top panel shows the response from 0 to 1,000 counts. The slope from 0 to 800 counts shows greater sensitivity, i.e., fewer radiance units per count. The bottom panel shows the response from 0 to 800 counts. This is the working range for ocean measurements from band 1.

SeaWiFS Prelaunch Radiometric Calibration and Spectral Characterization

**Table 1.** In the following tables (1–4), the process of calculating the knee and endpoint locations for the bilinear gains of SeaWiFS band 1 is shown. These calculations are made for Science Gain 1. Table 1 gives the input values and calculated sensitivities for the four channels of band 1. The sensitivities are calculated from the sphere radiances and the net counts.

Channel	Radiance [mW]	Measurement [counts]	Offset [counts]	Net Counts	Sensitivity [mW/count]
1	9.246	175	21	154	0.060039
2	9.246	871	23	848	0.010903
3	9.246	859	18	841	0.010994
4	9.246	871	21	850	0.010878

**Table 2.** Saturation counts and saturation radiances for the four channels. The saturation radiances are calculated from the saturation counts and the sensitivities. The offset has been removed from both the zero and the saturation counts.

Channel	Zero	Saturation Counts	Saturation Radiance [mW]
1	0	1,002	60.159
2	0	1,000	10.903
3	0	1,005	11.049
4	0	1,002	10.899

**Table 3.** Calculated instrument output at the saturation radiances for the four channels. The counts at the knees are calculated from the knee radiances and the sensitivities. The counts for each channel cannot exceed the saturation counts.

	Zero	Knee 1	Knee 2	Knee 3	Saturation
Counts—Channel 1	0.00	181.54	181.60	184.03	1,002.00
Counts—Channel 2	0.00	999.64	1,000.00	1,000.00	1,000.00
Counts—Channel 3	0.00	991.39	991.75	1,005.00	1,005.00
Counts—Channel 4	0.00	1,002.00	1,002.00	1,002.00	1,002.00
Sum of Counts	0.00	3,174.57	3,175.35	3,191.03	4,009.00
[Sum of Counts]/4	0.00	793.64	793.84	797.76	1,002.25
Radiance	0.00	10.90	10.90	11.05	60.16

**Table 4.** Knees and endpoint locations for the bilinear gains. These are the values in the last two rows of Table 3.

Location	Radiance [mW]	Counts
Zero	0.000	0.00
Knee 1	10.899	793.64
Knee 2	10.903	793.84
Knee 3	11.049	797.76
Saturation	60.159	1,002.25

late the number of counts from each channel at the three knees and the two endpoints of the bilinear gains (Table 3).

The counts from the four channels are summed and divided by four in Table 3. This duplicates the process within SeaWiFS. On orbit, the output from the channels, as selected by the instrument's electronics based on commands from the ground, will be summed. The result will be sent from SeaWiFS to the SeaStar spacecraft. This output will be sent minus its two least significant bits, which means that the output will be sent from the instrument to the spacecraft after division by four.

The radiances and counts at the three knees and the two endpoints are given in Table 4. The counts at zero radiance are zero. For these calculations, and for on-orbit operations, the zero offsets are removed at the start of the calculations. This initial step opens up a direct relationship between counts and radiances for ocean measurements. Below the first knee in the radiance region for ocean measurements, Table 3 gives the information for the calculation of the sensitivity of band 1: (10.899/793.64), or 0.013773 mW per count. Above the third knee in the radiance region for cloud measurements, the sensitivity

is  $(60.159-11.049)/(1002.25-797.76)$ , or 0.240158 mW per count. The ocean portion of the bilinear gain is 17.5 times more sensitive than the cloud portion. This difference in sensitivities becomes greater in sequence for bands 2 through 8.

The effect of slightly different sensitivities in the three high sensitivity channels is shown in Fig. 5. In this case, the knee is not sharp, but has two internal segments, rather than just one segment in and one segment out. This increases the region of uncertainty in the transition between the ocean and cloud sensitivity regimes.

The revised electronic configuration that gives SeaWiFS the ability to detect clouds, also defines the method in which the knees for the bilinear gains are calculated (see Tables 1–4). If the detector configuration for a band is changed, then the knees for the bilinear gains must be recalculated. If the sensitivities of the high sensitivity channels for a band are changed, i.e., by changing the gain for the band, then the knees for the bilinear gains must be recalculated. However, the sensitivity of the cloud channel, in this case channel 1 of band 1, remains fixed. It does not change with gain changes in the instrument. Only the sensitivities of the three high sensitivity channels for each band can be changed. For this reason, the upper endpoint in the bilinear gains does not change when the band's gains are changed.

## 4. MIRROR SIDES

### 4.1 Scan-to-Scan Differences

For the purpose of instrument calibration, SeaWiFS is to be considered as two separate, but nearly identical instruments: mirror side 1 and mirror side 2. This separation is necessary since the two sides of the half angle mirror (Fig. 2) have slightly different reflecting properties and slightly different alignments in the sensor's optical path. Mirror side differences translate into scan to scan differences since the two mirror sides are used alternately, i.e., from scan to scan in the SeaWiFS measurements. For this report the authors have not considered the geometric scan-to-scan differences generated by the small differences in the two mirror sides. The concern here is the radiometric effects of the differences. As shown below, these differences are a few tenths of a percent.

For SeaWiFS, there will be two sets of radiometric calibrations, identical in form but with slightly different calibration coefficients. Prelaunch calibration coefficients, tailored for the two mirror sides, are provided by SBRC, the instrument's manufacturer. After launch, however, tailored information of this sort will not be available. For the most part, SeaWiFS measurements of the moon will check only the average response of the two mirror sides, since the reflectivity of the lunar surface is not constant across its face. However, with diffuser measurements, it will be possible to monitor scan-to-scan (mirror side to mirror side)

differences in the instrument's output (Section 4.2). In addition, it will be possible to check scan-to-scan differences on orbit using Earth-exiting radiances from statistically uniform bodies of water, that is, from clear water regions.

These conditions lead to the following philosophy for monitoring the long-term repeatability of the radiometric sensitivity of SeaWiFS. On-orbit and ground-based measurements will be used to monitor the change, on average, of the eight instrument bands. Thus, neither of the two mirror sides is considered as prime, and neither as secondary. Measurements of the average radiometric calibration coefficients combined with measurements of scan-to-scan differences will be used to calculate the coefficients for the two mirror sides, in a manner that the values for the mirror sides are equally distant from the average. In addition to the measurements presented, ocean measurements on orbit can be used to check the magnitude of scan line-to-scan line differences.

### 4.2 Scan-to-Scan Difference Equation

Side-to-side differences in the half-angle mirror will be characterized by the manufacturer before launch. There may be changes in the side-to-side characteristics of the half-angle mirror during the course of the mission. The average reflectance for the two mirror sides is an inherent part in the 20 scans that cover the surface of the moon in a lunar measurement and in the 480 scan lines of a diffuser measurement. However, the magnitude of the side-to-side differences in the half-angle mirror can be tracked during standard measurements of the instrument's diffuser. During each diffuser measurement, there are 240 pairs of half-angle measurements between the two mirror sides to be used to calculate the differences. These differences transform into scan line-to-scan line differences in the ocean measurements. The magnitude of the scan to scan differences will be tracked as part of the onboard calibration information from SeaWiFS and will be used in the determination of the two sets of calibration coefficients. Strictly speaking, these differences are not part of the long-term radiometric calibration for the instrument.

Mirror side differences for a given SeaWiFS band are treated independently in the following equation:

$$R_1 = (C_1 + C_1)/(C_1 + C_2), \quad (1)$$

where  $R_1$  is the radiance value measured with side 1 of the half-angle mirror, relative to the average radiance from the two sides, with a value very close to unity;  $(C_1 + C_1)/(C_1 + C_2)$  is the calculation used to obtain  $R_1$ , with a value very close to unity; and  $C_1$  and  $C_2$  are measured values of the flight diffuser for sequential scan lines, as described above, in counts.  $R_1$  and  $R_2$  (defined immediately below) are dimensionless quantities.

The value for the radiance measured with side 2 of the half-angle mirror, relative to the average radiance from the two sides, can also be calculated directly:

$$R_2 = (C_2 + C_2)/(C_1 + C_2), \quad (2)$$

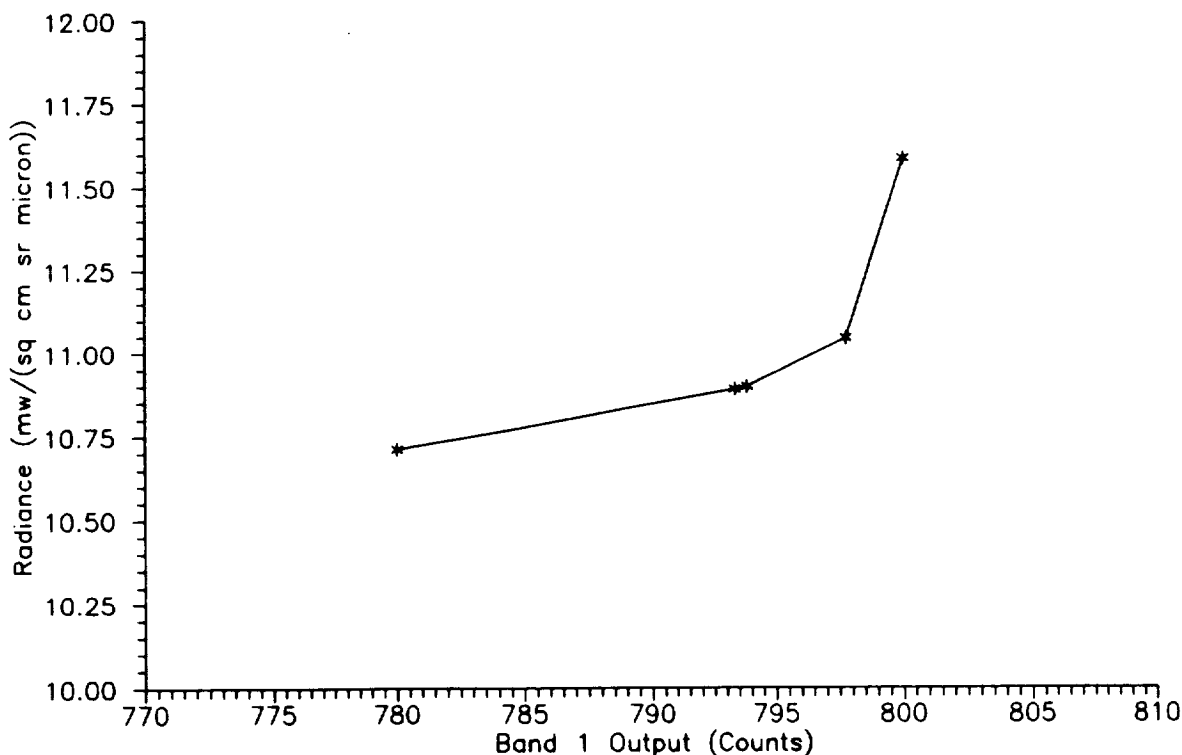


**Fig. 5.** An expanded view of the change in slope of the bilinear gain for band 1. This shows the effect of differences in the sensitivities of the three high sensitivity channels. The two segments between 793 and 798 nm are created as the two higher sensitivity channels saturate in turn. For “real world” measurements, the change in slope does not occur at one radiance level only.

where  $R_2$  is the radiance value measured with side 2 of the half-angle mirror, relative to the average radiance from the two sides, with a value very close to unity.

Both  $R_1$  and  $R_2$  are relative values, multipliers that will be applied to the calibration constants, below, to give the values for each of the mirror sides. These two constants are calculated from laboratory measurements by the manufacturer (Table 5).

## 5. CALIBRATION EQUATIONS

As with the equations for mirror side differences, the radiometric calibrations are identical in form for each of the SeaWiFS bands. Thus, the descriptions given here are representative of each band. The prelaunch radiometric calibrations for SeaWiFS are based on measurements by the manufacturer. On orbit, there will be no mechanism for monitoring changes of individual components within the radiometer. SeaWiFS carries no onboard calibrators. Among other things, there will be no means of determining spectral shifts in the instrument’s interference filters after

launch. In addition, there will be no means of isolating transmission changes from other elements in the SeaWiFS optical train. On orbit, it will be possible to monitor only relative changes in the output of the radiometer’s bands. Information on the type of internal changes within those bands will not be available. Before launch, there are absolute quantities in the prelaunch radiometric constants for the instrument that come from laboratory measurements. There is a program in progress to check the transfer of the prelaunch radiometric calibration of SeaWiFS to orbit at the start of on-orbit operations (Biggar et al. 1993). After that check is made, measurements on orbit will give only the changes in the instrument’s sensitivity relative to that at launch.

### 5.1 Calibration Equation Factors

There are several factors that must be considered in the determination of the radiometric sensitivity of the SeaWiFS radiometer. Laboratory measurements of the instrument’s sensitivity have been made with a fixed set up of the

commandable variables for the radiometer. For example, these measurements have been made at Science Gain 1, and the instrument's sensitivity at the other three gains has been determined relative to Science Gain 1. However, on orbit the long-term repeatability of the SeaWiFS measurements will be made, using scans of the moon at the lunar gain. The principal gain for monitoring instrument operation on orbit is different from the principal gain for laboratory measurements. For practical considerations, the knees and endpoints for the eight SeaWiFS bands have been calculated in terms of the radiometric sensitivity of the four channels in each band.

**Table 5.** Prelaunch mirror side factors.  $R_1$  and  $R_2$  are dimensionless quantities.

Band	Center Wavelength [nm]	$R_1$	$R_2$
1	412	1.002	0.998
2	443	1.001	0.999
3	490	1.001	0.999
4	510	1.001	0.999
5	555	1.002	0.998
6	670	1.002	0.998
7	765	1.001	0.999
8	865	1.003	0.997

The term *gain* has been present in discussions of the operation of the instrument since the inception of the Ocean Color Specifications. It is preferable to refer to the gains as sensitivity factors, with units of radiance per count. The higher the gain for a measurement, i.e., the greater the number of counts per unit radiance, the lower the saturation radiance, and the higher the sensitivity per count.

This format for the calibration equations reflects the on-orbit conditions for SeaWiFS. The SeaWiFS instrument has no onboard mechanism to monitor the absolute accuracy of the measured radiances. During the anticipated 5–10 year lifetime of the radiometer, the SeaWiFS Project will be able to detect relative changes in the sensitivity of the instrument only. After launch, lunar measurements will be used to monitor these changes as described below, and onboard measurements will be used to detect relative changes among the four electronic gains for each SeaWiFS band and among the four photodiodes for each band.

The relationships between individual gains are measured with a common electronic voltage, a calibration pulse, added to the photodiode output while the instrument views the inner surface of the back of the instrument. This process is discussed in more detail in Woodward et al. (1993). Relative changes among the individual detectors in a SeaWiFS band will be monitored by having the detectors view the instrument's diffuser sequentially several times while the diffuser is illuminated by the sun. This can be done, since each possible detector combination can be commanded from the ground. The relationship among the high

sensitivity detectors will be treated *comparatively*, i.e., examining the change with time in the output of any one of the high sensitivity detectors in comparison to the grouping comprised of the other detectors. Sufficient anomalous behavior of a single detector will cause the removal of that detector from the measurement set. Again, this process is discussed in more detail in Woodward et al. (1993).

Other factors in the radiometric calibration equations are not expected to change over time. These include the dependence of the radiometric sensitivity on the temperature of the focal planes and the dependence of the radiometric sensitivity on the scan angle of the measurement. Although there will be thermistors to measure the temperature of each focal plane during the SeaWiFS mission, there will be no on board means of measuring changes in the temperature dependence of the output from the detectors. In a like manner, no means has been found of checking, after launch, changes in the instrument's radiometric sensitivity at the edge of the SeaWiFS scan relative to the sensitivity at nadir. These factors are determined solely from prelaunch measurements by the manufacturer, as explained in a review of the CZCS calibration by Evans and Gordon (1994).

## 5.2 Long-Term Sensitivity

Long-term changes in the radiometric sensitivity of the eight SeaWiFS bands will be made using measurements of the reflected solar flux from the surface of the moon. These measurements will be complimented by vicarious, ground- and ocean-based measurements. The sun is considered as a stable, non-changing light source, and the surface of the moon is considered as unchanging over periods that are short on a geologic time scale. Variations in the solar flux incident on the lunar surface due to changes in the Earth-sun distance can be removed (Woodward et al. 1993). In a similar manner, variations in the reflectance of the moon due to small differences in the lunar phase angle and due to small changes resulting from lunar libration can also be removed. With these corrections the effective reflectance from the surface of the moon can be made essentially constant. Changes in the SeaWiFS measured values for the lunar radiance will be used directly to detect changes in the sensitivity of the instrument.

For solar measurements with the SeaWiFS diffuser, it is not possible to separate changes in the instrument sensitivity from changes in the diffuser reflectance in such a direct manner. All that can be derived from the diffuser measurements themselves is the product of the change in the instrument and of the change in the diffuser. There is an assumption, however, that will allow the diffuser and the lunar measurements to be tied together. Basically, the change in the reflectance of the diffuser is assumed to be linear over time periods of approximately one month (Cebula et al. 1988 and Herman et al. 1990). Experience with diffusers on previous satellite instruments has led to the explanation that diffuser degradation has been caused by the

coating of the diffuser with solarized organic and silicon-based materials that have outgassed from the spacecraft. The accumulation of thin layers of these materials does not lead to sharp step functions in the reflectivity of the diffuser over time.

Over longer time periods of one to several years, the change in the reflectance of the diffuser is expected to become an exponential function of time, asymptotically approaching zero change with time as the SeaWiFS mission ends. However, this 5–10 year long exponential function can be treated as a series of many linear segments that are a month in duration.

Using nearly simultaneous lunar and diffuser measurements, it is possible to separate changes in the sensitivity of the instrument, determined from lunar measurements, from changes in the reflectance of the diffuser. When the time-series of diffuser reflectances is normalized by lunar measurements, it is possible to use the assumption of a linear change in diffuser reflectivity to identify step changes in the instrument sensitivity that may occur between lunar measurements. Such changes were found in CZCS measurements (Evans and Gordon 1994).

### 5.3 Long-Term Sensitivity Equation

The long-term sensitivity equation for the radiometer contains only factors that can change during the lifetime of the SeaWiFS mission. These include two command variables that can be changed from the ground; the selection of the electronic gains, and the detector configuration. They also include time-dependent variables whose change can be monitored during the mission, the temperatures of the focal planes as measured by thermistors, and the long-term radiometric sensitivities of the instrument bands as determined through lunar and diffuser measurements.

The long-term sensitivity equation does not include the scan angle dependence of the radiometric sensitivity of the radiometer (also called scan modulation), i.e., the sensitivity of the instrument for measurements at the limb relative to those at nadir. These values are determined by the manufacturer and cannot be independently verified on orbit. The effect of scan modulation will be added to the overall radiometric sensitivity equation in the next section.

In addition, the long-term sensitivity equation does not include changes in the linearity in the detector response with input radiance. Again, these values are determined solely through measurements by the manufacturer and cannot be checked after launch. A discussion of the manufacturer's measurements is given below.

The on-orbit equation for the time dependent radiometric sensitivity of each SeaWiFS band, at nadir, has the following form:

$$L_{\text{nadir}} = K_1(t) \times K_2(gs, ds) \times (1 + K_3(T - T_{\text{ref}})) \times (C_{\text{out}} - C_{\text{dark}}). \quad (3)$$

The variables in (3) are defined as follows:

1.  $L_{\text{nadir}}$  is the measured radiance at nadir, in  $\text{mW cm}^{-2} \text{sr}^{-1} \mu\text{m}^{-1}$ .
2.  $K_1$ , which is a function of the time, is the primary instrument sensitivity factor expressed as the inverse of the number of days post-launch, and therefore equal to unity at the start of the SeaWiFS mission. This factor applies equally to each of the four gains in a SeaWiFS band.
3.  $t$  is the time, in days, after the start of on-orbit measurements by SeaWiFS.
4.  $K_2$  is the gain factor, in  $\text{mW cm}^{-2} \text{sr}^{-1} \mu\text{m}^{-1}$  per count.
5.  $gs$  is the gain selected by command from the ground and present in a datum from the spacecraft engineering telemetry that precedes each scan line.
6.  $ds$  is the detector configuration selected by command from the ground and present in a datum from the spacecraft engineering telemetry that precedes each scan line.
7.  $(1 + K_3(T - T_{\text{ref}}))$  is the focal plane temperature factor, a dimensionless value very close to unity.
8.  $K_3$  is the temperature dependence of the output from the detector, in terms of inverse degrees Celsius, with a value very close to zero, as measured by the manufacturer.
9.  $T$  is the measured temperature of the focal plane assembly, in degrees Celsius, calculated from a datum in the engineering telemetry stream associated with each scan line.
10.  $T_{\text{ref}}$  is the reference temperature for the temperature dependence,  $20^\circ \text{C}$ , set by the manufacturer.
11.  $C_{\text{out}}$  is the instrument output, in counts.
12.  $C_{\text{dark}}$  is the instrument dark restore value, in counts.

The calculation of the focal plane temperatures ( $T$ ) from the data in the spacecraft engineering telemetry requires several steps. As a result, the presentation of the temperature calculations is deferred to Section 8.0, where the eight values for  $K_3$ , one for each band, are also listed (Tables 10 and 11).

The primary instrument sensitivity for each SeaWiFS band,  $K_1(t)$ , is calculated from a combined set of lunar and diffuser measurements. There are also plans to derive this factor independently using ground based calibrations once the radiometer is collecting data on orbit. It is anticipated that the time series of  $K_1(t)$  values for periods through each lunar measurement will be updated and sent to the SeaWiFS stations approximately two weeks after that measurement. As the ensemble of lunar and diffuser measurements grows, improved time histories of the  $K_1(t)$  values will be supplied. In addition, as the rate of change of the  $K_1(t)$  values becomes understood, it will be possible to give improved, educated guesses regarding future changes in the  $K_1(t)$  values. Until reasonable time series for  $K_1(t)$

values are established, these  $K_1(t)$  values will be treated on orbit as constants during the time periods between the most recent and the next lunar measurement and then will be updated using the next lunar measurement.

Since all four gains for each SeaWiFS band—the four values of  $K_2(gs)$ —will be used frequently during the radiometer’s mission, calibration coefficients for all of the SeaWiFS bands will be contained in a periodically updated list that will be provided to each of the ground stations. These values will be given in a table of the knees and endpoints for the bilinear gains, using the form of Table 4. In addition, one word showing the command variable that determines the choice of the gain will be present in the engineering telemetry that precedes each scan line from the satellite.

The relative values for these gains will be monitored regularly during the mission (Woodward et al. 1993). The value for the lunar gain for each SeaWiFS band, i.e., the radiance per count for the lunar gain, will not change with time during the SeaWiFS mission. Since the change in the sensitivity of the instrument is determined through measurements of the moon, changes in the lunar gain will be found in  $K_1(t)$  for each band only. Changes in the values of the other gains relative to the lunar gain will be updated as determined. Changes in the gain ratios are anticipated to be small over time, if detectable at all. However, time series for the gain ratios for the eight instrument bands will be provided by the Project.

It is anticipated that the standard detector selection,  $ds$ , will not change during the SeaWiFS mission. For a given instrument band, that standard selection uses the sum of the output of the four detectors divided by four. Using the comparative method of the previous section, it is anticipated that none of the detectors will exhibit anomalous behavior and have to be removed from the measurement set. Should this occur, however, a new table of knees and endpoints for the bilinear gains will be supplied by the Project. In addition, a datum showing the command variable that determines the detector configuration will be present in the engineering telemetry that precedes each scan line from the instrument.

The focal plane temperature factor,  $1 + K_3(T - T_{\text{ref}})$ , contains two constants that are supplied from measurements by the radiometer’s manufacturer:  $K_3$  and  $T_{\text{ref}}$ . For all eight SeaWiFS bands, the constant  $T_{\text{ref}}$  is set to 20° C. The calculation of the temperature of the two detectors on each focal plane requires the conversion of engineering telemetry from the SeaStar spacecraft, in counts, into an analog signal from SeaWiFS, in volts, and then into temperature, in degrees Celsius. The conversion from volts to temperature requires a series of algebraic manipulations. These manipulations are not conceptually difficult, but they do require several steps of computation. The series of calculations required to obtain the focal plane temperatures is found in Section 8.0. This section also contains

the eight values that are required for the calculation of the temperature correction.

Thermal models of the operation of the SeaWiFS instrument indicate that the anticipated day-night temperature differences for a single orbit are on the order of 1° C. However, as the instrument’s thermal blankets age over the 5–10 year duration of the SeaWiFS mission, the average temperatures of the focal planes are anticipated to increase slowly at the rate of 1–2° Celsius per year.

## 5.4 Off-Nadir Measurement Differences

The primary laboratory measurements of the radiometric response of the SeaWiFS instrument have been made in the laboratory at nadir, i.e., pixel 643. Although not explicitly stated in the SeaWiFS performance specifications, it is important to know how the measurement at pixel 643 can be transferred to the other pixels in the scan. SBRC ran such tests during its characterization of the instrument. In the presentation of the test results, SBRC referred to the effect as *scan modulation*.

The data from these tests were taken approximately at nadir and at 100 pixel intervals above and below nadir. Data were taken for both mirror sides, and the off-nadir responses for the two mirror sides were identical at the 0.2% level, which is the resolution limit for the laboratory measurements. Overall the measurements can be summarized as follows:

1. All bands show changes in their responses with pixel number. These changes are small, ranging from 1% to 2% over the 1,285 pixels of a scan line.
2. The scan modulations for odd bands (bands 1, 3, 5, and 7) show a marked similarity with each other, as do the scan modulations for the even bands. The odd and the even bands, however, show distinctly different responses from each other.
3. The scan modulations can be fitted to quadratic equations easily. It is possible to account for the scan modulation in all eight bands with two equations, one for the even bands and one for the odd ones.
4. The measurements by SBRC show no mirror side differences in the scan modulation.

The data provided by SBRC did not include error bars for the individual radiometric measurements. From the results, however, it appears that the data have a scatter at one standard deviation of about  $\pm 0.3\%$ . This scatter falls above and below the linear results versus wavelength discussed above. The average values for the responses of the odd and even SeaWiFS bands are given in Fig. 6. The quadratic curves in Fig. 6 show the off-nadir corrections from the manufacturer for the odd and even bands.

The cause of the scan modulation has been explained as vignetting (shadowing) of the detectors during portions of the scan. The detectors can be considered as having

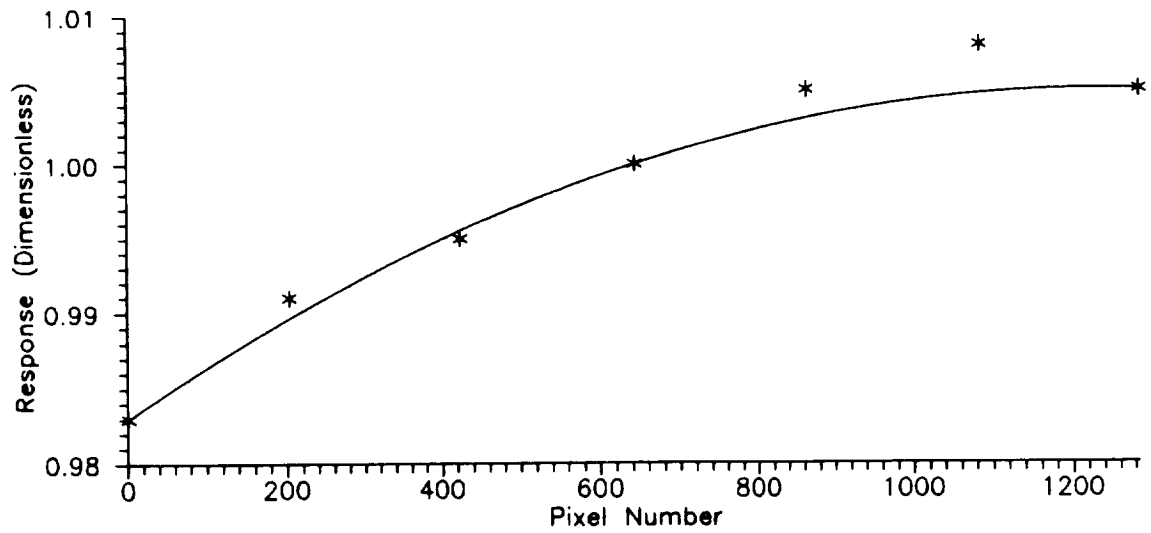
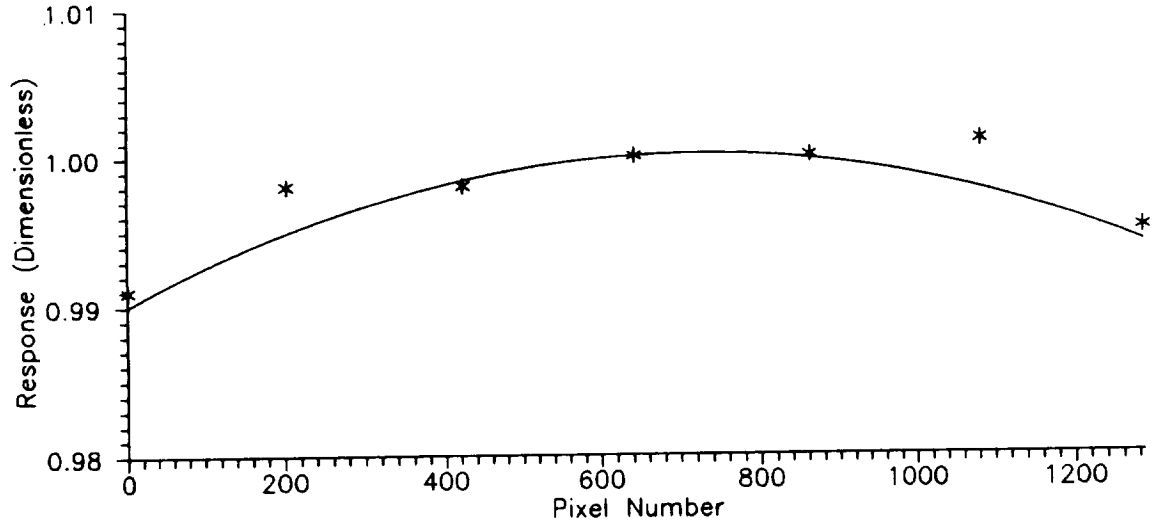


**Fig. 6.** Scan modulation measurements for the odd and even SeaWiFS bands. The results are given as relative differences from the nadir (pixel 643) value. The symbols show the average values from the laboratory measurements of the odd and even bands. The quadratic curves show the scan modulation corrections—see text for details. The top panel shows odd bands, and the bottom panel shows the even bands.

the image of the field stop imposed upon them. Any imperfection of the alignment of the instrument's optics will cause the image of the field stop to shift relative to the detectors. To minimize stray light entering the aft optics, the image of the field stop is 50% greater than the size of the detectors for each band. In the direction normal to the scan plane, this gives only a one-quarter pixel leeway on either side of the detectors. Imperfect alignment of the optics causes the image of the field stop to move relative to the focal plane assemblies. Increasing the size of the field stop, or cocking it slightly, could eliminate much of this effect. These changes were not part of the stray light improvements by SBRC. However, a portion of the stray light repairs to SeaWiFS involved work on the focal plane assemblies. The repositioning of the focal planes during their installation did affect the final scan modulation values slightly.

The quadratic response curves, calculated by SBRC, are based on measurements of the output of the SBRC integrating sphere over a period of about 30 minutes. To view the sphere, the instrument was rotated to seven angular positions, and the radiances from the sphere were recorded. The positions for the measurements were approximately 220 pixels apart and covered the range from 1–1,285 pixels. Small changes in the output of the sphere may have added a scatter of a few tenths of a percent to the measurements by the instrument.

The scan modulation response curves equal unity at nadir. For other pixels, the curves derived by SBRC give the difference of the instrument measurements, in relative terms, from the value at nadir. The corrections to the calibration equations are the inverse of the calculated instrument responses from SBRC. The SBRC response curves shows the output of odd bands at pixel 1 to be 1% lower than those at pixel 643. To correct for this, 1% must be added to the values from the odd bands at pixel 1.

This is the scan modulation correction:

$$K_4(\text{Pxl}) = \frac{1}{1 + A_0(\text{Pxl} - 643) + B_0(\text{Pxl} - 643)^2}, \quad (4)$$

where Pxl represents the pixel number, and where  $A_0 = 3.115 \times 10^{-6}$  and  $B_0 = -1.929 \times 10^{-8}$  for odd bands, and  $A_0 = 1.713 \times 10^{-5}$  and  $B_0 = -1.456 \times 10^{-8}$  for even bands.

For all bands,  $K_4(\text{Pxl})$  is equal to unity at nadir. As a result, this factor can be applied to (3) to cover all pixels in each scan. For a SeaWiFS band, the values over a scan line are given as

$$\begin{aligned} L_{\text{scan}} &= K_1(t) \times K_2(gs, ds) \\ &\times (1 + K_3(T - T_{\text{ref}})) \\ &\times K_4(\text{Pxl}) \times (C_{\text{out}} - C_{\text{dark}}), \end{aligned} \quad (5)$$

where  $L_{\text{scan}}$  is the measured radiance at any pixel in a scan, in  $\text{mW cm}^{-2} \text{sr}^{-1} \mu\text{m}^{-1}$ .

Equation (5) does not consider the mirror side differences in the instrument. Except for the variable,  $K_1$ , none

of the variables have any mirror side dependence. Based on considerations in the methods for determining long-term changes in the instrument's sensitivity,  $K_1$  has also been defined without a mirror side effect.

## 5.5 Full-Up Equations

The use of the radiometric calibration equations on orbit will require the consideration of the two sides of the half-angle mirror. This factor has been described above, including the factor  $R_1$  for mirror side 1 and  $R_2$  for mirror side 2. When these two factors are included, (5) can be modified to produce two equations with the form:

$$\begin{aligned} LS_1 &= R_1 \times K_1(t) \times K_2(gs, ds) \\ &\times (1 + K_3(T - T_{\text{ref}})) \\ &\times K_4(\text{Pxl}) \times (C_{\text{out}} - C_{\text{dark}}), \end{aligned} \quad (6)$$

and

$$\begin{aligned} LS_2 &= R_2 \times K_1(t) \times K_2(gs, ds) \\ &\times (1 + K_3 \times (T - T_{\text{ref}})) \\ &\times K_4(\text{Pxl}) \times (C_{\text{out}} - C_{\text{dark}}). \end{aligned} \quad (7)$$

The variables in (6) and (7) are defined as follows:

1.  $LS_1$  is the measured radiance for mirror side 1, in  $\text{mW cm}^{-2} \text{sr}^{-1} \mu\text{m}^{-1}$ .
2.  $R_1$  is the dimensionless multiplier for mirror side 1 from (1).
3.  $LS_2$  is the measured radiance for mirror side 2, in  $\text{mW cm}^{-2} \text{sr}^{-1} \mu\text{m}^{-1}$ .
4.  $R_2$  is the dimensionless multiplier for mirror side 2 from (2).

Equations (6) and (7) are the two on-orbit radiometric calibration equations for SeaWiFS.

## 5.6 Instrument Response Linearity

Equations (6) and (7) are based on the assumption that the measured radiance is a linear function of the number of counts in the instrument's output. The SeaWiFS performance specifications call for the output to be linear with radiance at the 1% level or better. For the six shortest wavelength SeaWiFS bands (412, 443, 490, 510, 555, and 670 nm), the measurements at SBRC show the linearity to be at the 0.5% level. For bands 7 and 8 (765 and 865 nm), the laboratory measurements show linearities that are better than the specifications, but not at the levels of the other six bands.

The measurements of the linearity of SeaWiFS were made using an integrating sphere. The radiances from the sphere were determined using a laboratory radiometer that compared the sphere's output to that from a standard lamp that has been calibrated by the National Institute of Standards and Technology (NIST). The radiances required for measurements of SeaWiFS at 765 and 865 nm are very

small when compared to the output from the standard lamp at these wavelengths. For the transfer radiometer, these levels were so low that noise in the transfer measurement approached 1%.

From this evidence, the conclusion is that the relatively poor linearity in the SeaWiFS laboratory measurements at 765 and 865 nm is due to limits in the quality of the characterization of the sphere itself. It is also concluded that the readings for all eight SeaWiFS bands are linear with input radiance at the level of 0.5% (Barnes et al. 1994). There is no term in the instrument's calibration equations for non-linear response.

## 5.7 Polarization Sensitivity

The degree of polarization of the eight SeaWiFS bands is measured in the laboratory using a polarizer that is rotated through 360° in 22.5° intervals. Over this angular range, the instrument bands should show two cycles of response. The response from SeaWiFS band 1 is shown in Fig. 7. There is little indication of the predicted two-cycle response. It is more reasonable to conclude that the variations in the instrument output shown in Fig. 7 are indicative of changes in the transmission of the polarizer with angle. Barnes et al. (1994) used Fourier analysis to expose the two-cycle signal. Their results indicate that polarization in the instrument is 0.25% or less.

The measurements in Fig. 7 are taken at pixel 633, near nadir. The response in this figure is also representative of the instrument responses at 30° and 55° from nadir. From the polarization measurements at these three angles, the polarization of SeaWiFS remains at 0.25% or less over a scan. There is no term in the instrument's calibration equations for polarization sensitivity.

## 6. GAIN FACTORS

The relative differences in the four sensitivity coefficients for each band result from different selectable gains in one of the intermediate amplifiers in the instrument's electronics. The SeaWiFS specifications give the gain requirements for gains 2, 3, and 4 relative to gain 1. Gain 1 is the principal science gain. Gain 2 is the secondary science gain with a radiometric sensitivity twice that for gain 1, that is, one count from Science Gain 2 represents half the radiance for one count from Science Gain 1.

### 6.1 Gain Ratios

#### 6.1.1 Individual Channels

The gains in the intermediate amplifiers have also been set up to give a three-quarters full scale output for lunar measurements and for solar measurements, using the flight diffuser. Details of the lunar and solar measurements can be found in McClain et al. (1992) and in Woodward et al. (1993). The gain values for the 32 SeaWiFS channels are

listed in Table 6 and are based on laboratory measurements by SBRC. The gain ratios are given with respect to Science Gain 1.

The gain ratios in Table 6 show little channel-to-channel variability. The four channels in band 1 can be taken as an example. For channel 1, the gain ratios for the four gains in Table 6 are all equal to unity. Channel 1 is the cloud channel, and those values should all be unity. In the calibration data from SBRC, the measured gain ratios for band 1—channel 1 are 1.016 ( $G_2/G_1$ ), 1.005 ( $G_3/G_1$ ), and 1.010 ( $G_4/G_1$ ). These differences are assumed to come from noise in the measured counts for each gain. That noise amounts to 2 or 3 counts out of 220. The data for each gain have a single calibration datum and a single zero. On orbit, there will be the capacity to take 25 calibration points and 25 zeros from each calibration pulse scan. This will improve the on-orbit gain ratios significantly when compared with the prelaunch measurements.

As a result, the gain ratios for the cloud channels have all been set to unity to eliminate the effects of noise in the measurements. In addition, there has been an averaging of gain ratios in the high sensitivity channels. For band 1—gain 2, the three high sensitivity bands all have the same gain ratio in Table 6 (1.988). In the calibration data from SBRC, the measured gain ratios are 1.987 (channel 2), 1.982 (channel 3), and 1.995 (channel 4). As with the measurements of the cloud channel, there is noise in these gain ratios. In the prelaunch data, the gain ratios have been set to the average of the three channels to remove noise. On orbit, it will be possible to measure these ratios with greater precision. Until then, it is not possible to distinguish between noise in the gain measurements of the high sensitivity channels and small differences in their gains.

#### 6.1.2 Combinations of Channels

The gain ratios in Table 6 are given for individual channels. It is possible to calculate these ratios for combinations of channels. Such ratios can be calculated for the standard SeaWiFS detector configuration, 4:1 TDI, where the output is the sum of the four channels. The calculations are based on the procedure outlined in Tables 1–4. They can be explained by using the values from SeaWiFS band 1. The gain ratios for the high sensitivity channels for band 1—gain 2 are 1.988 (Table 6). This means that a channel will produce 1.988 counts per unit radiance at gain 2 if the channel gives one count per unit radiance at gain 1. Conversely, if gain 1 has a sensitivity of one unit of radiance per count, gain 2 will have a sensitivity of 1/1.988 unit of radiance per count.

For gain 2 calculations, 1/1.988 is the fractional multiplier applied to the sensitivities for channels 2, 3, and 4 from Table 1. For gain 2, the sensitivities of these channels are approximately 0.005 mW per count (Table 1). With these three sensitivities and the sensitivity for channel 1,

**Table 6.** Gain ratios for the SeaWiFS channels, relative to Gain 1. The gains for the cloud detection channels for each band do not change with the gain selection.

<i>Band</i>	<i>Channel</i>	<i>Gain 1</i>	<i>Gain 2</i> ( $G_2/G_1$ )	<i>Gain 3</i> ( $G_3/G_1$ )	<i>Gain 4</i> ( $G_4/G_1$ )
1	1	1.000	1.000	1.000	1.000
	2	1.000	1.988	1.320	1.681
	3	1.000	1.988	1.320	1.681
	4	1.000	1.988	1.320	1.681
2	1	1.000	1.989	1.319	1.682
	2	1.000	1.989	1.319	1.682
	3	1.000	1.989	1.319	1.682
	4	1.000	1.000	1.000	1.000
3	1	1.000	1.000	1.000	1.000
	2	1.000	1.989	0.896	1.681
	3	1.000	1.989	0.896	1.681
	4	1.000	1.989	0.896	1.681
4	1	1.000	1.989	0.789	1.682
	2	1.000	1.989	0.789	1.682
	3	1.000	1.989	0.789	1.682
	4	1.000	1.000	1.000	1.000
5	1	1.000	1.000	1.000	1.000
	2	1.000	1.989	0.642	1.595
	3	1.000	1.989	0.642	1.595
	4	1.000	1.989	0.642	1.595
6	1	1.000	1.989	0.364	0.665
	2	1.000	1.989	0.364	0.665
	3	1.000	1.989	0.364	0.665
	4	1.000	1.000	1.000	1.000
7	1	1.000	1.000	1.000	1.000
	2	1.000	1.987	0.311	0.575
	3	1.000	1.987	0.311	0.575
	4	1.000	1.987	0.311	0.575
8	1	1.000	1.991	0.261	0.499
	2	1.000	1.991	0.261	0.499
	3	1.000	1.991	0.261	0.499
	4	1.000	1.000	1.000	1.000

which has not changed, it is possible to work through the calculations in the manner of those in Table 2 and 3. The results give three new knees for the bilinear gains, both in radiance and in counts. The upper endpoint remains the same, since the sensitivity for channel 1 has not changed.

Using the zero values plus those from the first knee in the bilinear gain, it is possible to calculate the sensitivity of band 1 in the radiance region for ocean measurements. The ratio of the sensitivities for gain 1 and gain 2 give the gain ratio for these gains with the standard detector configuration (Table 7). Table 7 also lists the gains that are used for lunar and solar measurements. These lunar and solar gains agree with the gains required by the SeaWiFS performance specifications.

From this discussion, it follows that the calculation method in Tables 1-4 is fundamental to the operation of

the bilinear gains. If the gain of a channel or combination of channels changes, then new knees must be calculated using the procedure from Tables 1-4.

## 6.2 Lunar Measurements

Once on orbit, the monitoring of the long-term repeatability of SeaWiFS measurements will be done by viewing the moon. On orbit, the changes in the sensitivities of the science gains will be based on measurements of the moon at the lunar gains. The lunar gains will be treated as a constant throughout the SeaWiFS mission. Changes in the measured lunar radiance, with the real lunar radiance remaining constant, will result in corresponding changes to the variable  $K_1$ , also described in (3). The lunar gains in these interchannel measurements will be kept constant,

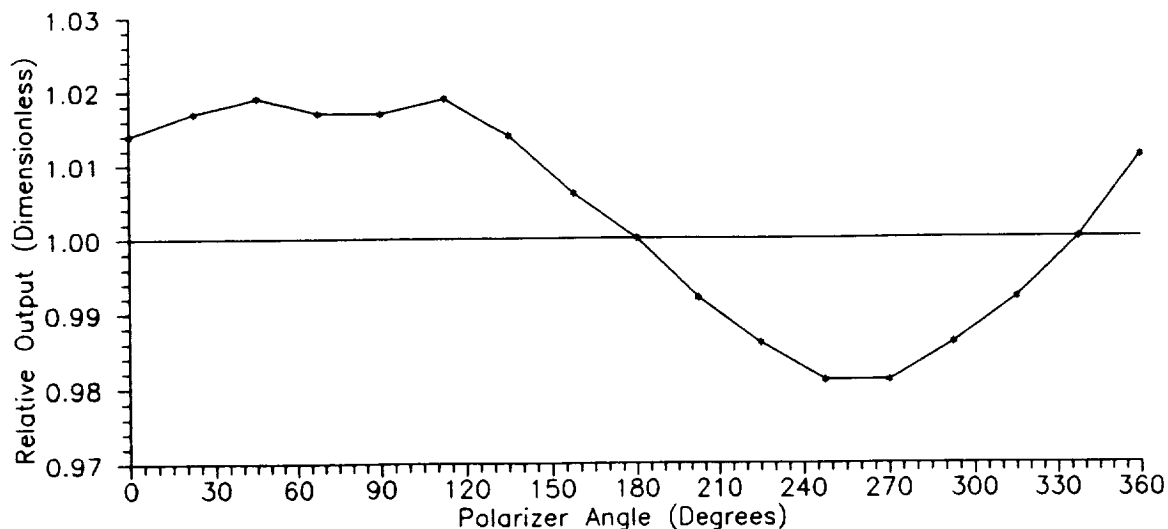


Fig. 7. Polarization sensitivity of SeaWiFS band 1 (412 nm).

and the gain ratios for the other gains will be allowed to vary. These are important considerations for an instrument whose long-term repeatability will be monitored by lunar, rather than terrestrial, measurements. Among other things, these considerations require a change in viewpoint from terrestrial to lunar measurements by those tracking changes in the instrument's sensitivity on orbit.

**Table 7.** SeaWiFS gain values for the standard detector configuration. These values are given relative to gain 1. The nominal value for gain setting 2 is 2. The gains used for the lunar measurement and for the solar diffuser measurement are shown. These gains cover the measurement regions from zero radiance to the first knees in the bilinear gains.

Band	Gain 1	Gain 2	Gain 3	Gain 4
1	1.000	1.931§	1.302	1.642†
2	1.000	1.940	1.303†	1.648§
3	1.000§	1.951	0.900†	1.655
4	1.000§	1.955	0.796†	1.658
5	1.000§	1.961	0.652†	1.579
6	1.000	1.969	0.376†	0.671§
7	1.000	1.969	0.323†	0.583§
8	1.000	1.975	0.272†	0.507§

§ Gain used for solar diffuser measurement.

† Gain used for lunar measurement.

The SeaWiFS calibration plan (McClain et al. 1992) includes a program of ground based measurements, primarily measurements of water-leaving radiances with field

instruments, in conjunction with SeaWiFS measurements on orbit. This calibration plan has been developed to make both the vicarious and satellite measurements traceable to a single set of laboratory standards so that ground and on orbit measurements can be reconciled. For the vicarious measurements, there is an ongoing program of round-robin intercalibrations of field instruments using NIST-traceable standards (Mueller 1993). The reconciliation of vicarious and on-orbit measurements also requires knowledge of the atmospheric transmission of light at the SeaWiFS wavelengths. For the SeaWiFS mission, this knowledge is derived from a set of models of the atmosphere that include light scattering by molecules of air, *Rayleigh* scattering, and by small particles, *Mie* scattering (H. Gordon, pers. comm.). These models will play a fundamental role in the reconciliation of the on-orbit radiance measurements from SeaWiFS and the water-leaving radiance measurements from field instruments.

The on-orbit monitoring scheme for the long-term repeatability of SeaWiFS measurements as described here, and also found in Woodward et al. (1993), comprises a closed set of measurements made by the satellite instrument only. The set of ground based measurements proposed in the SeaWiFS calibration plan (McClain et al. 1992) will be performed in conjunction with SeaWiFS measurements during satellite overpasses of the ground, or ocean, sites. The ground based measurements will complement the set of satellite based, long-term repeatability measurements described here. Ultimately, the combined

**Table 8.** Input values and calculated sensitivities for the eight SeaWiFS bands. The radiances, the measurement counts, and the offset counts come from laboratory data. The sensitivities are calculated from the radiances and the net counts. The values are given for Science Gain 1, the standard gain for SeaWiFS ocean measurements.

<i>Band</i>	<i>Channel</i>	<i>Radiance</i> [mW]	<i>Measurement</i> [counts]	<i>Offset</i> [counts]	<i>Net Counts</i>	<i>Sensitivity</i> [mW/count]
1	1	9.246	175	21	154	0.060039
	2	9.246	871	23	848	0.010903
	3	9.246	859	18	841	0.010994
	4	9.246	871	21	850	0.010878
2	1	9.122	883	18	865	0.010546
	2	9.122	887	21	866	0.010533
	3	9.122	878	16	862	0.010582
	4	9.122	153	18	135	0.067570
3	1	7.216	127	21	106	0.068075
	2	7.216	899	22	877	0.008228
	3	7.216	905	21	884	0.008163
	4	7.216	903	19	884	0.008163
4	1	5.970	856	21	835	0.007150
	2	5.970	855	20	835	0.007150
	3	5.970	856	19	837	0.007133
	4	5.970	111	21	90	0.066333
5	1	4.692	98	26	72	0.065167
	2	4.692	840	22	818	0.005736
	3	4.692	837	22	815	0.005757
	4	4.692	828	17	811	0.005785
6	1	1.682	540	21	519	0.003241
	2	1.682	538	17	521	0.003228
	3	1.682	544	33	511	0.003292
	4	8.058	168	21	147	0.054816
7	1	9.885	253	23	230	0.042978
	2	2.057	915	20	895	0.002298
	3	2.057	913	21	892	0.002306
	4	2.057	922	27	895	0.002298
8	1	1.063	671	20	651	0.001633
	2	1.063	670	24	646	0.001646
	3	1.063	671	18	653	0.001628
	4	10.283	320	20	300	0.034277

set of satellite based and ground based measurements will form the basis for the understanding of the SeaWiFS data set.

## 7. CALIBRATION CONSTANTS

### 7.1 SeaWiFS Radiometric Calibration

The laboratory results of the SeaWiFS radiometric calibration are given in Table 8. The 32 listings in the table show the input radiances and output counts for each channel of each band from the laboratory measurements. The values are given for Science Gain 1. The sensitivities for the channels are calculated from the radiances and the net

counts. The values from Table 8 are sufficient to calculate the knees and endpoints for each band for all detector combinations at Science Gain 1. The procedure outlined in Tables 1–4 can be applied to any combination of channels. For example, it is possible to combine channel 1 of band 1, taken once, with channel 2 of that band, taken three times, to create a truly bilinear response, a response with only one knee.

As discussed in Section 6.1, the gain ratios can be applied to the sensitivities in Table 8 to calculate the knees for each band for gains 2, 3, and 4. The endpoints for these gains will not change. The zero remains zero, and the upper endpoint is a function of the sensitivity of the cloud channel, which also does not change. Both the radiance

levels and count values for the knees are a function of the gain setting since the sensitivities of three of the channels change, while the cloud channel remains constant.

## 7.2 Out-of-Band Correction

There is an artifact of the radiometric calibration that has not been discussed in the calibration data from SBRC. The radiometric calibration of the instrument was performed with an integrating sphere as the source of radiance. The sphere has a wavelength dependent output that can be approximated by a 2,850 K blackbody. This source has a peak output near 1,000 nm (Section 9.8, Fig. 17). On orbit, SeaWiFS will measure input radiances with spectral shapes that are similar to that from a 5,900 K blackbody, which has a peak output near 490 nm.

The bandwidths for the SeaWiFS bands are 20 nm wide for bands 1 through 6, and 40 nm wide for bands 7 and 8. For these bandwidths, the spectral shape of the source has little effect (Section 11). The SeaWiFS bands, however, have small out-of-band responses (Section 9). The photodiodes in each SeaWiFS band have a slightly different output when illuminated by a 2,850 K or 5,900 K source. This output difference is of the order of a few percent or less (Section 9.10). This output difference is also the same for each channel of a band. The cloud and high sensitivity channels for a band all have the same fractional change in output when measuring these two sources. The out-of-band effect changes the sensitivities of all four channels in a band identically.

## 7.3 Bilinear Gain Calibration Constants

The calibration constants for the SeaWiFS bands are listed in Table 9. The table gives the endpoints and the knees for each band and gain. These values are given for the standard detector combination, i.e., for the sum of the four channels in each band.

Using the radiance levels and count values in Table 9, it is possible to calculate the radiance corresponding to each count for each band. Table 9 is the basis for the calculation of the gain factors ( $K_2$  values) used in (3). For computational purposes, it is also possible to prepare a lookup table for each band and for each gain. The lookup table would have approximately 32,000 entries, with about 1,000 entries for each of the four gains for each of the eight bands. This lookup table applies only to the standard detector configuration. Any changes to that configuration would require the recalculation of Table 9. It would also require the creation of a new lookup table, if one was used in the on-orbit data reduction.

The knees and endpoints for band 1–gain 1 in Table 9 are not the same as those in Table 4. The radiances for channel 1–gain 1 in Table 9 are 3.7% greater than the corresponding radiances in Table 4. This is the result of the application of the out-of-band correction discussed in Section 9.10. There is a smaller output from the photodiodes

for band 1 when it is exposed to a 5,900 K source, as measured on orbit, than when it is exposed to a 2,850 K source, measured in the laboratory. The counts per unit radiance of this band will be smaller on orbit than they are in the laboratory.

It will take a 3.7% greater radiance to saturate the channels of band 1 on orbit than is required to saturate them in the laboratory. Thus, the radiances at the knees and the upper endpoint for band 1–gain 1 in Table 9 are 3.7% greater than those in Table 4. These are the radiances at which each channel of the band saturates.

The fractional change from the out-of-band correction has only changed the radiances at the knees and the upper endpoint. The count values have remained the same. This results from the fact that the out-of-band correction affects the sensitivity of each channel in a band identically. For band 1, each channel changes by 3.7%. For the other bands, the fractional change is different (Section 9.10, Table 12). The out-of-band corrections have been applied to all bands and all channels in Table 9.

## 7.4 Out-of-Band Contributions

The out-of-band responses for the eight SeaWiFS bands are parts of the instrument's radiometric calibration. In that calibration, the instrument views a broad area of known radiance, and records the output from the bands in counts. The counts from each band include the out-of-band contribution. Those out-of-band contributions are functions of the spectral shape of the source that is measured. The SeaWiFS laboratory calibration has the out-of-band correction for a 2,850 K source factored into its results. If the instrument measures a source with this spectral shape, these measurements automatically contain the appropriate out-of-band corrections.

The prelaunch calibration equations for SeaWiFS contain correction terms that convert the out-of-band responses from a 2,850 K source to a 5,900 K source. As a result, the SeaWiFS calibration equations now have the out-of-band correction for a 5,900 K source factored into them. The 5,900 K spectral shape closely duplicates the spectral shape for SeaWiFS ocean measurements. The errors that arise from the use of the 5,900 K out-of-band corrections for ocean measurements are estimated to be small, i.e., a few tenths of a percent. If an alternate out-of-band correction is to be used, then the 5,900 K correction must be removed from the measurement results, and a new out-of-band correction inserted in its place.

# 8. TEMPERATURE FACTORS

## 8.1 Dependence Coefficients

The information about the temperature sensors for the focal plane assemblies includes the temperature dependencies of the output of the eight SeaWiFS bands, the  $K_3$

**Table 9.** Prelaunch calibration constants for the SeaWiFS bilinear gains. These values have been corrected for out-of-band response (see Table 12 for the conversion factor). These values are given for the standard detector configuration (each channel used once). For all bands and at all gain settings, the instrument was calibrated to give zero counts at zero radiance.

Band	Gain	Knee 1		Knee 2		Knee 3		Saturation	
		Radiance	Counts	Radiance	Counts	Radiance	Counts	Radiance	Counts
1	1	793.64	11.313	793.84	11.317	797.76	11.469	1,002.25	62.445
	2	771.09	5.691	771.27	5.693	774.89	5.769	1,002.25	62.445
	3	782.64	8.571	782.83	8.547	786.60	8.688	1,002.25	62.445
	4	775.26	6.731	775.45	6.734	779.12	6.824	1,002.25	62.445
2	1	789.10	10.734	791.34	10.778	792.93	10.837	1,004.75	69.062
	2	769.69	5.397	771.85	5.420	773.33	5.449	1,004.75	69.062
	3	779.67	8.140	781.86	8.174	783.40	8.218	1,004.75	69.062
	4	773.27	6.382	775.44	6.408	776.94	6.444	1,004.75	69.062
3	1	779.55	8.343	780.61	8.360	782.00	8.401	1,002.25	69.576
	2	764.62	4.194	765.64	4.202	766.96	4.224	1,002.25	69.576
	3	783.05	9.315	784.11	9.333	785.52	9.379	1,002.25	69.576
	4	767.39	4.963	768.42	4.973	769.74	4.998	1,002.25	69.576
4	1	778.79	7.175	779.00	7.178	779.28	7.185	1,002.75	66.599
	2	765.37	3.607	765.57	3.609	765.84	3.612	1,002.75	66.599
	3	786.02	9.098	786.23	9.101	786.52	9.110	1,002.75	66.599
	4	767.85	4.267	768.05	4.268	768.32	4.272	1,002.75	66.599
5	1	769.72	5.794	771.63	5.815	774.33	5.872	1,001.25	65.556
	2	758.77	2.913	760.64	2.923	763.23	2.952	1,001.25	65.556
	3	782.02	9.029	783.97	9.062	786.80	9.152	1,001.25	65.556
	4	761.50	3.631	763.38	3.645	766.00	3.681	1,001.25	65.556
6	1	763.41	3.211	763.48	3.212	764.36	3.223	1,000.00	54.322
	2	756.05	1.615	756.12	1.615	756.97	1.620	1,000.00	54.322
	3	789.32	8.831	789.40	8.832	790.36	8.861	1,000.00	54.322
	4	770.87	4.829	770.95	4.830	771.85	4.846	1,000.00	54.322
7	1	759.48	2.300	763.07	2.317	763.69	2.323	1,000.25	43.193
	2	752.87	1.158	756.41	1.166	757.01	1.169	1,000.25	43.193
	3	788.94	7.390	792.73	7.442	793.43	7.460	1,000.25	43.193
	4	769.31	3.999	772.97	4.027	773.61	4.036	1,000.25	43.193
8	1	762.22	1.618	762.77	1.620	763.74	1.626	1,002.50	34.001
	2	756.28	0.813	756.82	0.813	757.77	0.817	1,002.50	34.001
	3	796.06	6.206	796.64	6.213	797.74	6.237	1,002.50	34.001
	4	774.20	3.243	774.76	3.246	775.78	3.258	1,002.50	34.001

values. The reference temperature for the temperature dependence ( $T_{\text{ref}}$ ) has been set to 20° C by SBRC. The variable  $K_3$  and the constant  $T_{\text{ref}}$  are used in (3), (5), (6), and (7). The  $K_3$  values for the eight SeaWiFS bands are listed in Tables 10 and 11.

The temperature corrections require knowledge of the temperatures of the focal plane assemblies. The conversion of the engineering information in the scan lines from SeaStar into focal plane temperatures requires two steps (Sections 8.2 and 8.3). Since there is only one temperature sensor per focal plane assembly, the derived temperatures for bands 1 and 2 will be identical, as will those for bands

3 and 4, and so forth. Thus, the coefficients for the calculation of these pairs of temperatures should be identical in the following sections.

## 8.2 Data Conversion

In this section, the term *voltages* is used to refer to voltages from SeaWiFS.

### 8.2.1 SeaStar Counts to Voltage

The voltages for every analog telemetry output from SeaWiFS range from 0–5.11 volts. These voltages are trans-

mitted to the ground by SeaStar as 8 bit binary words. Since the counts from the SeaWiFS radiance measurements are transmitted in 10 bit binary words, the analog telemetry values are also packaged in 10 bits. However, for the analog telemetry values, only eight of those 10 bits per word are used.

**Table 10.** Values in the temperature dependence equations. This table contains the temperature dependency coefficients ( $K_3$ ) and the coefficients to convert OSC telemetry counts to temperature sensor output volts ( $K_5$  and  $K_6$ ).

Band	$K_3$ [ $(^\circ\text{C})^{-1}$ ]	$K_5$ [volts/count]	$K_6$ [volts]
1	0.000901	0.020	0.0
2	0.000585	0.020	0.0
3	0.000420	0.020	0.0
4	0.000390	0.020	0.0
5	0.000391	0.020	0.0
6	0.000151	0.020	0.0
7	0.000106	0.020	0.0
8	0.000078	0.020	0.0

**Table 11.** Current output for the current source diodes ( $K_7$ ). These data are given for a temperature of  $20^\circ\text{C}$ . A correction must be applied to these data at other temperatures. Values are given for the prime and backup temperature sensors for each focal plane assembly. The backup sensor for bands 3 and 4 is inoperative.

Band	$K_7$ (prime) [mA]	$K_7$ (backup) [mA]
1	0.493	0.484
2	0.493	0.484
3	0.492	Inoperative
4	0.492	Inoperative
5	0.491	0.497
6	0.491	0.497
7	0.486	0.492
8	0.486	0.492

The SeaStar spacecraft will convert the analog voltages from SeaWiFS using an ADC with a 5.12 volt reference voltage. This will eliminate the need for scaling amplifiers between SeaWiFS and the ADC. Since an 8 bit binary signal ranges from 0–255 counts, each count will have a value of 0.02 volts, with 0 counts equal to 0 volts. This corresponds to temperature sensor voltages that range from 0–5.10 volts. This is the basis for the coefficients  $K_5$  and  $K_6$  in Tables 10 and 11. The conversion equation for SeaStar telemetry counts to SeaWiFS temperature sensor voltages is linear:

$$V_T = K_5 \times C_{\text{temp}} + K_6. \quad (8)$$

The variables in (8) are defined as:

1.  $V_T$  is the output from the focal plane temperature sensor, in volts.
2.  $K_5$  is the spacecraft analog-to-digital (AD) conversion factor, in volts per count.
3.  $C_{\text{temp}}$  is an 8-bit digital word in the SeaStar telemetry, in counts.
4.  $K_6$  is the offset in the spacecraft AD conversion, in volts.

## 8.2.2 Voltage to Focal Plane Temperature

The temperature detection circuit for each focal plane assembly uses a precision thermistor in parallel with a 16.2 Kohm resistor. The current through the thermistor-resistor pair is provided by a current source diode that has a nominal output of 0.48 mA. The actual output of the current sources at  $20^\circ\text{C}$  are given in Tables 10 and 11. The output from the temperature sensor is the voltage across the thermistor-resistor pair as caused by the current from the diode. With knowledge of this voltage drop and of the current from the source, it is possible to calculate the effective resistance for the thermistor-resistor pair. With knowledge of the value of the resistor, 16.2 Kohm, it is then possible to calculate the actual resistance of the thermistor. From the thermistor resistance, the temperature of the focal plane assembly is derived using a conversion equation that is specific for the type of thermistor in the temperature sensor.

There is a small, additional complication to this calculation. The output from the current source diode has a small temperature dependence. The correction for current source diodes requires an approximate temperature ( $TC$ ) for the focal plane assembly.  $TC$  is good to about  $2^\circ\text{C}$  over the range from  $5^\circ\text{C}$  to  $45^\circ\text{C}$ . The details of these calculations will be presented in a series of steps below. The calculated focal plane temperatures are accurate to  $0.3^\circ\text{C}$ . This includes the uncertainty in the digitization of the temperature sensor voltages by the SeaStar spacecraft.

1. Calculate the approximate temperature, with

$$TC = (5 - V_T) \times 40/3, \quad (9)$$

where  $TC$  is the approximate focal plane temperature, in degrees Celsius.

2. Calculate the current from the current source diode, including its temperature correction, with

$$ICS = K_7 - (0.0013 \times (TC - 20)), \quad (10)$$

where  $ICS$  is the current from the current source diode, in mA;  $K_7$  is the current from the diode at  $20^\circ\text{C}$ , in mA (Tables 10 and 11); and  $(0.0013 \times (TC - 20))$  is the temperature correction for the diode source, in mA.

3. Calculate the effective resistance for the thermistor-resistor pair, with

$$R_E = V_T / ICS, \quad (11)$$

where  $R_E$  is the effective resistance for the thermistor-resistor pair, in Kohms.

4. Calculate the resistance for the thermistor, with

$$R_T = (16.2 \times R_E)/(16.2 - R_E), \quad (12)$$

where  $R_T$  is the resistance of the thermistor, in Kohms.

5. Calculate the focal plane temperature from the thermistor resistance using the following conversion equation.

$$T = -341 + 5398.94/(\ln(254898 \times R_T)), \quad (13)$$

where  $T$  is the focal plane temperature, in degrees Celsius, and the constants are given values for the type of thermistor used in the temperature sensors.

The variable  $T$ , given for each SeaWiFS band, is used in equations (3), (5), (6), and (7). The working range for these temperature calculations is about  $+5^\circ\text{C}$  to  $+45^\circ\text{C}$ , which roughly corresponds to the range 1.7–5.0 volts, or about 85–250 counts.

## 9. SPECTRAL RESPONSE

SBRC's primary method for determining the spectral response of SeaWiFS is based on the measurement of the individual piece parts in the instrument's optical train. The transmission and reflection characteristics of the piece parts and the responsivity of the detectors are multiplied together to give the optical throughput of the eight SeaWiFS bands at 1 nm intervals. The results of the calculations are given as amperes of electrical current from the photodiode per watt of radiant flux at each 1 nm interval. This throughput must be combined with a radiance source having the spectral shape of the sun to give the total output of each band for the full range of wavelengths.

SBRC's secondary method is based on a system level measurement using a monochromatic light source. This source employs a single monochromator to provide light input with a spectral width of about 1 nm and with a known radiant flux at each wavelength. In this method, the output of the photodiode is measured, in amperes, for a known radiant flux from the monochromator, in watts, at each 1 nm interval, allowing the calculation of the throughput of the instrument. This throughput is equivalent to that from the piece part measurements. For SBRC, the system level measurements give a double check of the piece part calculations. The piece part values give the prime measure of spectral response.

The system level measurements work reasonably well in the wavelength range where there is at least a minimal output from the band's photodiode. There are, however, regions outside of the pass bands of the radiometer's optical components where the throughput of the system is sufficiently close to zero, such that essentially no measurable current comes from the photodiode. In these wavelength regions, noise in the system level measurements dominates

the results. The piece part results give much better values, since they are based on measurements of individual components, each having a small throughput. At the system level, the measurements in these regions include the product of these small throughput contributions, which creates an overall throughput at the system level that is immeasurably small.

The following sections contain discussions of the spectral responses of the individual parts for each SeaWiFS band. These individual parts are shown in the aft optics schematic (Fig. 3). It is important to note that the piece part measurements in the following sections have been made of interference filters taken from the production run for the SeaWiFS flight filters. The piece part measurements have not been made with the actual flight filters.

### 9.1 Mirrors

There are five mirrors in the optical train for SeaWiFS. Four of these are shown in Fig. 3. They are the primary mirror, the polarization scrambler, the half-angle mirror, and the collimator. The fifth mirror, a folding flat mirror (not shown) is located after the collimating mirror (Fig. 17 of Woodward et al. 1993). Each of these mirrors uses silver as the reflecting surface, and four of these mirrors have essentially the same spectral response. The reflectivity of one of these four nearly identical mirrors has been measured at several wavelengths in the laboratory by SBRC. Values between these wavelengths have been calculated by linear interpolation. Figure 8 (top) shows the reflectivity of one of the silver mirrors.

As part of the modifications to reduce stray light in SeaWiFS, the polarization scrambler was reworked to move ghosts, in the direction normal to the scan plane, onto the primary image. In this modification, the front surface of the optical plate over the silver mirror in the scrambler was tilted slightly, relative to the mirror. This change has given the scrambler a slight wedge shape. A spectral scan was made by SBRC of the reflectivity of the reworked polarization scrambler. This spectral response is also shown in Fig. 8 (top).

The model for the combined reflectances of the five mirrors, including that for the polarization scrambler, is shown in Fig. 8 (bottom). At each wavelength, the reflectance for the silver mirror in Fig. 8 (top) is multiplied by itself four times and then multiplied by the reflectance of the polarization scrambler. This calculation accounts for the net reflectance of these five mirrors in series in the SeaWiFS optical train.

### 9.2 Lenses

There are four sets of lenses in the SeaWiFS aft optics (Fig. 3). These sapphire lenses are spectrally flat over wavelengths from 300–1,000 nm, covering the region of the

SeaWiFS Prelaunch Radiometric Calibration and Spectral Characterization

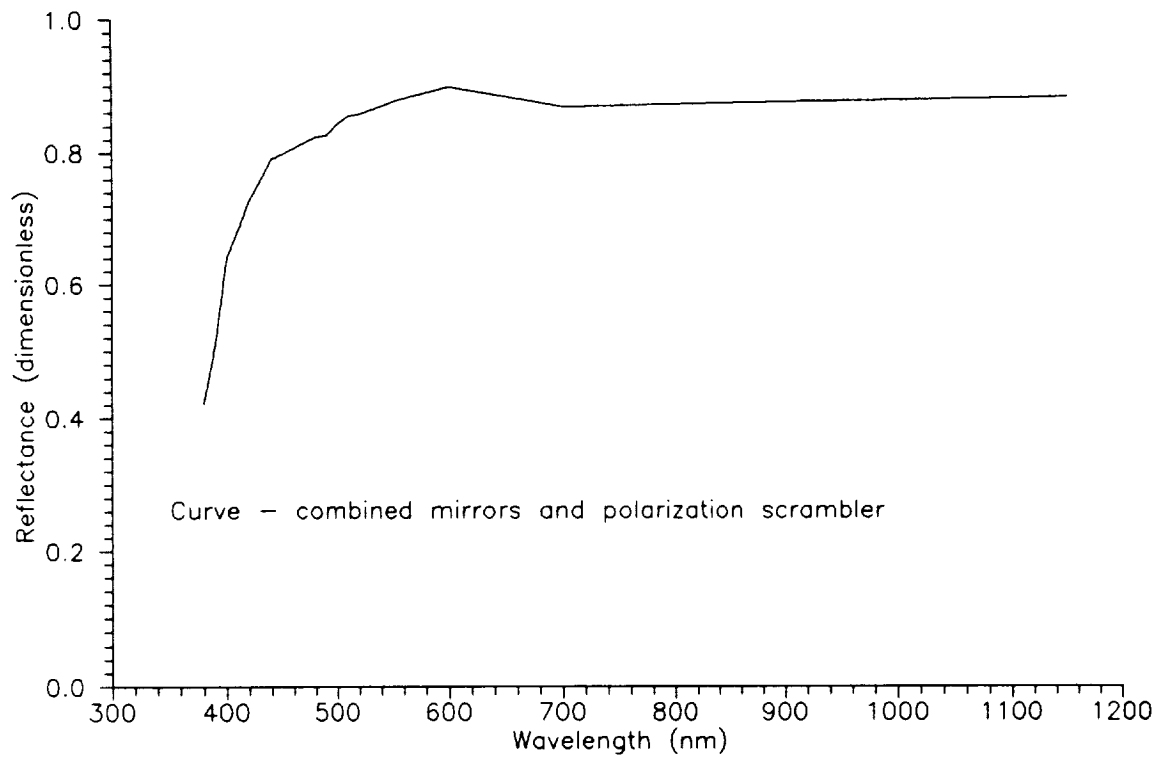
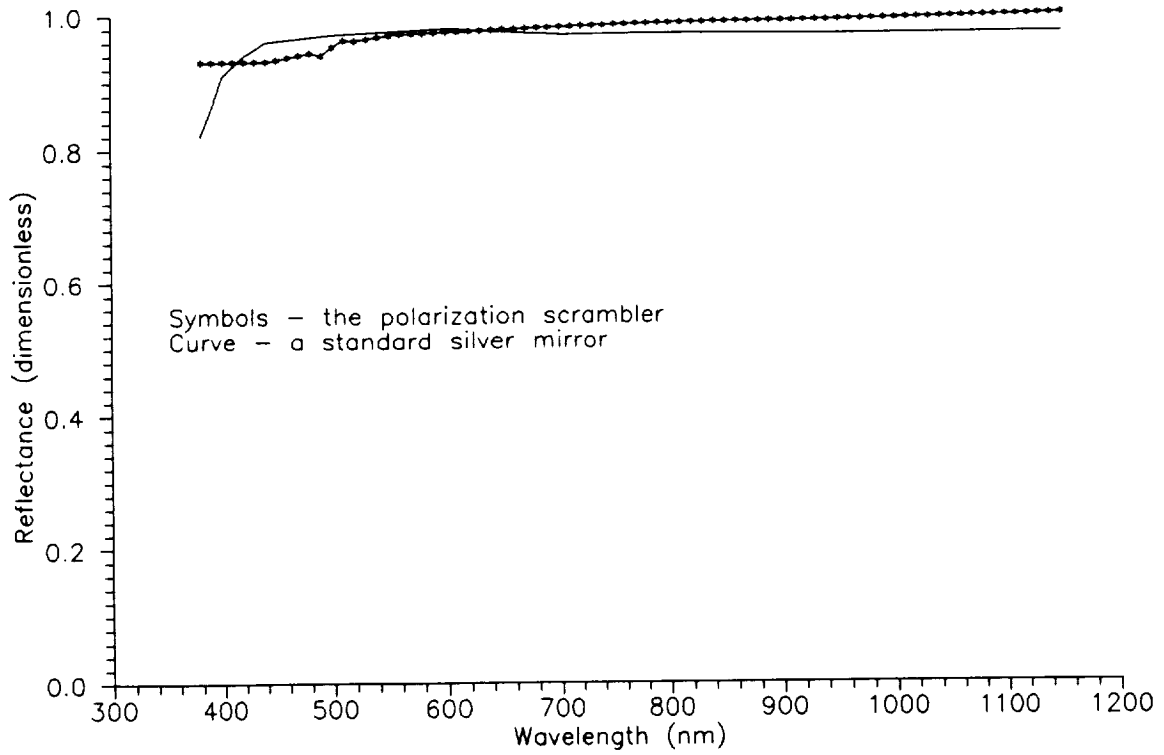


**Fig. 8.** SeaWiFS mirror reflectances. The top panel shows measured values for a standard silver mirror and for the polarization scrambler. The bottom panel shows the reflectance model for the four mirrors and the polarization scrambler in series in the SeaWiFS optical train.

SeaWiFS measurements. The lenses have transmittances of 99%. They are not included in the spectral response calculations. The lenses focus the collimated light that has passed through the dichroics onto the focal plane assemblies. The angle with which this light converges must be considered in the measurements of the spectral response of the narrowband interference filters.

### 9.3 Dichroics

The SeaWiFS radiometer uses three dichroics. In the SeaWiFS application, these dichroics transmit light for wavelengths above a reference wavelength in the dichroic's design and reflect light below the reference wavelength. The three SeaWiFS dichroics perform a prefiltering of the radiance from the Earth, limiting the range of wavelengths that reach the interference filters on each focal plane.

The dichroics and focal plane assemblies in SeaWiFS are shown in schematic form in Fig. 3. In the schematic, the light to the focal plane assembly for bands 7 and 8 (765 and 865 nm) passes in a straight line through two dichroics. These dichroics are numbered 1 (nearest the collimator) and 3. The light for bands 5 and 6 (555 and 670 nm) is transmitted by dichroic 1 and then reflected by dichroic 3. In Fig. 3, the focal plane assembly for bands 5 and 6 is located on the far right.

The focal plane assembly for bands 1 and 2 (412 and 443 nm) is located behind the BG39 filter in Fig. 3. The light for this focal plane is reflected off dichroics 1 and 2. Dichroic 2 is located to the left of dichroic 1 in Fig. 3. The remaining focal plane assembly, for bands 3 and 4 (490 and 510 nm), receives light reflected from dichroic 1 and transmitted by dichroic 2. This focal plane assembly is located on the left most side of Fig. 3.

For each focal plane assembly, and its pair of SeaWiFS bands, light is either transmitted or reflected by two dichroics. These dichroics play a major role in forming the shapes of the spectral responses of the eight SeaWiFS bands. This is particularly true in establishing the out-of-band response of the instrument. The performance specifications sent from SBRC to its filter manufacturer call for the use of the dichroics to remove the transmission spikes in regions well away from the pass band of the interference filters. This has limited the number of filter elements required for the interference filters and has helped increase the transmission of the interference filters to almost 100% at their center wavelengths.

Figure 9 gives the spectral responses for the two dichroics in the optical train for band 1. Figure 9 (top) gives the reflectance curve for dichroic 1. The cutoff for reflection by this dichroic falls between 510 nm (band 4) and 555 nm (band 5), separating the four shortest wavelength bands from the four longest. When viewing Fig. 9 (top), it should be remembered that a dichroic either transmits light or reflects it. The dichroics and the interference filters

in SeaWiFS are designed without light absorbing components. In regions where the reflectance is near 100%, the transmittance is near 0%.

Figure 9 (bottom) gives the reflectance curve for dichroic 2. Its cutoff wavelength is between 443 nm (band 2) and 490 nm (band 3). Dichroics 1 and 2 keep most of the longer wavelength radiation from the Earth from reaching bands 1 and 2, which limits the wavelength range over which the interference filters need to work.

For wavelengths above 1,140 nm, the SBRC measurements of dichroic 1 (Fig. 9, top) gave reflectances lower than the resolution of the laboratory equipment. For these wavelengths, the laboratory readings were zero. The values from the dichroics contribute to spectral responses presented in the following sections. These results are presented as a set of logarithmic plots. As a result, the zero values for dichroic 1 in this technical memorandum have been replaced with amounts that are equal to the lowest reflectance in the rest of the dichroic measurements. Similar measures have been taken at other places where the SBRC data set has values of zero.

### 9.4 Broadband Filters

There are two pieces of Schott color glass filters in the SeaWiFS aft optics assembly (Fig. 3). These broadband filters were not part of the original SeaWiFS optical design. The two filters (BG39 and BG26 in the figure) were added to the instrument after the SeaWiFS critical design review. Both broadband filters transmit in the blue-green region of the visible spectrum and reflect in the red.

The transmission curve for the BG39 filter is shown in Fig. 10 (top). This filter was added to the focal plane assembly for bands 1 and 2 to provide additional suppression of transmission spikes from the interference filters in the red. These spikes do not present a significant problem for the 412 and 443 nm bands on orbit. The broadband filter was added to aid in the radiometric calibration of bands 1 and 2 in the laboratory.

The light source used for the radiometric calibration of the instrument does not have the same spectral shape as the sun. The sun, with the approximate spectral shape of a 5,900 K blackbody, has a peak flux output at a wavelength of 491 nm. The integrating sphere in the SBRC laboratory has the spectral shape of a 2,850 K blackbody and a maximum light output at 1,017 nm. This is true of all integrating spheres since all use tungsten lamps as light sources. Blackbody radiation is described in Section 9.8.

In relative terms, the laboratory light source produces considerably more light in the red portion of the spectrum than in the blue-green. In relative terms, this excess of red light from the integrating sphere accentuates the out-of-band transmission spikes from the interference filters. When using the integrating sphere, the so-called *red leak* for band 1 (412 nm) is about 30% of the transmitted light through the filter's pass band.

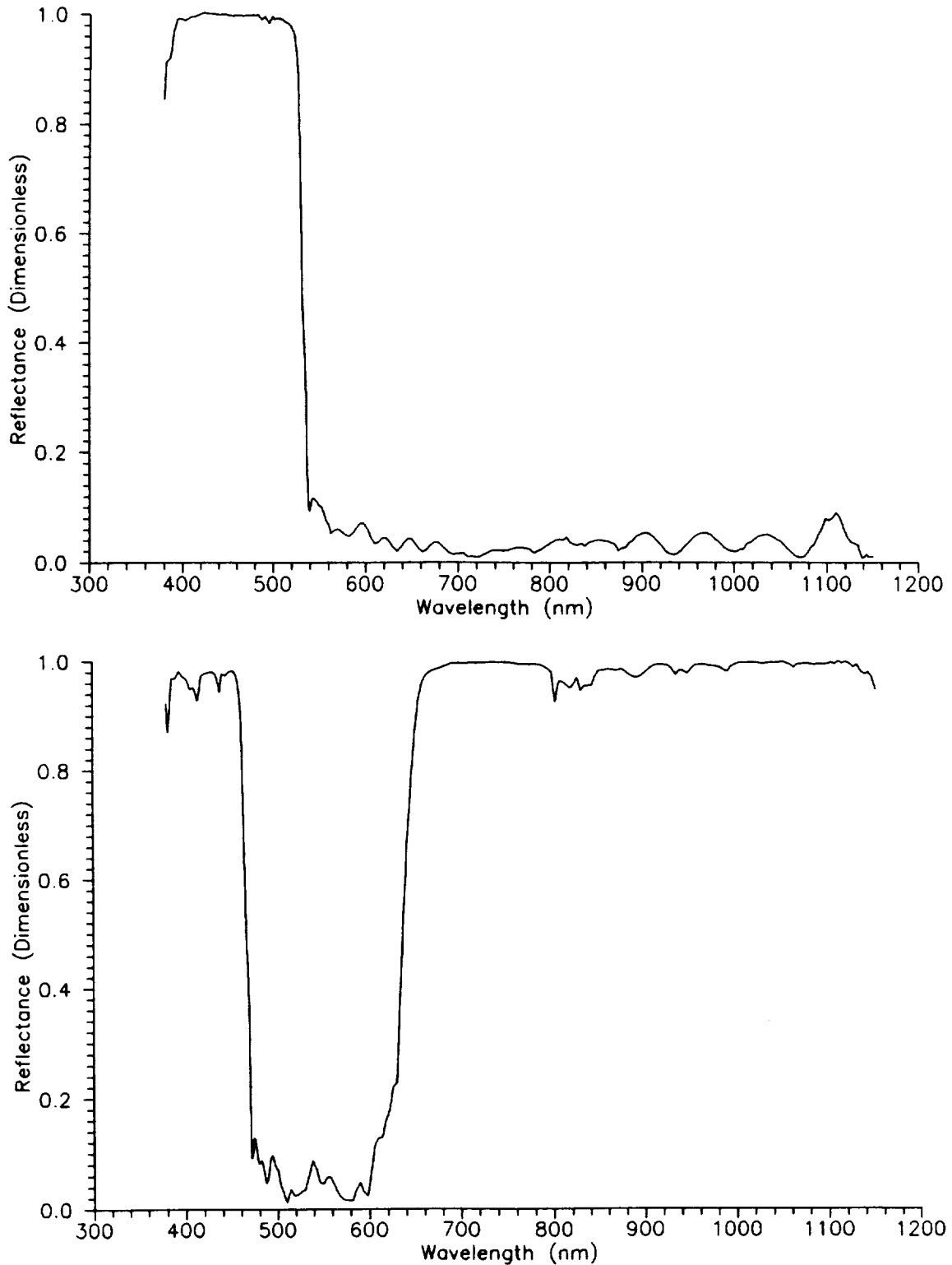


**Fig. 9.** Reflectance curves for SeaWiFS dichroics 1 and 2. These dichroics are in the optical train for bands 1 and 2 (412 and 443 nm). The top panel shows the reflectance curve for dichroic 1. This element separates bands 1 through 4 from bands 5 through 8. The bottom panel shows the reflectance curve for dichroic 2. This element separates bands 1 and 2 from bands 3 and 4.

The sun (or a 5,900 K blackbody) produces much more radiance flux in the blue-green region than in the red. For sunlight, the *red leak* through the 412 nm interference filter is less than 1%. As a result, the BG39 filter has little use to SeaWiFS on orbit. The filter has been of great utility in the laboratory measurements which are required before the instrument is placed in orbit.

The BG26 filter has been added to the instrument to reduce the amount of light in the two longest SeaWiFS bands (765 and 865 nm). This reduced optical signal has helped the stray light characteristics for these bands. Although the BG26 filter has not been added to change spectral shapes in the instrument, its spectral effects must still be considered.

The transmission spectrum for the BG26 filter is given in Fig. 10 (bottom). Both colored glass filters have been measured in the laboratory at SBRC. The measurements have been made at several wavelengths. Values between these wavelengths have been calculated by linear interpolation. With its position at the entrance to the focal plane assembly, this filter affects the transmission of all eight SeaWiFS bands. Figure 10 (bottom), however, shows that the curve has very little spectral shape over the pass bands of the eight SeaWiFS interference filters. The BG26 broadband filter is spectrally flat over SeaWiFS band 1 and adds next to nothing to its spectral shapes.

## 9.5 Photodiode Responsivity

The responsivity of the photodiode used in SeaWiFS, expressed in terms of mA of current out per mW of radiant flux in, has been measured at SBRC. These measurements are made for one of the diodes in the production batch used for the instrument. SeaWiFS employs 32 photodiodes, and it is impractical to measure the spectral response of each. As a result, there has been only one measurement at SBRC. The diode's response curve shows little structure over the 10 and 20 nm half-widths of the eight SeaWiFS bands (Fig. 11, top).

There is, however, structure in Fig. 11 (top) around the 412 and 443 nm wavelengths. This results from noise in the measurement at SBRC and not from the wavelength dependence of the efficiency of the photodiode. The SBRC measurements of the spectral response curve were performed using the same equipment as the system level test of the wavelength dependence from SeaWiFS. Light from a monochromator was used to illuminate a NIST calibrated photodiode and then to illuminate the SeaWiFS diode. The response curve in Fig. 11 (top) was calculated using these data and the NIST calibration curve for the reference photodiode. The monochromator used a tungsten lamp for its source, and the measurements had low light levels in the blue wavelengths and increased noise at wavelengths below 500 nm.

This artificial structure at the blue end of Fig. 11 (top) was removed using a second order polynomial fit of the

data from 406–490 nm. These fitted results replace the laboratory measurements over wavelengths from 380–490 nm. The measured values and the fitted curve are shown in Fig. 11 (bottom). The extrapolation of the fitted curve to 380 nm removes unwarranted structure in the out-of-band response of the bands below 400 nm, although the extrapolation creates some additional error in the instrument level spectral response curves below 400 nm. This error, however, is a small part of values that are already close to zero. The spectral response calculations in this technical memorandum use the fitted curve from 380–490 nm.

Elements of the SeaWiFS optical train, other than the photodiodes, transmit or reflect a fraction of the input radiance. In the calculation of the optical throughput of the instrument, they are dimensionless. It is the photodiodes that convert mW of radiant flux into mA of electrical current. The diodes integrate the radiant flux over the wavelength range where the optics have a non-zero response. For each channel, the electronics transform this current into voltage, amplify the voltage, and change the voltage into counts with an ADC. This process gives the fundamental radiometric conversion factor for SeaWiFS, mW of radiance flux per count.

## 9.6 Detector-to-Detector Differences

For the ocean color instrument, the performance specifications address spectral uniformity for an instrument with multiple detectors. SeaWiFS has four detectors per band which are cut from a single piece of silicon substrate and lie in a single line. The individual detectors are 0.025 cm square with a 0.005 cm saw cut in the substrate between them. The total length of the detector array is 0.117 cm. All four detectors lie under the same narrowband interference filter. Assuming a reasonable uniformity in the silicon substrate and in the interference filters, the spectral responses for the four detector elements in each band are assumed to be essentially identical. The response curve for each band is dominated by the band's interference filter, with the photodiode adding little to the band's spectral response. The specifications call for the central wavelength of each channel to be within +0.5 nm of the central wavelength of all four channels. The prelaunch acceptance report (Barnes et al. 1994) shows the SeaWiFS instrument to meet this specification.

## 9.7 Narrowband Filters

The spectral shape for each SeaWiFS band is dominated by the band's narrowband interference filter. The response of this filter gives the principal definition of the following for each SeaWiFS band: the center wavelength; the band edges, from the full width at half maximum; and the extended band edges, from the 1% power points. The transmission curve for the 412 nm narrowband interference filter from 380–580 nm is shown in Fig. 12 (top). This

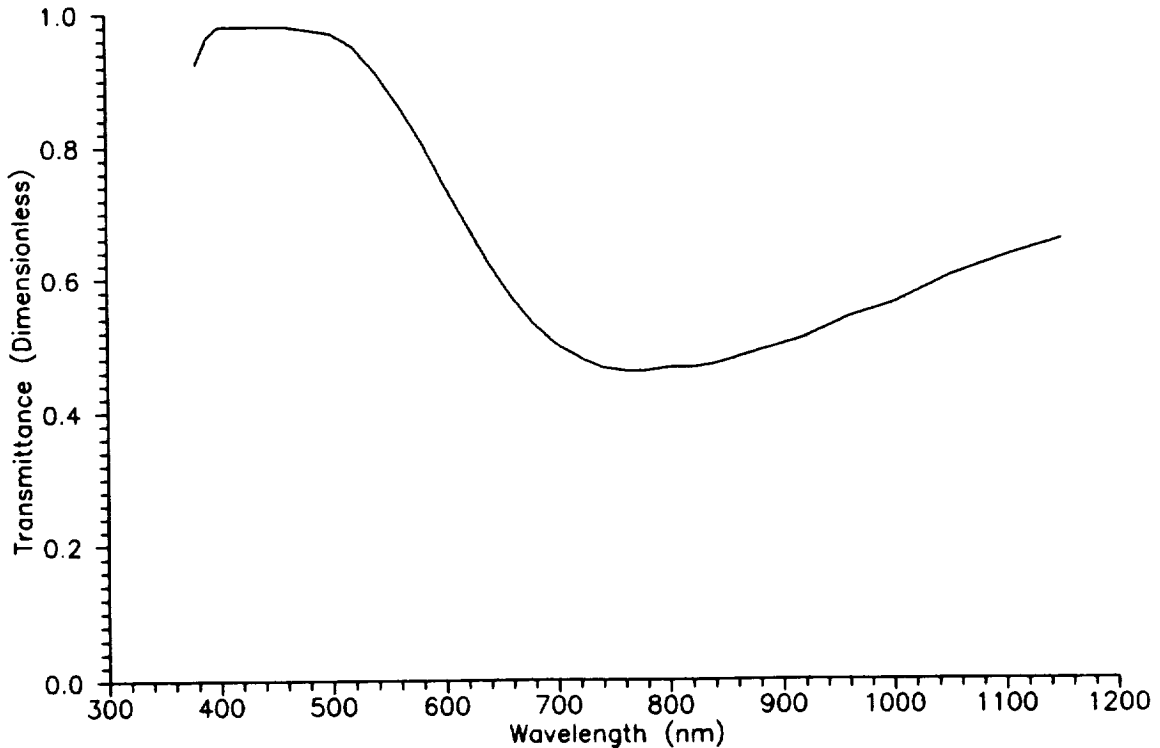
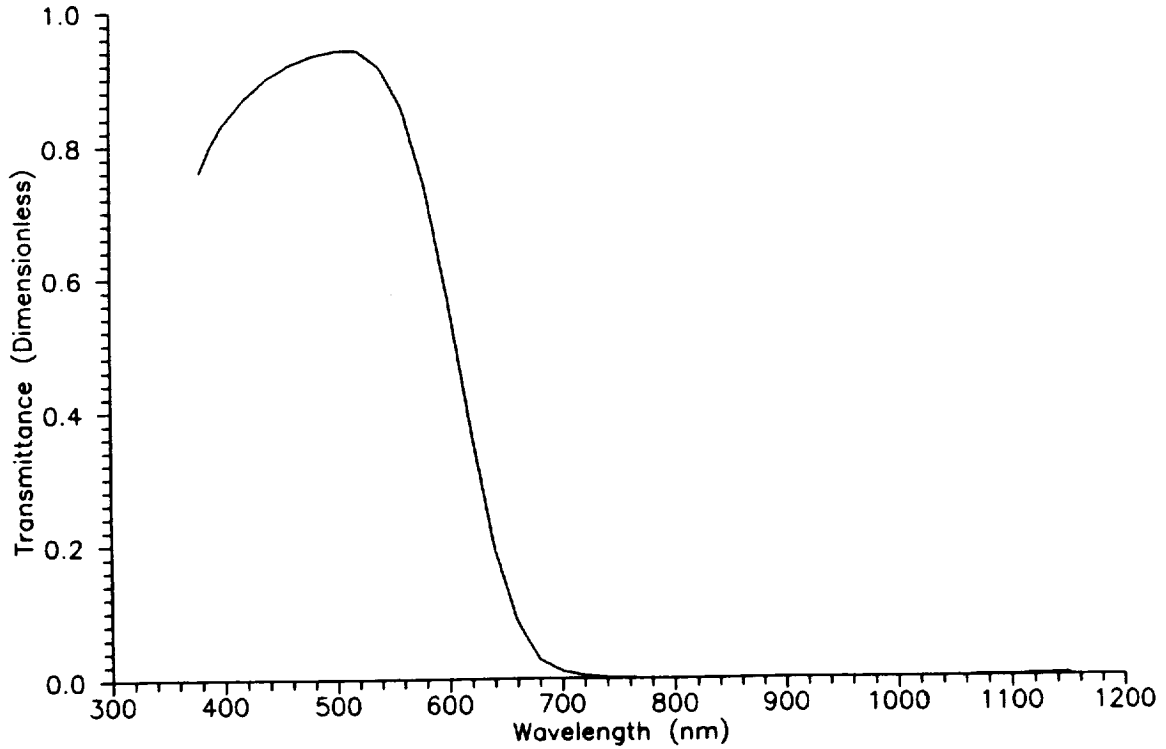


**Fig. 10.** Transmission curves for the SeaWiFS color glass filters. The top panel shows the transmission curve for broadband filter BG39. This filter forms a part of the optical train for bands 1 and 2 (412 and 443 nm). The bottom panel shows the transmission curve for broadband filter BG26. This filter is part of the optical train for all eight SeaWiFS bands.

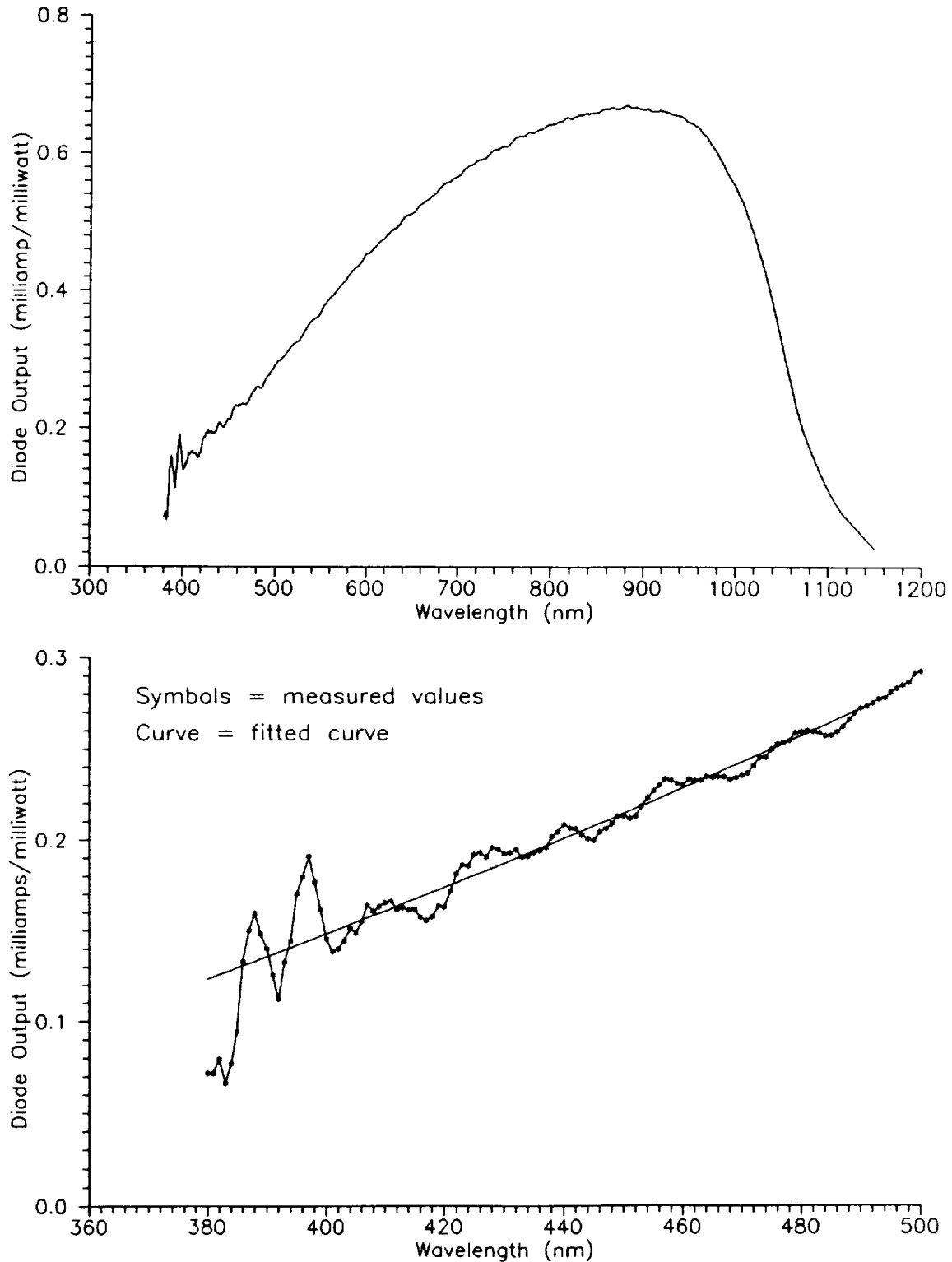


**Fig. 11.** Spectral response curve for the SeaWiFS photodiodes. The top panel shows the measured response curve for the diodes from 380 to 1150 nm. The bottom panel shows the measured values for the photodiodes and the fitted curve from 380 to 550 nm. The spectral response calculations in this technical memorandum use the fitted curve from 380 to 490 nm.

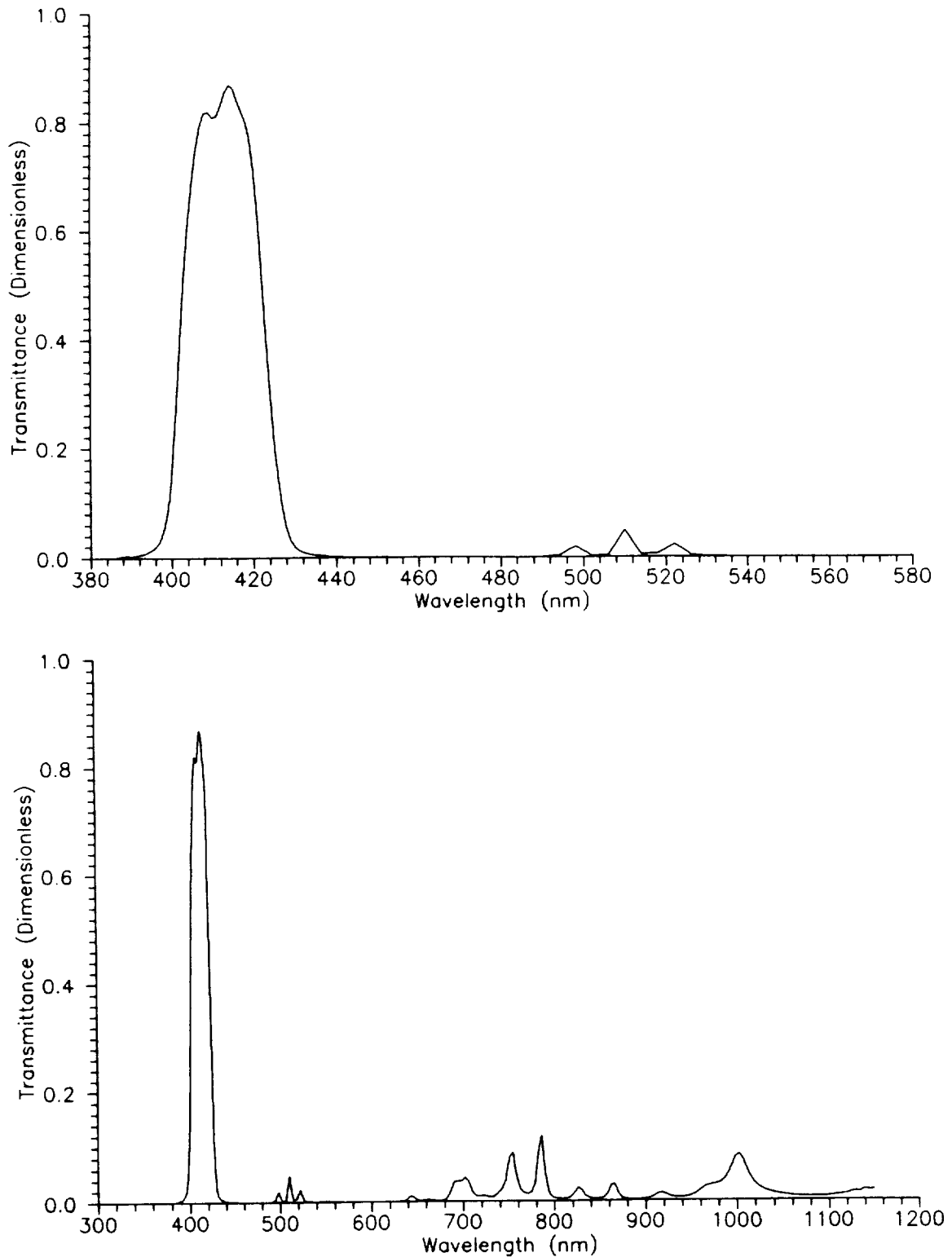


**Fig. 12.** Transmission curve for the 412 nm narrowband interference filter. Vertical scale in linear units. The top panel shows the transmission curve from 380–580 nm covering the pass band of the filter and the out-of-band response near 500 nm. The bottom panel shows the transmission curve for the filter from 380 to 1150 nm showing the complete set of out-of-band responses.

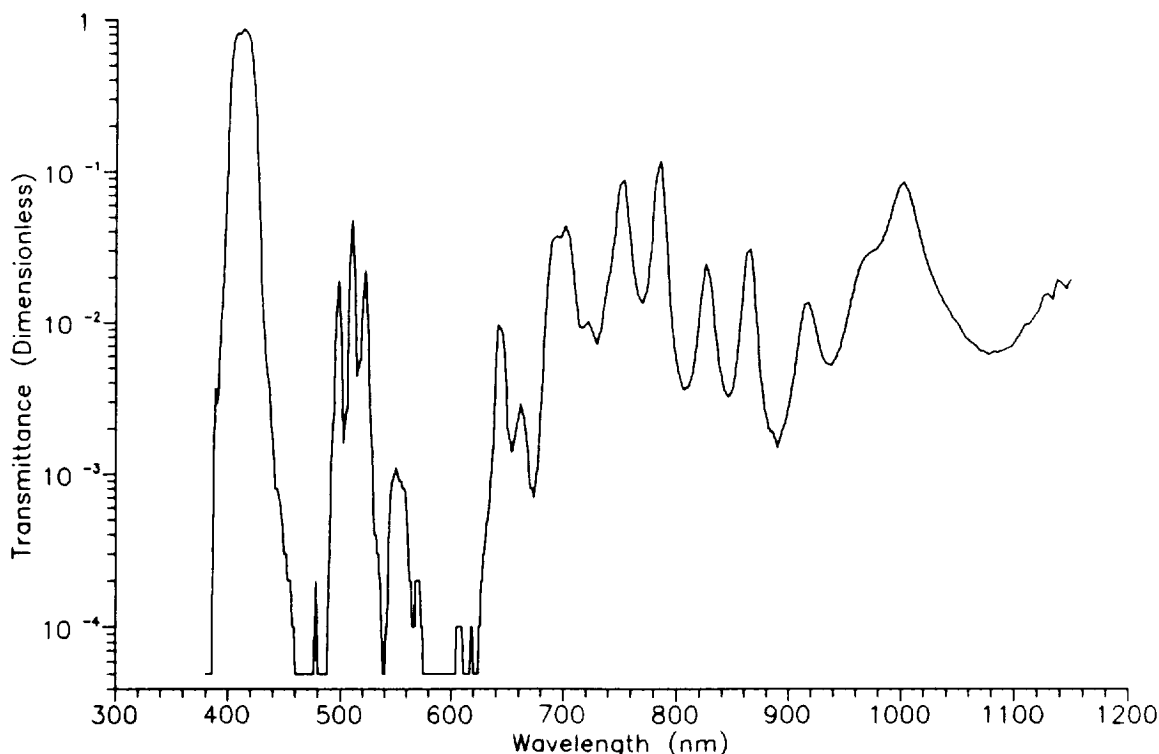


**Fig. 13.** Transmission curve for the 412 nm filter. The vertical scale is given in logarithmic units. This accentuates the out-of-band response of the filter.

curve, with its linear ordinate, shows the features and the shape of the pass band of the filter. Figure 12 (top) also shows the out-of-band transmission leak near 500 nm.

Figure 12 (bottom) shows the response of the filter from 380–1,150 nm. The curve for the same filter is also given in Fig. 13 with a logarithmic ordinate. Figure 13 shows the large and the small out-of-band components of the filter. Some of these peaks are substantial. The SeaWiFS optical train for bands 1 and 2, however, contains dichroics and a BG39 broadband color glass filter to reduce these out-of-band components.

The SeaWiFS radiometer uses a scrambler to remove any polarization that may be present in the input radiance to the instrument, although polarization is not a consideration in the measurement of the interference filters. The lenses between the dichroics and the focal plane assemblies (Fig. 3) convert the collimated light into converging light with a relative aperture ( $f$ -number) of 2. For this  $f$ -number, the distance between the lenses and the focal plane assemblies is twice the diameter of the opening in the lens assemblies. This converging angle has been included in the measurements of the narrowband interference filters in the laboratory.

The measurements of the SeaWiFS interference filters at SBRC have been made with laboratory equipment having a resolution of 0.0001 transmission units. There are data points in the test results where the transmission of the filters is less than that threshold. In the laboratory results, these points have been given transmission values of zero. For this report, the zero values have been replaced with one-half of the resolution of the measurements, i.e., at 0.00005 transmission units. This allows for plots of the results on a logarithmic axis.

For each SeaWiFS band, the dichroics substantially reduce the out-of-band transmission spikes. Figure 14 (top) shows the net result for the interference filter for band 1 (from Fig. 12, top) combined with the response curves for the band's two dichroics (from Figure 9, top and bottom). This figure uses a logarithmic ordinate to emphasize the characteristics outside of the filter's pass band. As shown in Fig. 14 (top), the out-of-band response is reduced significantly when compared with Fig. 13.

A BG39 filter has been added to the instrument to further reduce the out-of-band response for the 412 nm channel. The inclusion of the BG26 and BG39 filter responses to Fig. 14 (top) give the result in Fig. 14 (bottom). The

out-of-band response of band 1 above 600 nm is more than four orders of magnitude below the transmission peak at 412 nm.

Figure 15 shows the addition of the mirror and the photodiode responses to Fig. 14 (bottom). Figure 15 gives the spectral response of SeaWiFS band 1 (412 nm) to a spectrally flat light source. At each wavelength from 380–1,150 nm, this theoretical source provides a radiance of  $1 \text{ mW cm}^{-2} \text{ sr}^{-1} \mu\text{m}^{-1}$ . At each wavelength, the photodiode converts this radiance into picoamperes of current. The integral of this current over wavelength gives the total output of the photodiode, in nanoamperes, for such a source. Figure 15 provides an intermediate step in the spectral response calculations, since SeaWiFS views sources that have specific spectral shapes, both in the laboratory and on orbit. In addition, Fig. 15 marks the point in the spectral calculations where the measurements of the band edges, i.e., 50% power points, and extended band edges, i.e., 1% power points, are made to show compliance with the SeaWiFS specifications.

The inclusion of the photodiode and the mirror responses to the data set in Fig. 15 has the effect of increasing the out-of-band response for band 1 relative to the response for the data sets in Fig. 14 (top and bottom). This can be seen in the relative size of the peak near 650 nm in Fig. 15 (bottom). The diode and mirror responses have enhanced this peak in Fig. 15 (bottom) between four and five times relative to its size in Fig. 14 (top and bottom). The 650 nm peak lies below the resolution of Fig. 14 (bottom), and is four orders of magnitude below the transmission peak in Fig. 15 (bottom).

## 9.8 Blackbody Radiation

For an idealized blackbody radiator, the radiance can be given as a function of temperature and wavelength. For the purposes of calculations, the equation can be used in the following form (Wyatt 1978):

$$L(\lambda) = \frac{1.191066 \times 10^8}{\lambda^5 (e^{1.43883 \times 10^4 / \lambda T} - 1)}, \quad (14)$$

where  $\lambda$  is the wavelength, in  $\mu\text{m}$ ;  $T$  is the temperature, in kelvins; and  $L$  is the radiance, in  $\text{W m}^{-2} \text{ sr}^{-1} \mu\text{m}$ .

The radiance values from (14) can be converted directly into units of  $\text{mW cm}^{-2} \text{ sr}^{-1} \mu\text{m}^{-1}$ , the units for SeaWiFS measurements. The radiance values from this equation increase at all wavelengths with increasing temperature, and the peak of the curve shifts toward shorter wavelengths with increasing temperature. These two effects are significant, since the laboratory measurements for SeaWiFS are made with light sources that use tungsten lamps having blackbody temperatures near 2,850 K, while the sun approximates a 5,900 K source for wavelengths in the blue and the visible (Allen 1973 and Warneck 1988). For this reason, the SeaWiFS performance specifications require

that the out-of-band response for the SeaWiFS bands be determined for a source with the spectral shape equivalent to the sun.

There are xenon arcs and other laboratory sources that mimic the wavelength dependent shape of the blackbody shape of the sun better than tungsten lamps. These laboratory sources do not have the inherent stability of integrating spheres using sets of tungsten lamps. In addition, these other sources cannot be easily adjusted over the range of intensities necessary for the calibration of the instrument. As a result, laboratory radiometric measurements of the SeaWiFS bands have been made using sources with tungsten lamps and then calculated for a solar-equivalent spectral shape.

A 5,900 K blackbody closely approximates the spectral shape for the maximum anticipated radiances from the Earth found in the SeaWiFS performance specifications (Barnes et al. 1994). When the 5,900 K curve is normalized to the eight cloud radiances in the specifications (Fig. 16), the relative standard deviation of the curve values from the cloud radiances is 5%, with the values from the curve falling low in bands 1, 2, and 6. A fine tuning of the temperature of the solar equivalent blackbody temperature to other temperatures near 5,900 K will have no significant effect on the spectral response calculations for SeaWiFS.

Figure 17 (top) shows the response of SeaWiFS band 1, 412 nm, to a source with the shape of a 5,900 K blackbody. The flux from the blackbody curve has been normalized at 412 nm to the typical saturation radiance for band 1 from the SeaWiFS performance specifications,  $13.63 \text{ mW cm}^{-2} \text{ sr}^{-1} \mu\text{m}^{-1}$  (Barnes et al. 1994). Figure 17 (bottom) shows the same response but to a 2,850 K blackbody normalized at 412 nm.

In addition, the vertical scale for Fig. 17 (bottom) is 15 times greater than that for Fig. 17 (top). The radiation curve for the 2,850 K blackbody peaks at 1,017 nm, far to the red of the normalization wavelength, 412 nm. The normalized 5,900 K curve in Fig. 17 (top) would appear as a small hump in Fig. 17 (bottom). The illumination of SeaWiFS band 1 at the SeaWiFS saturation radiance level with the SBRC integrating sphere also illuminates this band with considerable light in the red region. At 1,000 nm, the illumination is about 16 times greater than the illumination at the band's center wavelength. This is a factor that must be considered in the transfer of the SeaWiFS radiometric calibration in the laboratory to the calibration on orbit.

The system response curves in Fig. 15 are given for a spectrally flat source with a radiance of  $1 \text{ mW cm}^{-2} \text{ sr}^{-1} \mu\text{m}^{-1}$ . The two blackbody radiance curves in Fig. 17 use the same units. This allows a direct calculation of the response of SeaWiFS band 1 to 2,850 K and 5,900 K sources that have a radiance of 13.63 mW at 412 nm. Figure 18 shows the differences between the output of SeaWiFS band 1 when exposed to 2,850 K and 5,900 K blackbody sources.

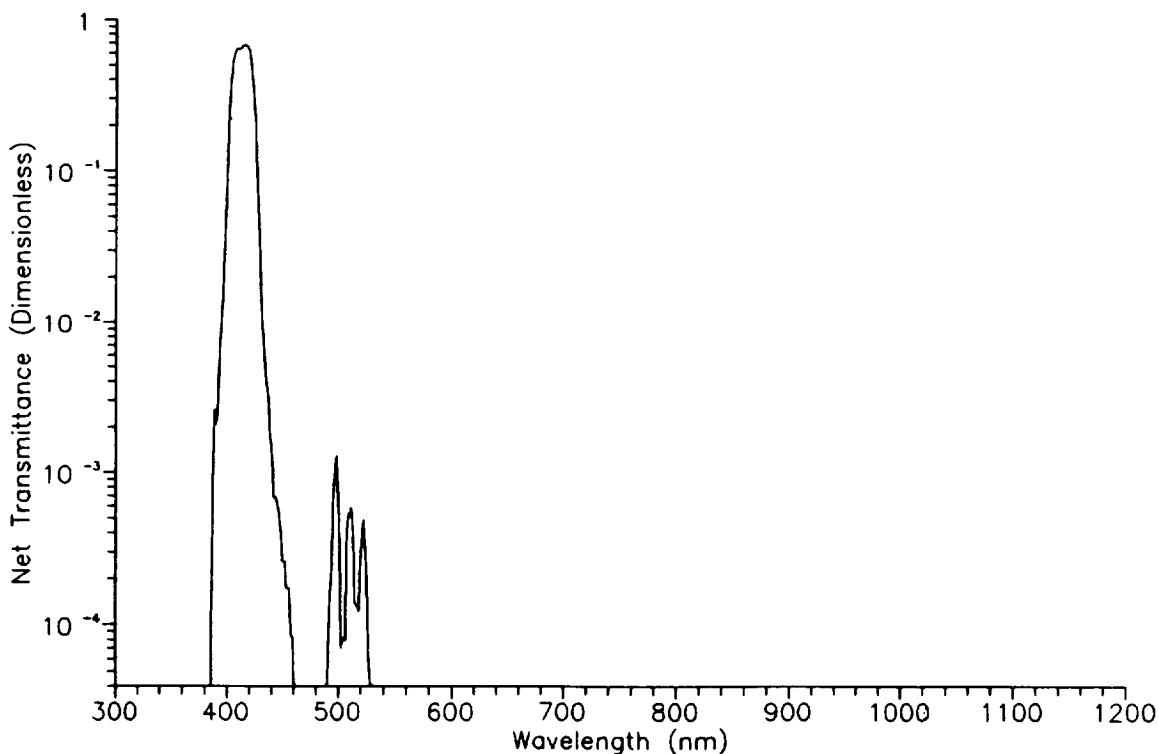
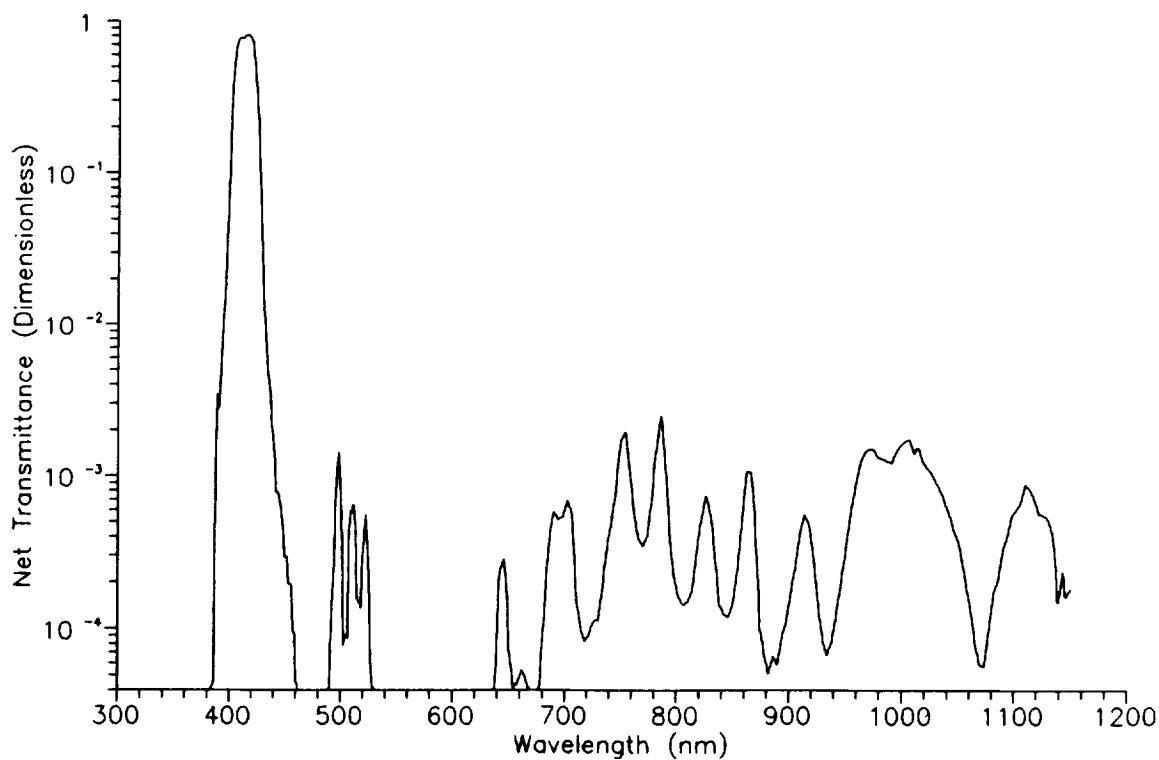


**Fig. 14.** Combined transmission curves for the interference filter, dichroics, and broadband filters in SeaWiFS band 1. The top panel shows the combined curve for the interference filter and dichroics. Compared with Fig. 10, the out-of-band response has been reduced by about two orders of magnitude. The bottom panel shows the combined curve for the interference filter, dichroics, and broadband filters. The out-of-band response above 600 nm has been further reduced by two orders of magnitude.

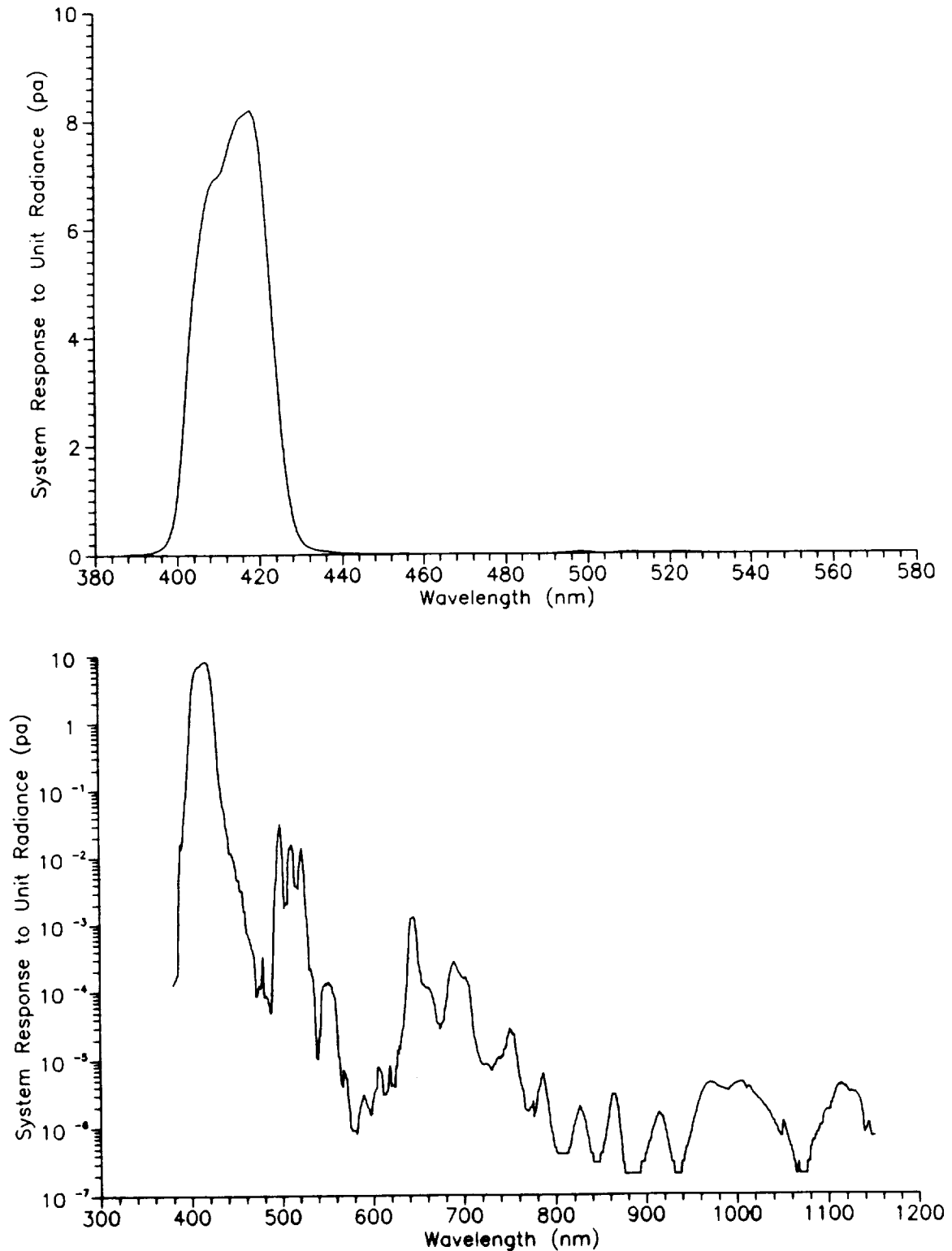


**Fig. 15.** System response curve for SeaWiFS band 1. This includes the optical components and the photodiode response to a spectrally flat light source with a radiance of  $1 \text{ mW cm}^{-2} \text{ sr}^{-1} \mu\text{m}^{-1}$ . The top panel shows the system response on a linear scale. The out-of-band response near 500 nm is barely noticeable. The bottom panel shows the system response on a logarithmic scale.

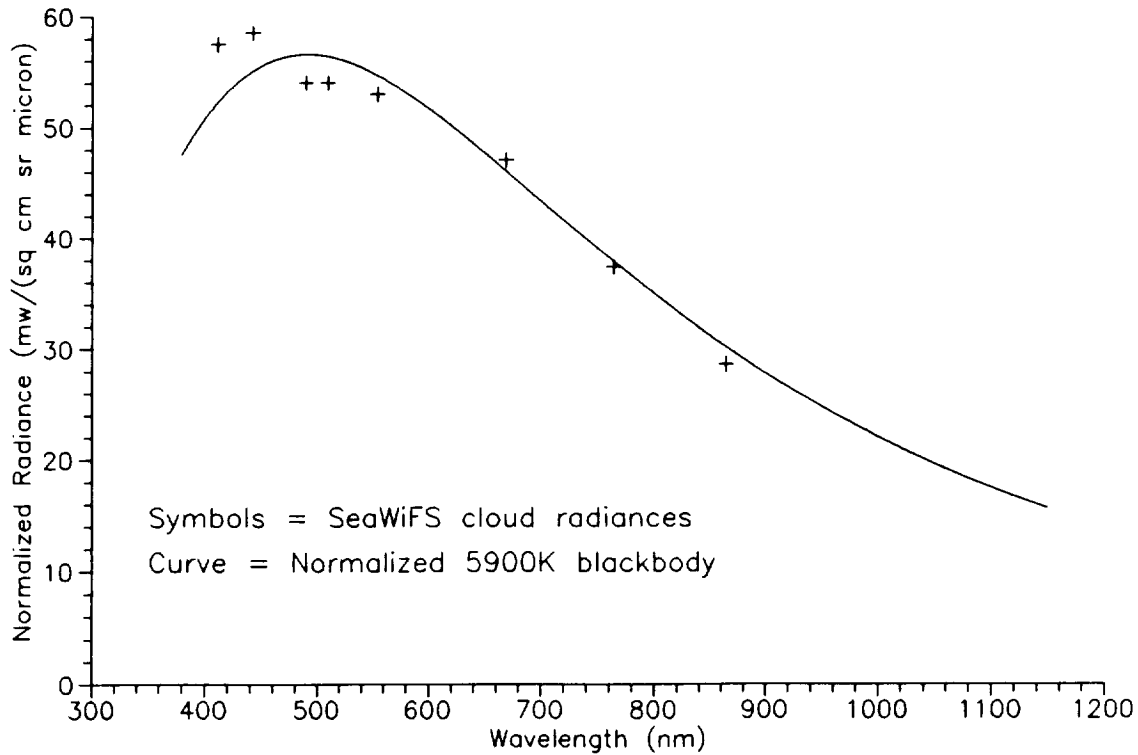


**Fig. 16.** Radiance curve for a 5,900 K blackbody normalized to the cloud radiances from the SeaWiFS performance specifications.

The spectral response characteristics for the other seven SeaWiFS bands are calculated in a manner that is the same as the method that has been described here for band 1. The spectral responses of all eight bands to a 5,900 K source are shown below (Figs. 19–24). The integrated output of the instrument for the 2,850 K and 5,900 K blackbody temperatures must be used in ratios to convert the laboratory measured radiance calibration for SeaWiFS to the in-flight calibration. For SeaWiFS band 1, the laboratory measurements will give a slightly greater number of counts per unit radiance than will the measurements on orbit. The results of these calculations for all eight SeaWiFS bands are given below.

The performance specifications for SeaWiFS allow out-of-band responses that are less than 5% of those within the extended band edges, which are defined by the 1% power points. These out-of-band response specifications cover the response of the instrument to a radiance source that mimics the sun. Calculations for all eight bands, using the 5,900 K blackbody, are also given in Section 12. In addition, the band edges and extended band edges for all of the SeaWiFS bands are tabulated in Section 11. These

values are calculated for a spectrally flat light source, a 5,900 K blackbody, and for a 2,850 K source.

### 9.9 Absolute Throughput

Using additional information, including the collection aperture for the instrument and the instrument’s field of view, SBRC has calculated the absolute throughput for the eight SeaWiFS bands. Using these data and the output of the instrument when illuminated by an integrating sphere, SBRC has calculated the sphere radiance based ultimately on the piece part curves. The worst comparison between the calculated and measured sphere radiances was for band 1 (412 nm). For this band, the output of the instrument was about 50% greater than expected in the calculations. Absolute instrument throughput is not investigated here.

### 9.10 Spectral Response Curves

In previous sections, the spectral responses of SeaWiFS band 1 for three light sources have been given: spectrally flat, 5,900 K blackbody, and 2,850 K blackbody. The radiances from the two blackbody light sources were normalized to the expected saturation radiance for band 1 at

SeaWiFS Prelaunch Radiometric Calibration and Spectral Characterization

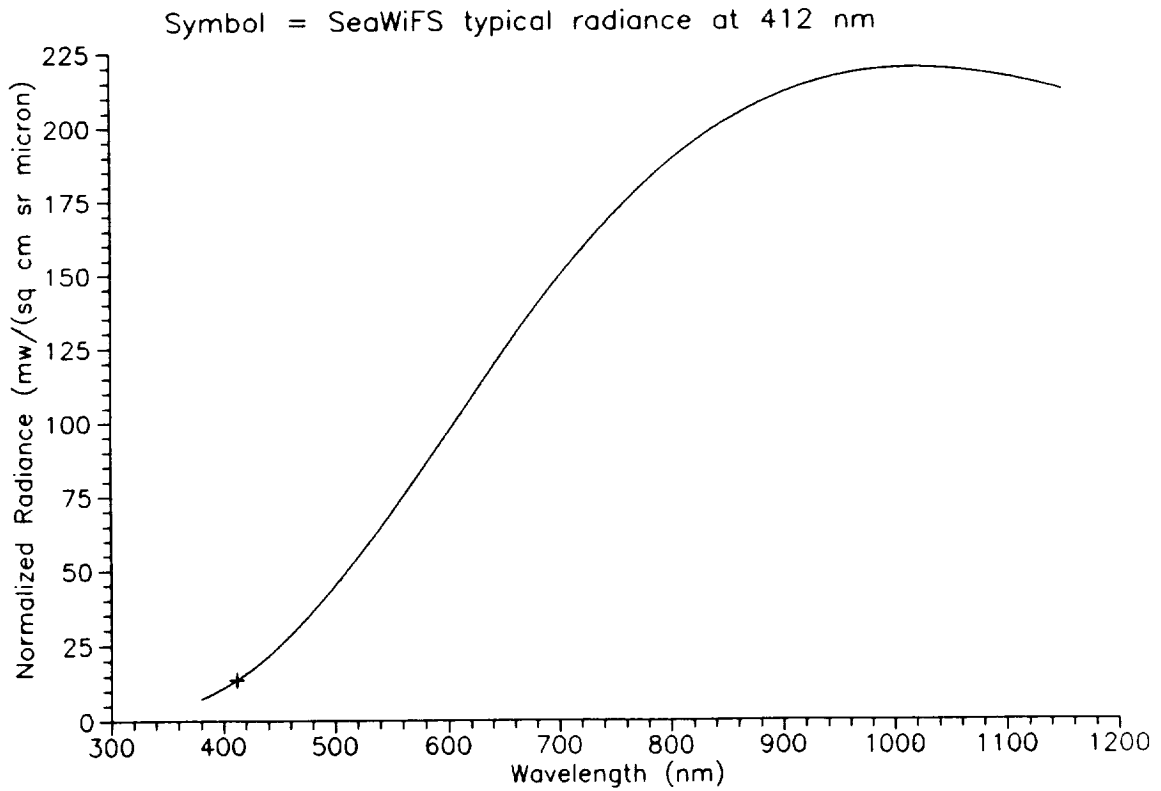
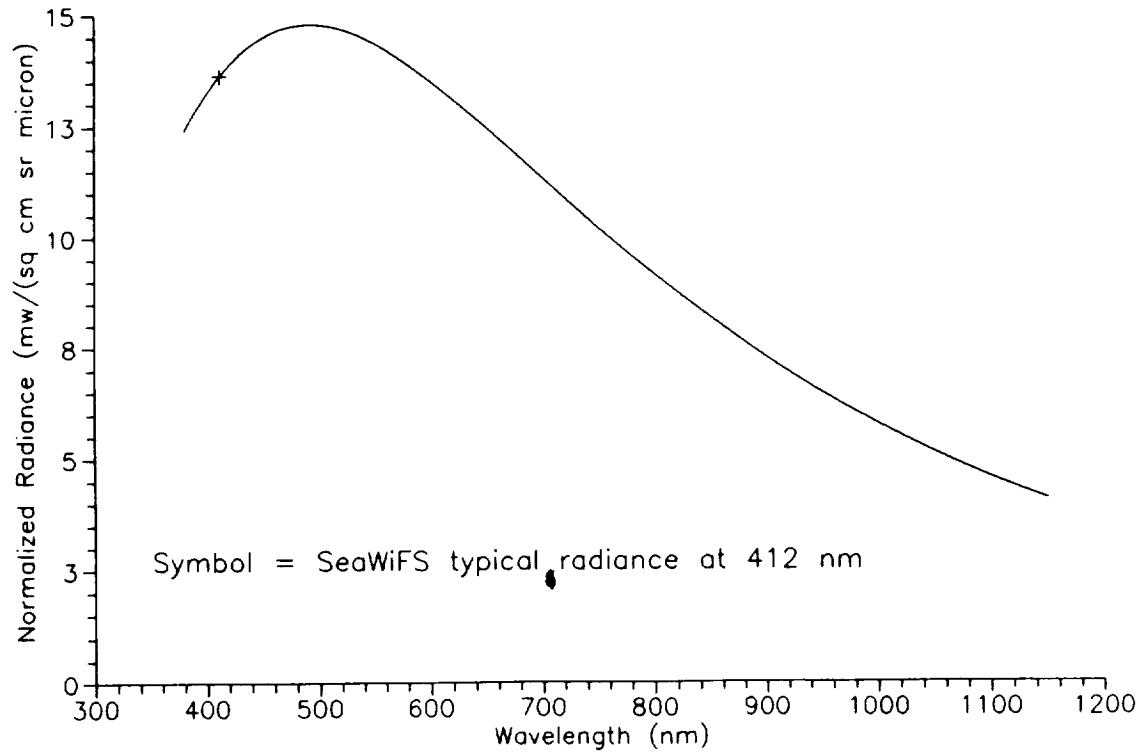


**Fig. 17.** Blackbody radiance curves normalized to the saturation radiance at 412 nm from the SeaWiFS specifications. The top panel shows the curve for a 5,900 K blackbody that approximates the solar spectrum. The bottom panel shows the curve for a 2,850 K blackbody that approximates the SBRC integrating sphere.

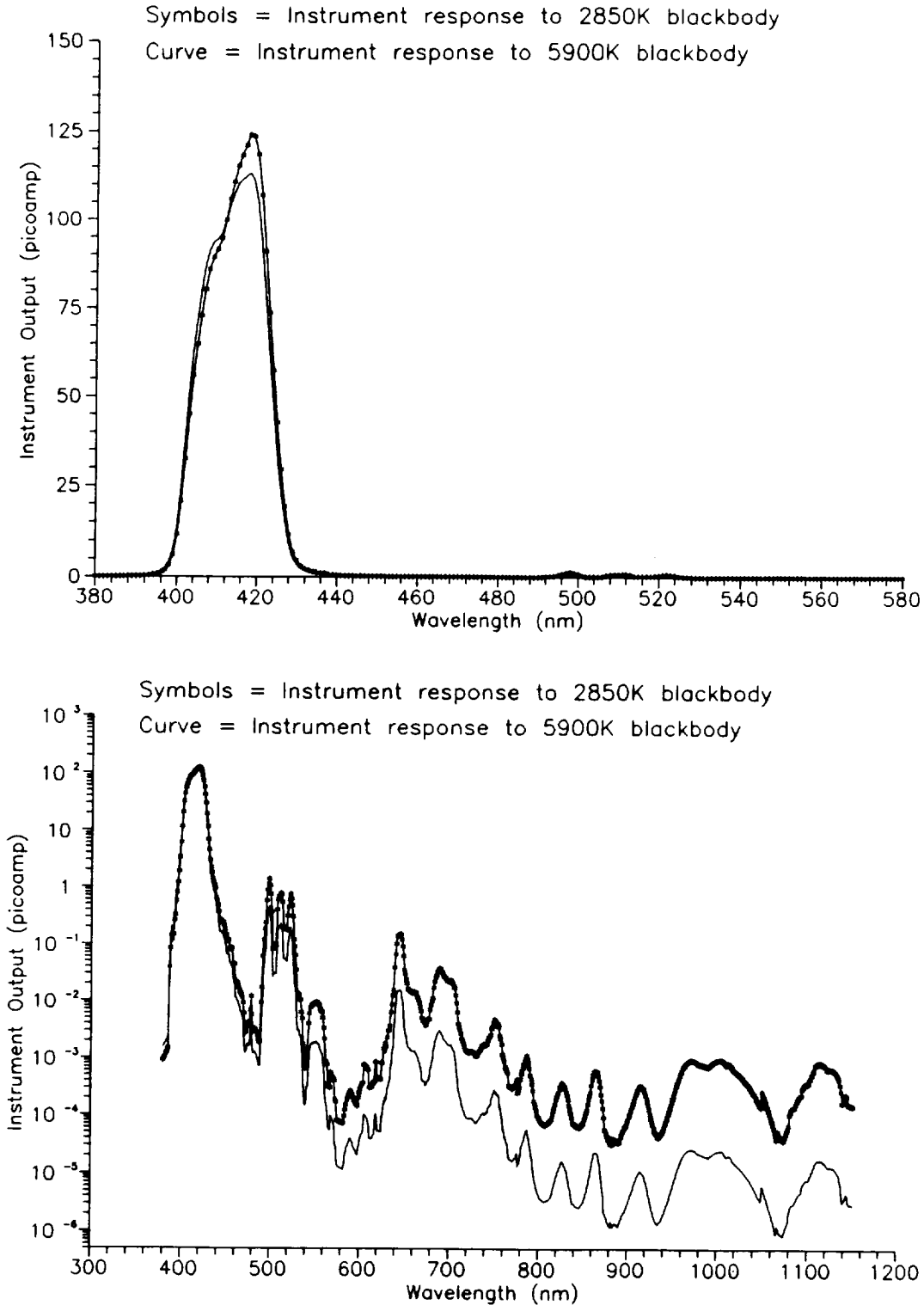


**Fig. 18.** Instrument output for the two blackbodies. The differences in the instrument's responses to the laboratory and flight sources are a factor in the on-orbit radiometric calibration of the SeaWiFS. The top panel shows the instrument output using a linear scale. This demonstrates the in-band differences from the two light sources. The bottom panel shows the instrument output using a logarithmic scale. This shows the out-of-band differences.

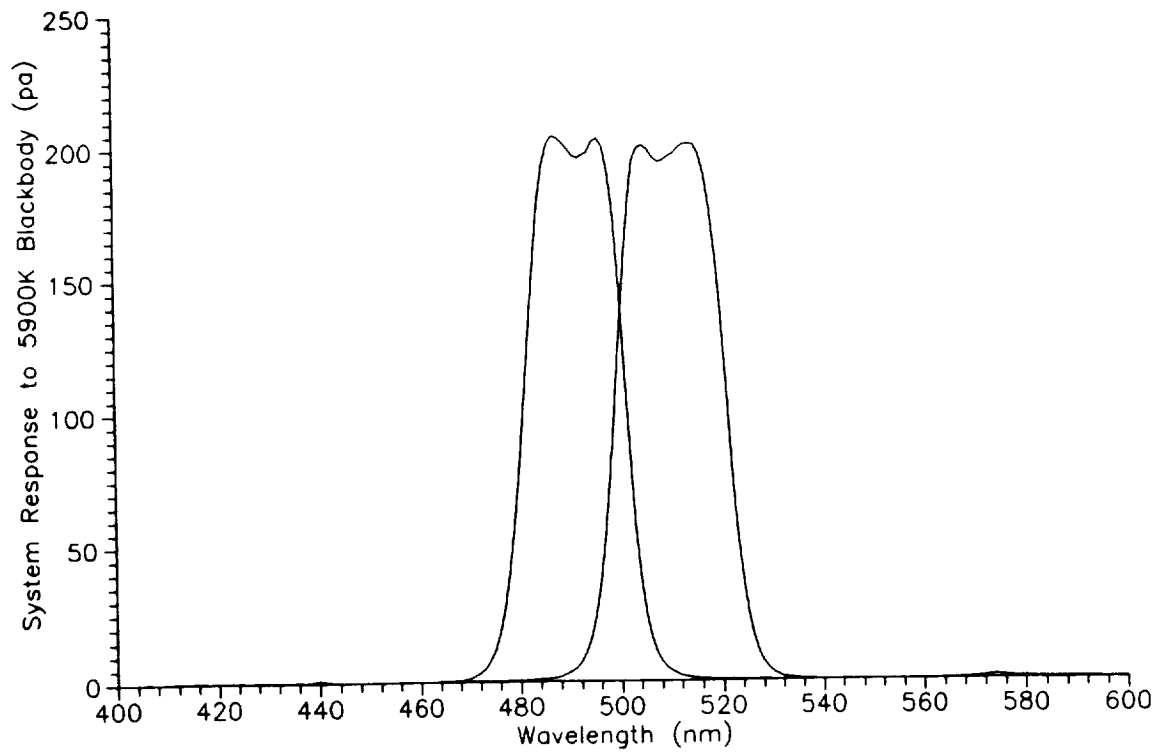
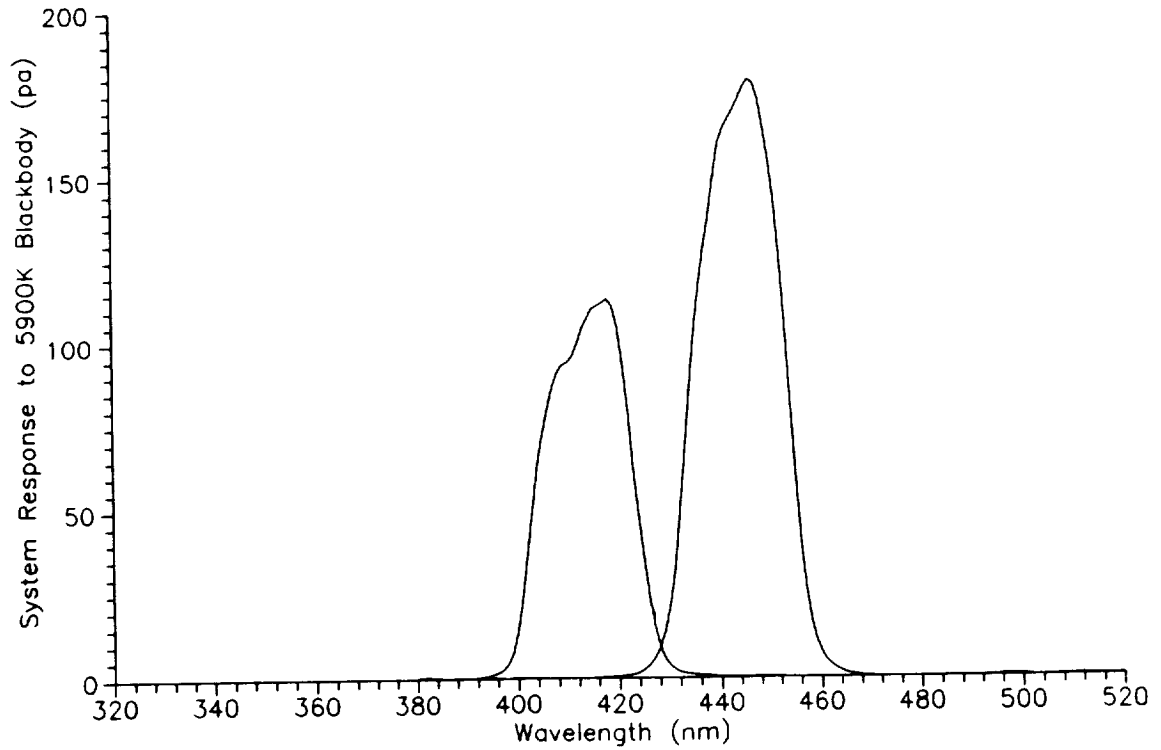


**Fig. 19.** Instrument output for the SeaWiFS bands. These are the responses of the instrument to a 5,900 K blackbody. The linear scale shows the in-band responses. The top panel shows Bands 1 and 2 (412 and 443 nm). The bottom panel shows Bands 3 and 4 (490 and 510 nm).

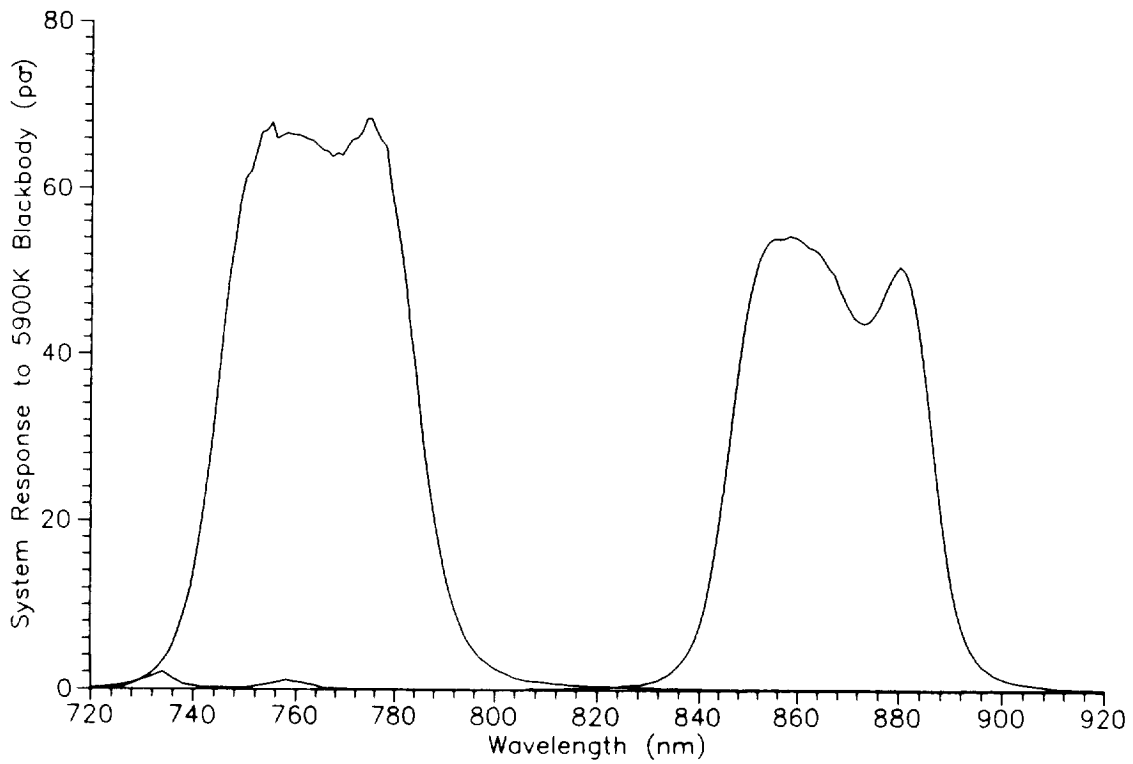
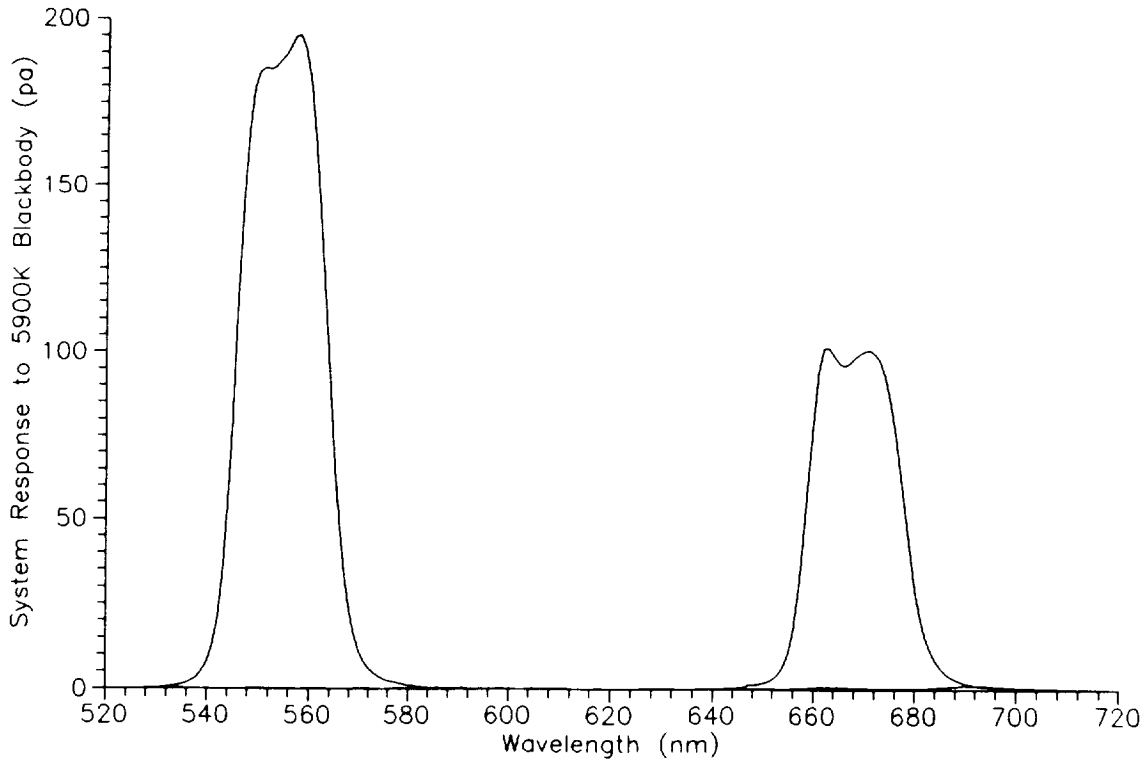


**Fig. 20.** Instrument output for the SeaWiFS bands. These are the responses of the instrument to a 5,900 K blackbody. The linear scale shows the in-band responses. The top panel shows Bands 5 and 6 (555 and 670 nm). The bottom panel shows Bands 7 and 8 (765 and 865 nm).

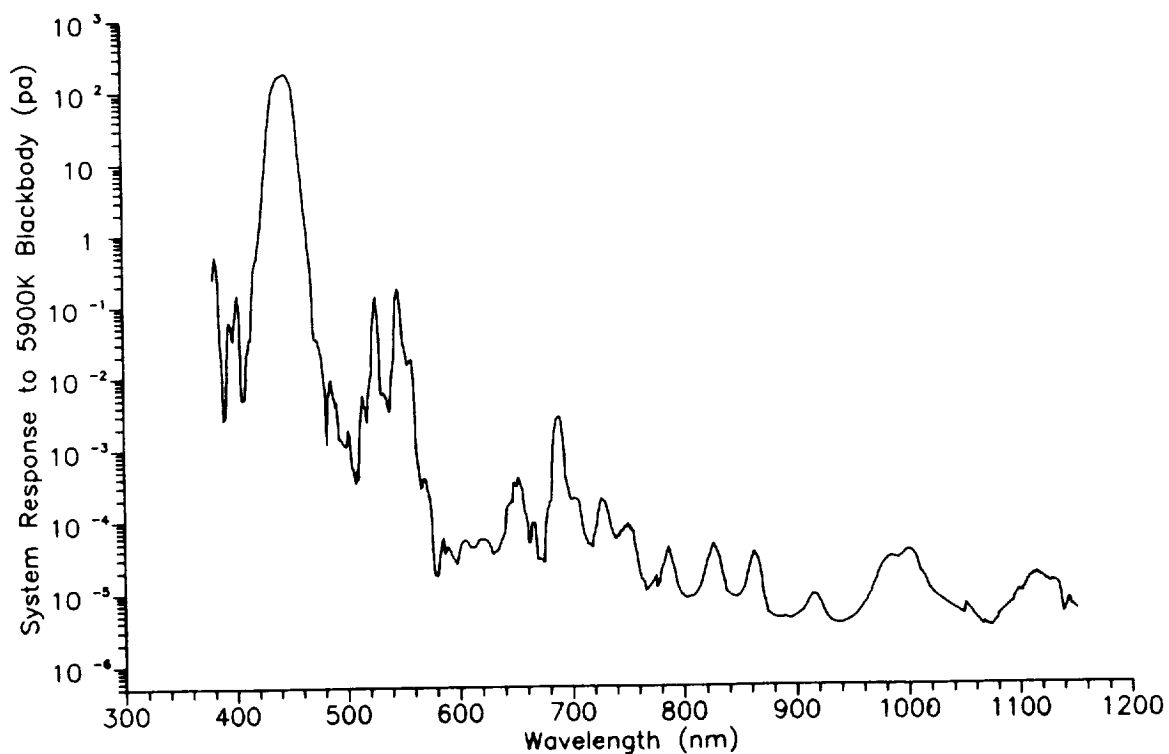
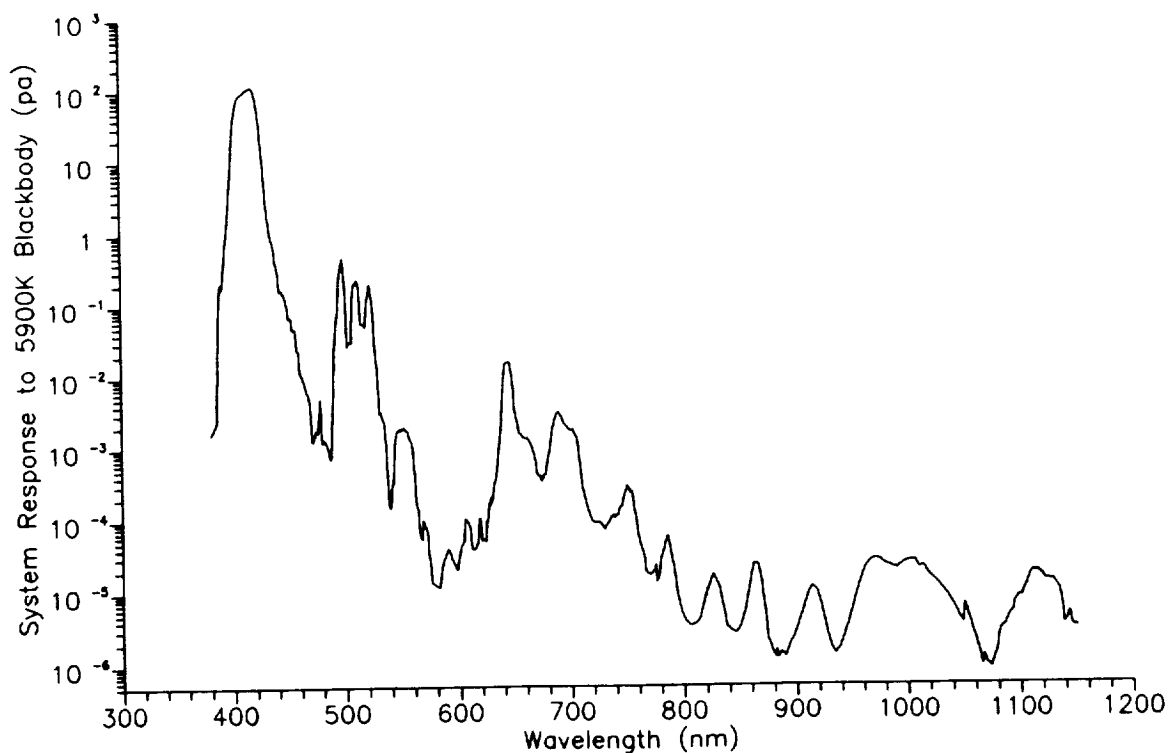


**Fig. 21.** Instrument output for the SeaWiFS bands. These are the responses of the instrument to a 5,900 K blackbody. The logarithmic scale shows the out-of-band responses. The top panel shows Band 1 (412 nm). The bottom panel shows Band 2 (443 nm).

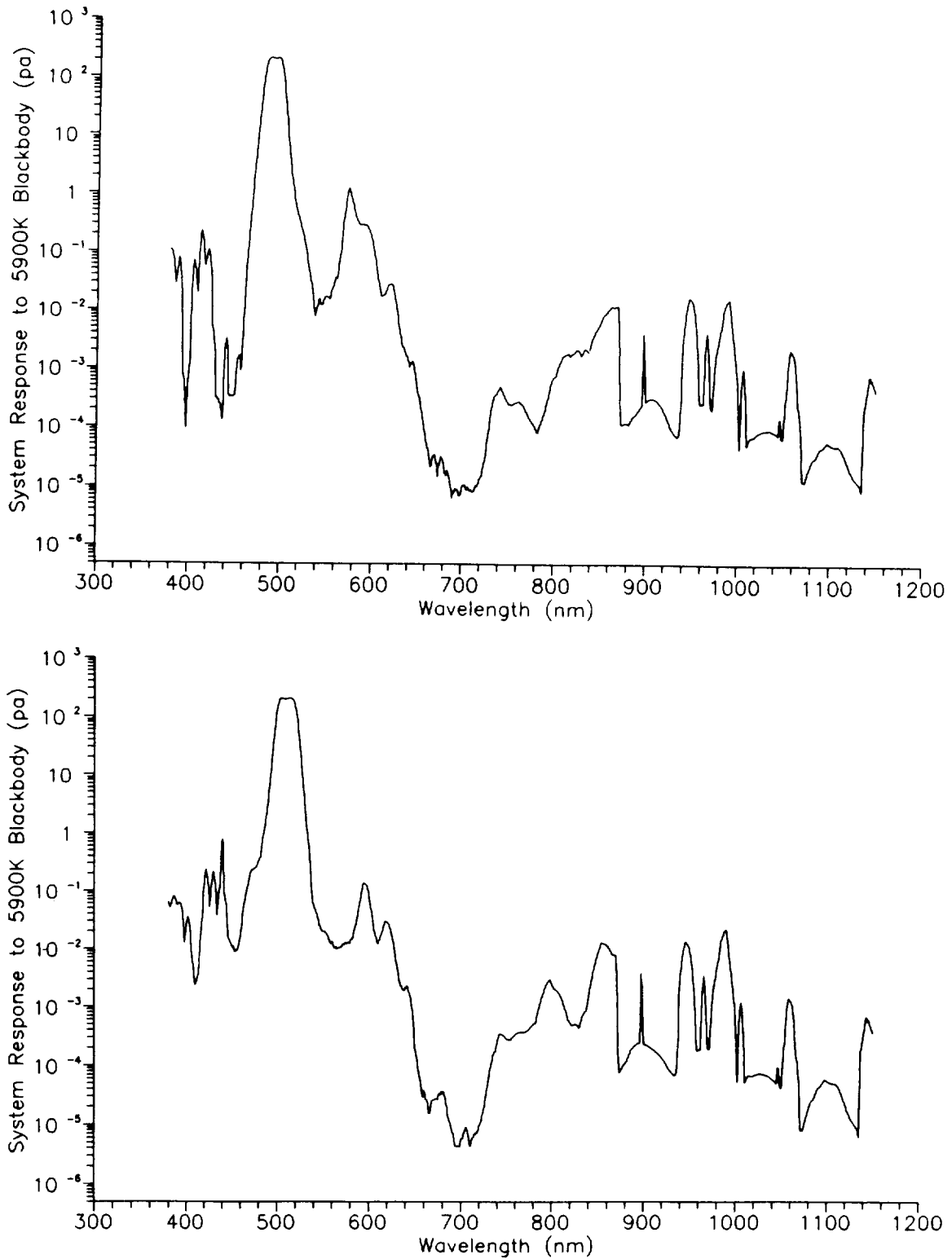


**Fig. 22.** Instrument output for the SeaWiFS bands. These are the responses of the instrument to a 5,900 K blackbody. The logarithmic scale shows the out-of-band responses. The top panel shows Band 3 (490 nm). The bottom panel shows Band 4 (510 nm).

## SeaWiFS Prelaunch Radiometric Calibration and Spectral Characterization

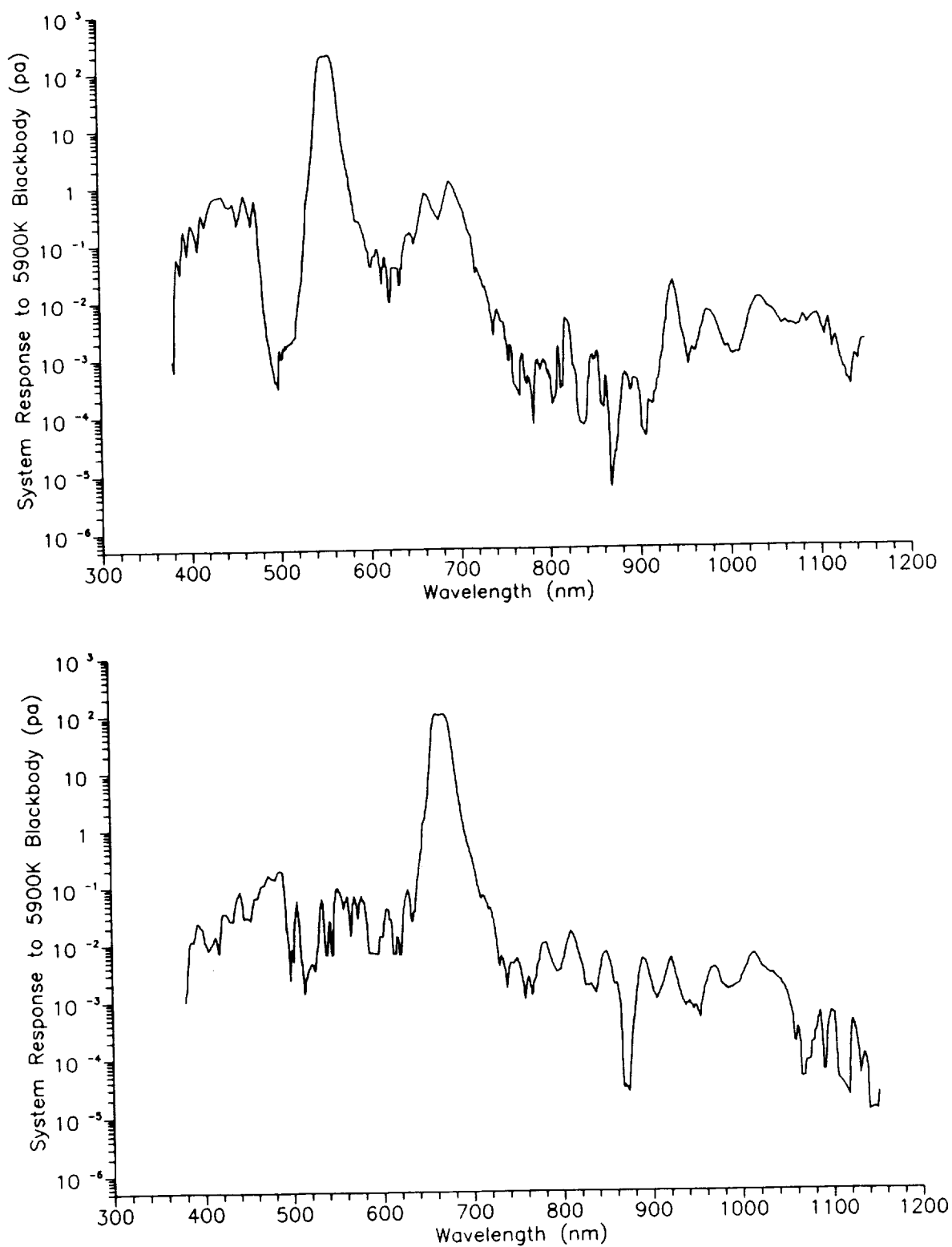


**Fig. 23.** Instrument output for the SeaWiFS bands. These are the responses of the instrument to a 5,900 K blackbody. The logarithmic scale shows the out-of-band responses. The top panel shows Band 5 (555 nm). The bottom panel shows Band 6 (670 nm).

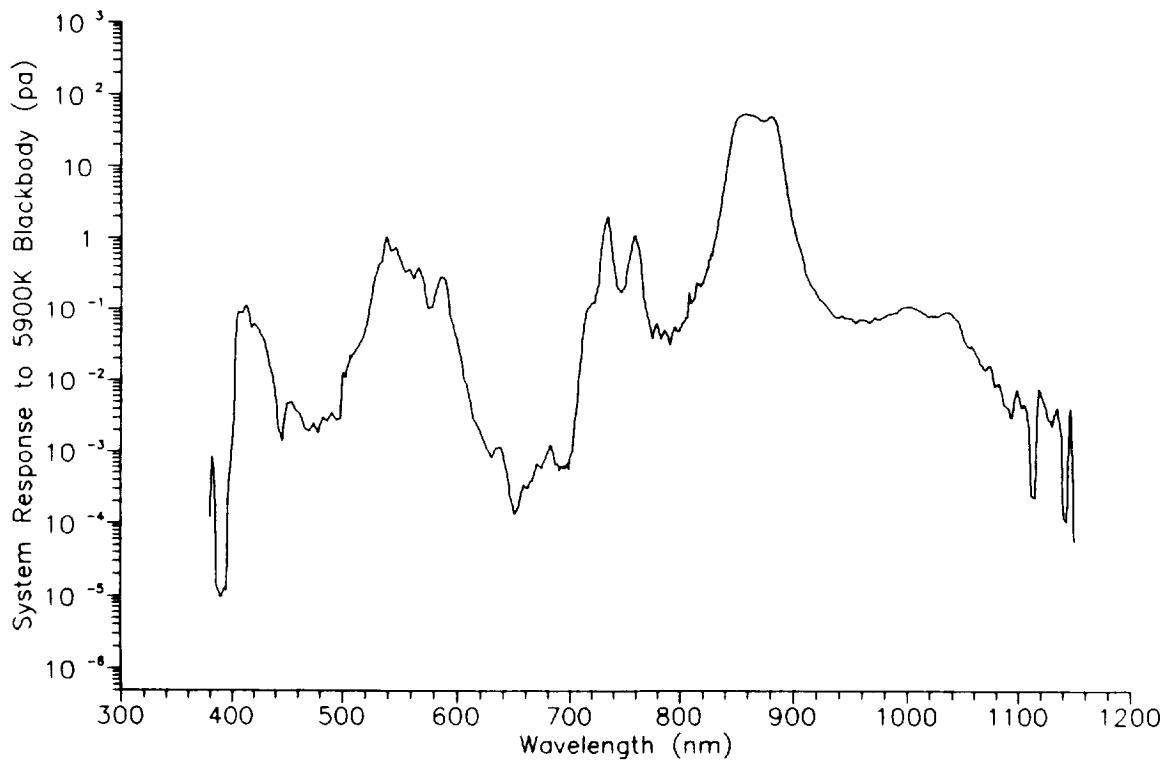
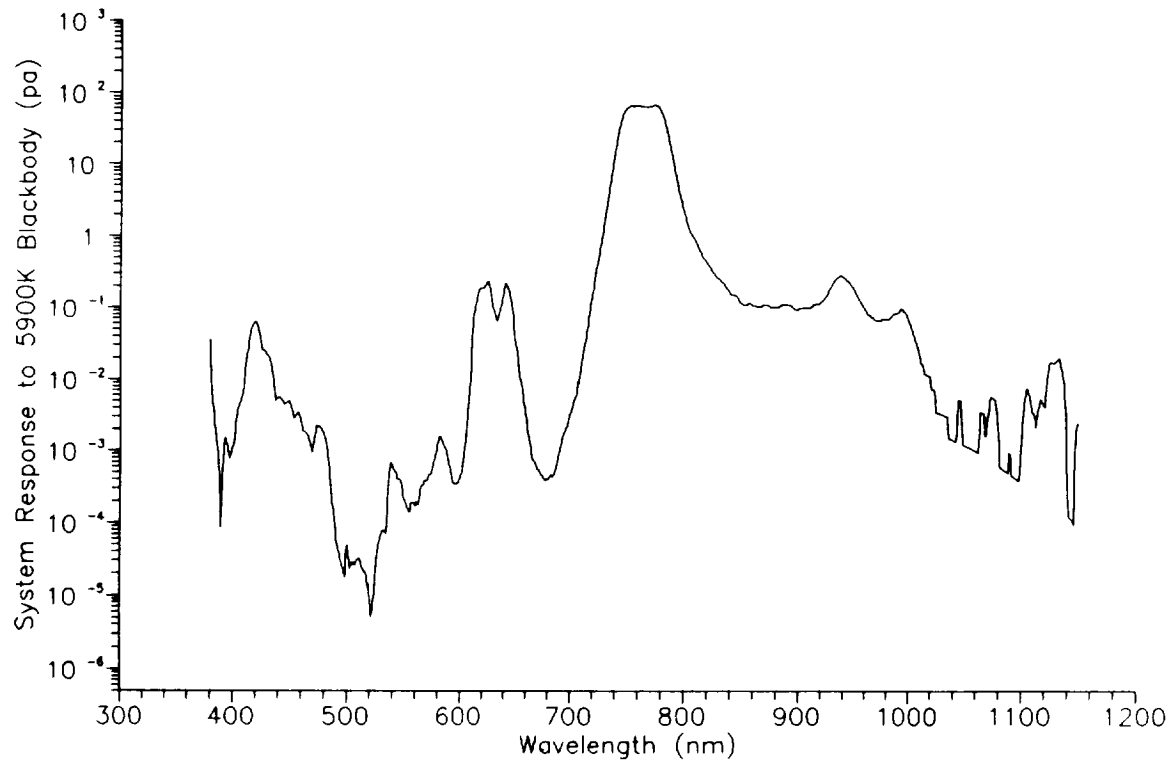


**Fig. 24.** Instrument output for the SeaWiFS bands. These are the responses of the instrument to a 5,900 K blackbody. The logarithmic scale shows the out-of-band responses. The top panel shows Band 7 (765 nm). The bottom panel shows Band 8 (865 nm).

the band's nominal center wavelength, 412 nm. For the overview of the responses of the eight SeaWiFS bands in this section, the response of the eight bands to a 5,900 K blackbody source, a source that approximates the solar spectrum will be shown. For each of the bands, the 5,900 K radiance has been normalized to the expected saturation radiance at that band's nominal central wavelength.

Figure 19 (top) gives the in-band responses for the 412 and 443 nm channels, and Fig. 21 gives their out-of-band responses. The plots in Fig. 21 show that the interference filters for the two bands exhibit similarities, especially evident in their out-of-band transmittances near 500–560 nm. The similarities between the filters seem reasonable, since their peak transmittances are only 30 nm apart. For bands 1 and 2, the components in the optical train—other than the interference filters—are the same, so the similarities in Fig. 21 come from the filters, themselves.

For band 1, and to a lesser extent for band 2, there has been a reduction in the blue side of the in-band response of the filter. This can be seen most easily in a comparison of the size of the left side transmission peak in the band 1 interference filter near 406 nm in Fig. 12 (top) with the corresponding system response peak in Fig. 15 (top). Both the mirror reflectances (Fig. 8, bottom) and the photodiode output (Fig. 11, top) act to trim the blue side of the output from the interference filter for band 1. Combined with the shape of the 5,900 K blackbody response near 412 nm (Fig. 17, top), these elements are responsible for the reduction in the portion of the peak nearest the blue end of the spectrum of band 1 in Fig. 19 (top). To a lesser extent, these elements are also responsible for the reduced blue side peak in the response of band 2. For both bands 1 and 2, the system responses are about one-half nanometer more to the red side than the responses of the interference filters.

The in-band responses for SeaWiFS bands 3 and 4 are shown in Fig. 19 (bottom), and the out-of-band responses are shown in Fig. 22. As was seen for bands 1 and 2, the out-of-band responses for bands 3 and 4 show marked similarities (Fig. 22). This is particularly true for the transmission curves for the 490 and 510 nm interference filters (not shown) above 800 nm. In this region, the interference filters transmit 70% to 80% of the incident radiation. However, the two dichroics in the optical path for these bands effectively remove most of this flux before it reaches the filters.

Figure 20 (top) gives the in-band responses for the 555 and 670 nm channels, and Fig. 23 gives their out-of-band responses. Figure 20 (top) shows an out-of-band leak between 690 and 700 nm. This peak and a second out-of-band peak around 450 nm are more clearly seen in Fig. 23. In relative terms, the out-of-band response of band 5 is just over twice that for band 6. The calculations of the out-of-band responses for the eight SeaWiFS bands are summarized in Section 12.0.

The in-band responses for SeaWiFS bands 7 and 8 are shown in Fig. 20 (bottom), and the out-of-band responses are shown in Fig. 24. These bands have been designed with twice the spectral widths of the other SeaWiFS bands. The small scale structure, i.e., the lack of smoothness in the peak of the curve for band 7 (765 nm) is an artifact of the measurement of the band's interference filter by SBRC. Interference filters of the type used in SeaWiFS exhibit a much smoother spectral response. Band 8 (865 nm) shows the greatest out-of-band leakage for the SeaWiFS set, both in absolute and relative terms. However, its 3.7% out-of-band response is well within the 5% maximum value in the SeaWiFS performance specifications.

Figures 21–24 shows the output of the photodiodes for each SeaWiFS band in picoamperes per nanometer (from 380–1,150 nm). The actual current from the photodiode is the sum of the band output over the entire wavelength range. The photodiode serves to integrate the instrument's spectral response. The integrals, i.e., summations, of the spectral responses of the eight SeaWiFS bands are given in Table 12. These summations are given for the responses to a 5,900 K blackbody (Figs. 21–24) and to a 2,850 K blackbody (not shown). In the calculations for each band, both sources give the saturation radiance for the band at the band's nominal center wavelength (for band 1, 13.63 mW at 412 nm; for band 2, 13.25 mW at 443 nm; and so forth).

Table 12 also provides factors which allow conversion between the 2,850 K light source used in the laboratory and a 5,900 K source that mimics the sun. For band 1 (Table 12), the output of the photodiode in response to a 5,900 K source is almost 4% less than the output in response to a 2,850 K source. Correction factors, similar to the ones in Table 12, must be used in the transfer of the laboratory radiometric calibrations to orbit.

The out-of-band responses for the eight SeaWiFS bands are part of the instrument's radiometric calibration. In that calibration, the instrument views a broad area of known radiance, and records the output from the bands in counts. The counts from each band include the out-of-band contributions which are functions of the spectral shape of the source that is measured. The SeaWiFS laboratory calibration has the out-of-band correction for a 2,850 K source factored into its results. If the instrument measures a source with that spectral shape, those measurements automatically contain the appropriate out-of-band corrections.

The prelaunch calibration equations for SeaWiFS contain correction terms that convert the out-of-band responses from those for a 2,850 K source to those for a 5,900 K source. As a result, the SeaWiFS calibration equations now have the out-of-band correction for a 5,900 K source factored into them. The 5,900 K spectral shape duplicates the spectral shape for SeaWiFS ocean measurements closely. The errors that arise from the use of the 5,900 K

**Table 12.** Integrated instrument responses for the eight SeaWiFS bands. The results are given for responses in nanoamperes to 2,850 K and 5,900 K blackbody radiance sources. The radiances for the blackbody sources are normalized to the expected saturation radiance for each band at the nominal center wavelength for each band. The conversion factor gives a fractional multiplier to convert the laboratory instrument response using a 2,850 K blackbody to the response on orbit using a 5,900 K source. These results are calculated over the wavelength range from 380–1,150 nm.

Band	Response to 2,850 K Source [nA]	Response to 5,900 K Source [nA]	Conversion Factor	Normalization Wavelength [nm]	Normalization Radiance [mW cm <sup>-2</sup> sr <sup>-1</sup> μm <sup>-1</sup> ]
1	2.275	2.190	0.963	412	13.63
2	3.493	3.435	0.983	443	13.25
3	4.424	4.336	0.980	490	10.50
4	4.624	4.613	0.998	510	9.08
5	3.749	3.717	0.991	555	7.44
6	2.069	2.092	1.011	670	4.20
7	2.875	2.859	0.995	765	3.00
8	2.249	2.274	1.011	865	2.13

out-of-band corrections for ocean measurements are estimated to be small, or a few tenths of a percent. If an alternate out-of-band correction is to be used, then the 5,900 K correction must be removed from the measurement results and a new out-of-band correction inserted in its place.

## 10. SYSTEM LEVEL RESPONSE

System level measurements of the spectral response of SeaWiFS were made using a 0.5 m monochromator, illuminated with a 100 W halogen lamp, as a light source. The slits on the monochromator were adjusted to give a spectral resolution for the source (full width at half maximum) of 0.9 nm at 546 nm. The wavelength accuracy of the monochromator was checked using five emission lines, in first and second order, from a mercury lamp.

The relative output energy from the monochromator was measured using a photodiode with a known quantum efficiency, i.e., with a known number of mA of current out per mW of radiant flux in. The output of this photodiode, after amplification and conversion to mW of radiant energy, is shown in Fig. 25. No effort was made to determine the complete set of geometric (goniometric) factors in the illumination of the calibrated photodiode, such as the area of illumination of the diode and the solid angle of the illuminating light. Figure 25 gives relative values, only. Since the comparisons in this section are of spectral responses normalized to 100%, the calculation of absolute radiances is not necessary.

In previous sections, the calculated piece part results for the SeaWiFS bands were convolved with the spectral shapes of blackbody sources to give the responses of the instrument to laboratory and solar spectra. For the comparisons in this section, the shape of the halogen lamp and monochromator light source must be removed from the system level measurements of the SeaWiFS bands. This is done by dividing the output of the bands by the values in

Fig. 25 and normalizing the result to 100%. This gives the system level response to a light source that is spectrally flat over the wavelength range from 380–1,100 nm. For the piece part measurements, the responses to a spectrally flat source have also been calculated (Fig. 15).

Data from the SeaWiFS instrument in the system response tests has been taken from the output of the preamplifiers for each band. These voltages have been amplified with a lock-in amplifier and digitized with a 12 bit ADC. This modification to data acquisition gives the tests a sensitivity to low light levels that is orders of magnitude better than the resolution of the standard digital output from the sensor. Piece part calculations, however, still give results that are one to two orders of magnitude more sensitive than the minimum detectable limit of the system level measurements.

The piece part and the system level spectral response curves for the eight SeaWiFS bands are shown in Figs. 26 and 27. The system level measurements have been made over 60 nm wavelength ranges, centered for each band's nominal pass band. In Figs. 26 and 27, the piece part wavelength ranges have been trimmed to the same ranges as the system level results. For this reason, the spectral curves for bands 7 and 8 float above the horizontal axis in Fig. 27 (bottom). The system level measurements for bands 7 and 8 do not come down to the abscissa.

The band edge values from the piece part and system level measurements are given in the next section. All of the band edges, which give the full width at half maximum for the spectral response, are within 1 nm for the two sets of measurements here—with the exception of two, the lower band edges for band 3 and band 7 (Fig. 26, bottom, and Fig. 27, bottom). In all cases, however, each band edge measurement is within the performance specifications for the instrument.

The shapes of the peaks for the two measurement sets show differences. Requirements for these shapes are not

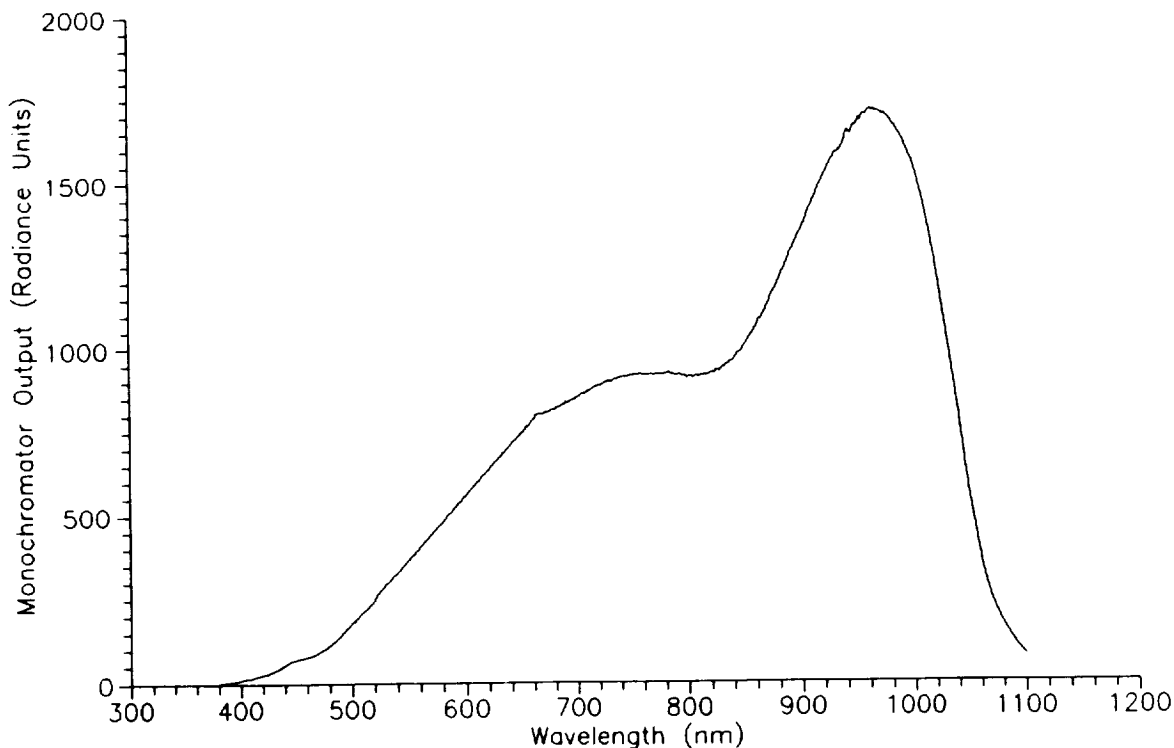


**Fig. 25.** Spectral shape of the light source for the system level spectral response Measurements. The curve gives the output of a photodiode with known quantum efficiency which is illuminated by the output slit of the monochromator. Geometric (goniometric) factors, such as the illuminated area of the photodiode, are not included in the calculation of the curve, so absolute radiance values are not given in the ordinate for the graph.

part of the SeaWiFS specifications. Both the piece part and the system level results are within the requirements of the specifications, and the measurement sets are final and will not be repeated. The most reasonable explanation for the differences is that the system level measurements have been made with the flight filters, and the piece part measurements have been made with filters from flight spares that have come from the same lot as the flight parts.

During the thermal vacuum testing of SeaWiFS, in the spring of 1993, the focal plane assembly for bands 5 and 6 was replaced due to an electrical problem. When the interference filter for band 5 was removed from the old focal plane assembly, it was chipped. A replacement filter was placed in the new assembly. The system level measurements for bands 5 and 6 were not repeated after thermal vacuum testing. As a result, the system level measurements for band 5 no longer represent the actual flight unit but represent a band with an interference filter that has come from the same lot as the flight part, like the piece part measurements.

For band 1 (Fig. 26, top), the shape of the system level spectral response resembles the transmission curve for the 412 nm interference filter (Fig. 12, top). It seems likely that the model for the mirror reflectances (Fig. 8, bottom) shows too sharp a reduction in reflectance at the lowest wavelengths. Such an effect would remove too much of the blue side of the piece part results in Fig. 26 (top).

There are differences between the piece part and the system level response curves. The piece part results are considered prime, and the system level measurements are considered backup checks. The differences between the two sets of measurements are sufficiently small, and the system level results verify the piece part results. The comparison of the out-of-band measurements for the eight bands are given in Figs. 28–31. The comparisons are given for the responses to a spectrally flat radiance source. This is the arrangement used to calculate the band edges to check agreement with the SeaWiFS performance specifications. Figures 28–31 show the limited dynamic range for the system level measurements. To improve the sensitivity of the

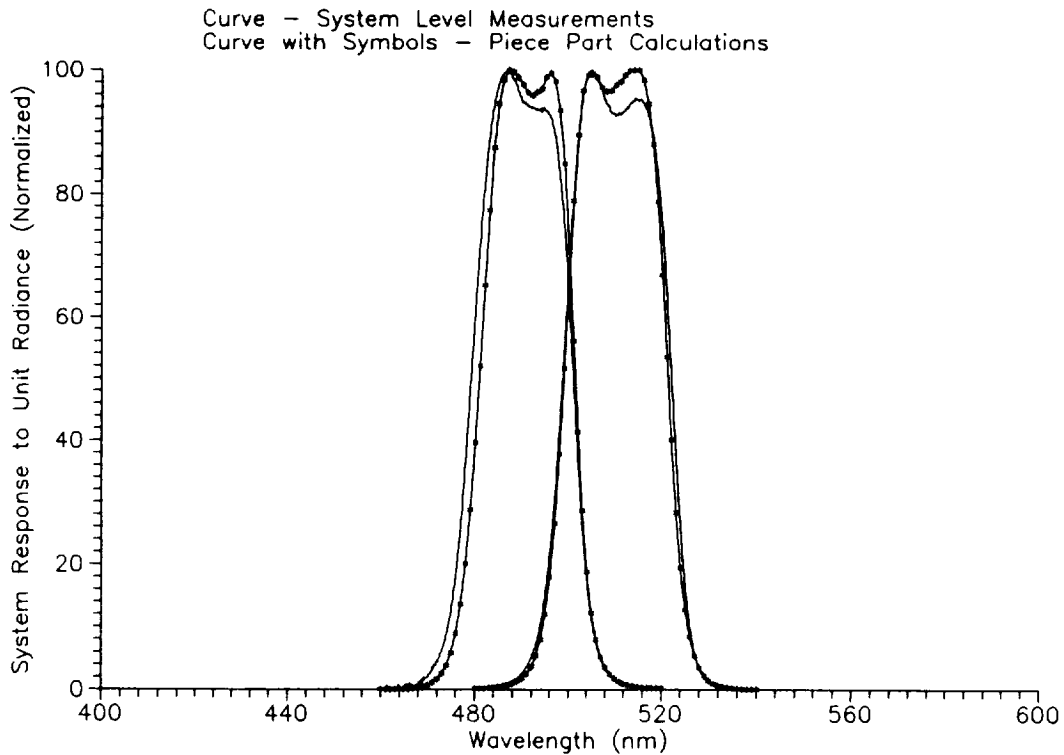
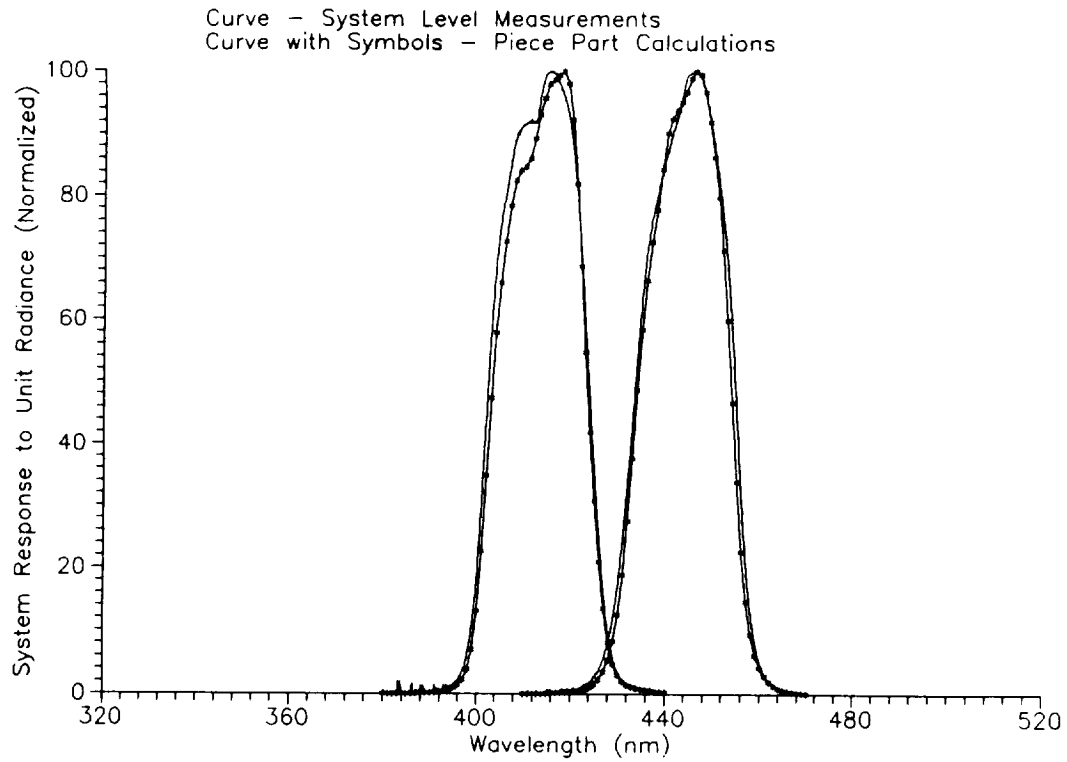


**Fig. 26.** Spectral responses for the SeaWiFS bands. The curves show the response of the bands to a spectrally flat source as measured at the system level and as calculated from piece part measurements. The responses are normalized to 100%. The top panel shows Bands 1 and 2 (412 and 443 nm). The bottom panel shows Bands 3 and 4 (490 and 510 nm).

## SeaWiFS Prelaunch Radiometric Calibration and Spectral Characterization

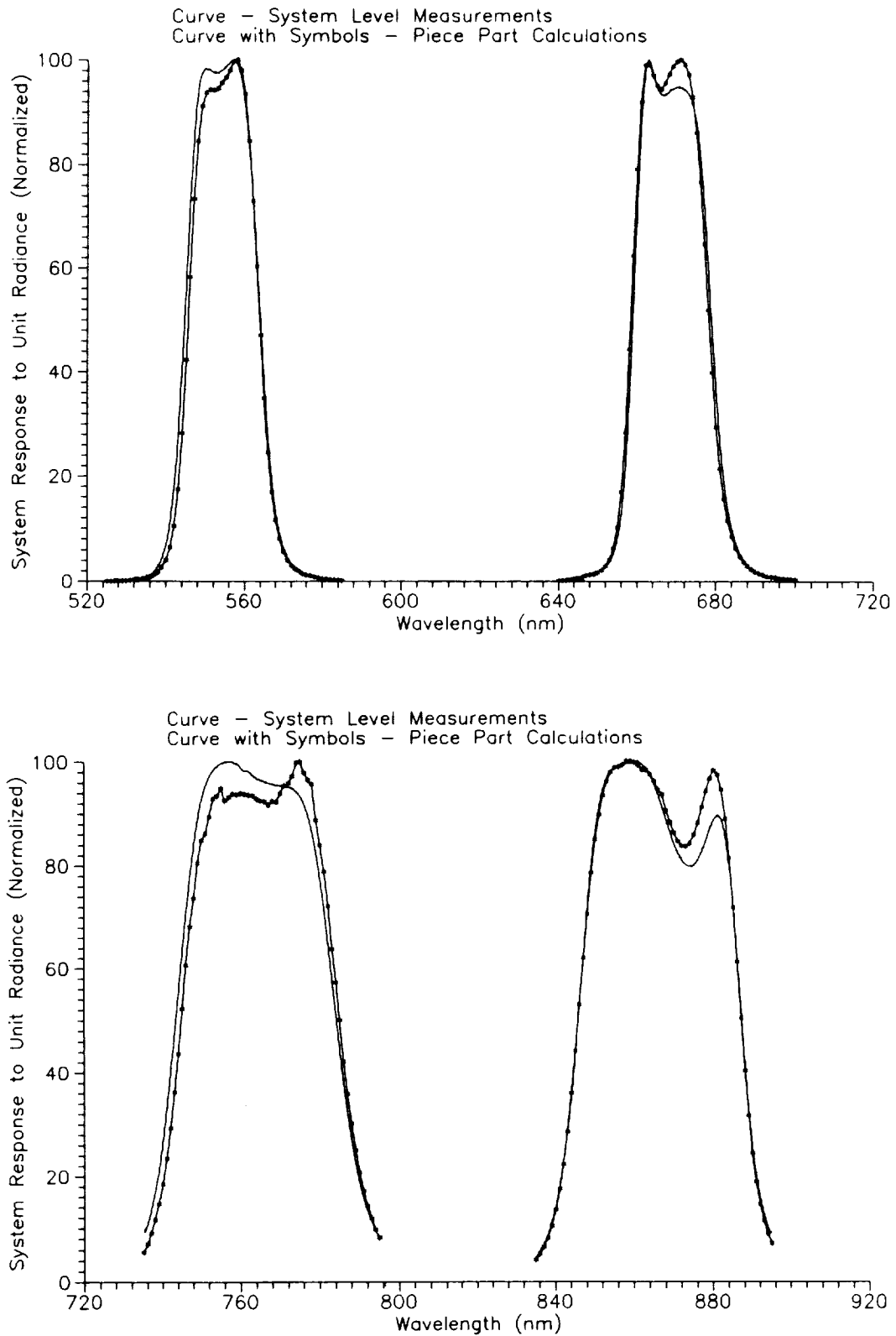


**Fig. 27.** Spectral responses for the SeaWiFS bands. The curves show the response of the bands to a spectrally flat source as measured at the system level and as calculated from piece part measurements. The responses are normalized to 100%. The top panel shows Bands 5 and 6 (555 and 670 nm). The bottom panel shows Bands 7 and 8 (765 and 865 nm).

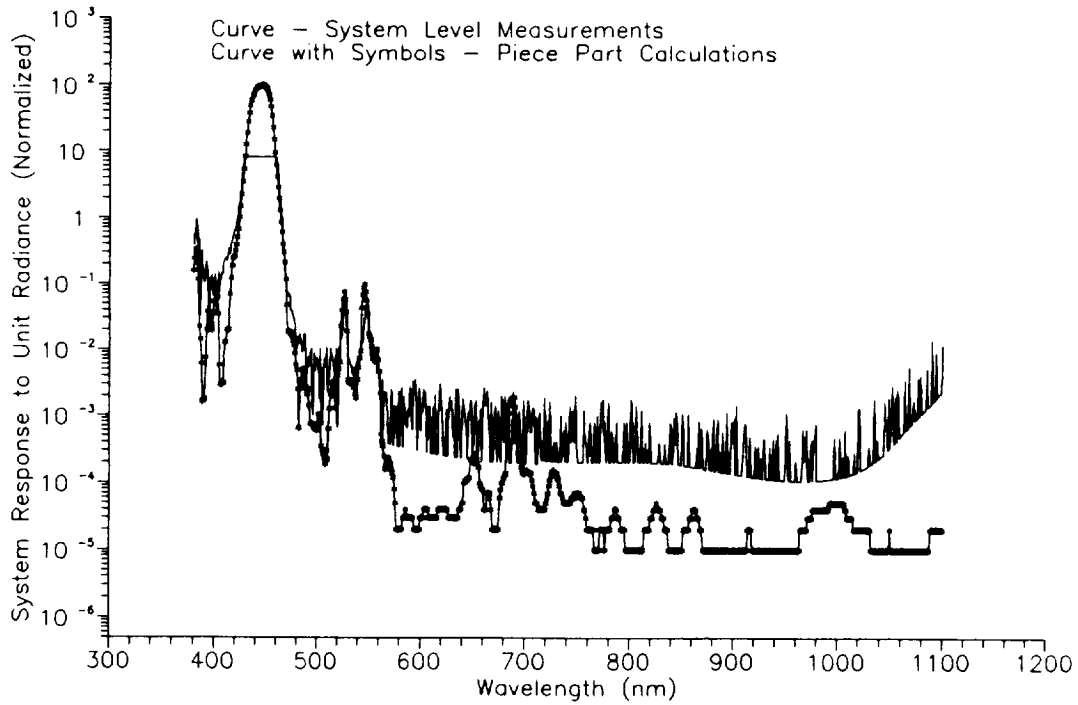
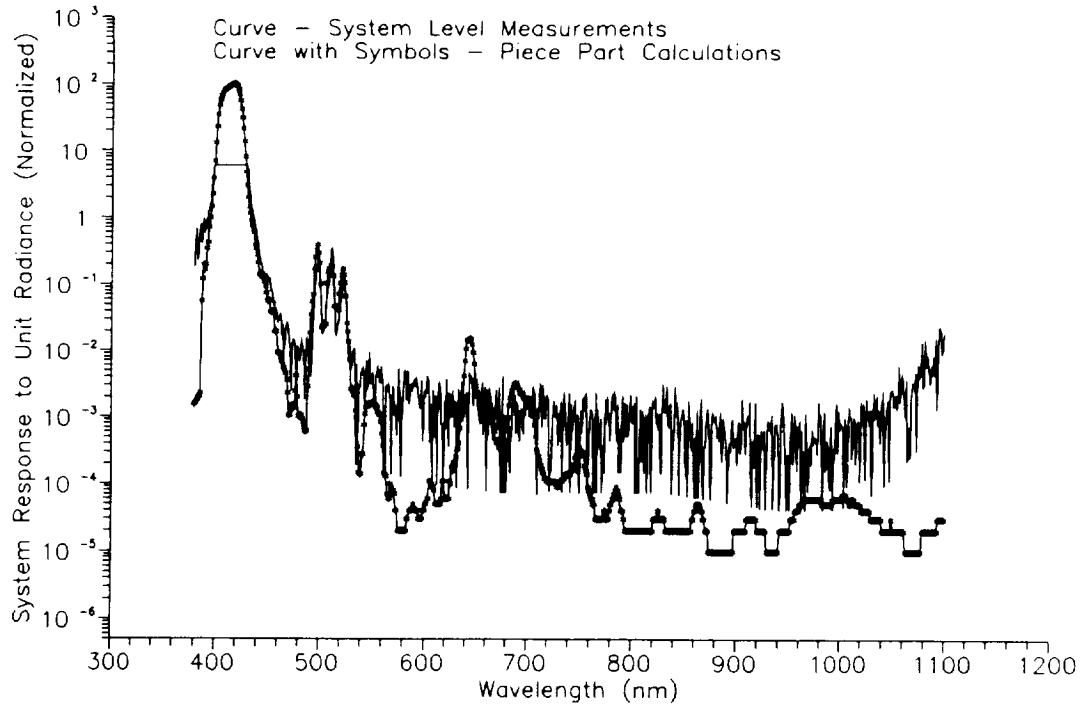


**Fig. 28.** Out-of-band measurements for the SeaWiFS bands. The curves show the response of the bands to a spectrally flat source as measured at the system level and as calculated from piece part measurements. The responses are normalized to 100%. The top panel shows Band 1 (412 nm). The bottom panel shows Band 2 (443 nm).

## SeaWiFS Prelaunch Radiometric Calibration and Spectral Characterization

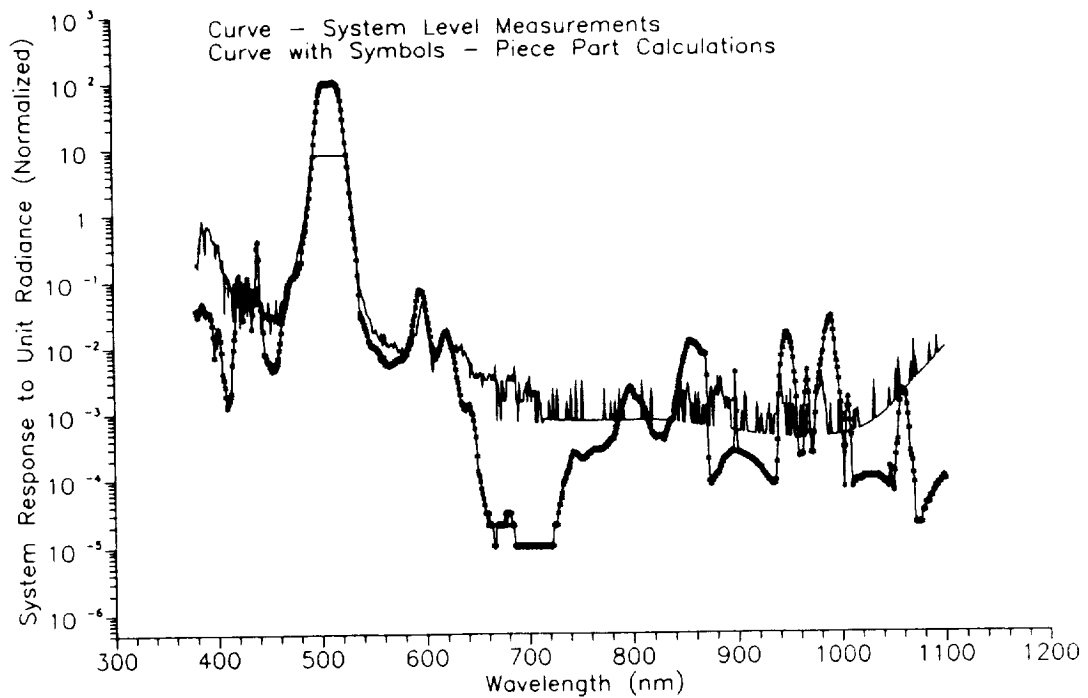
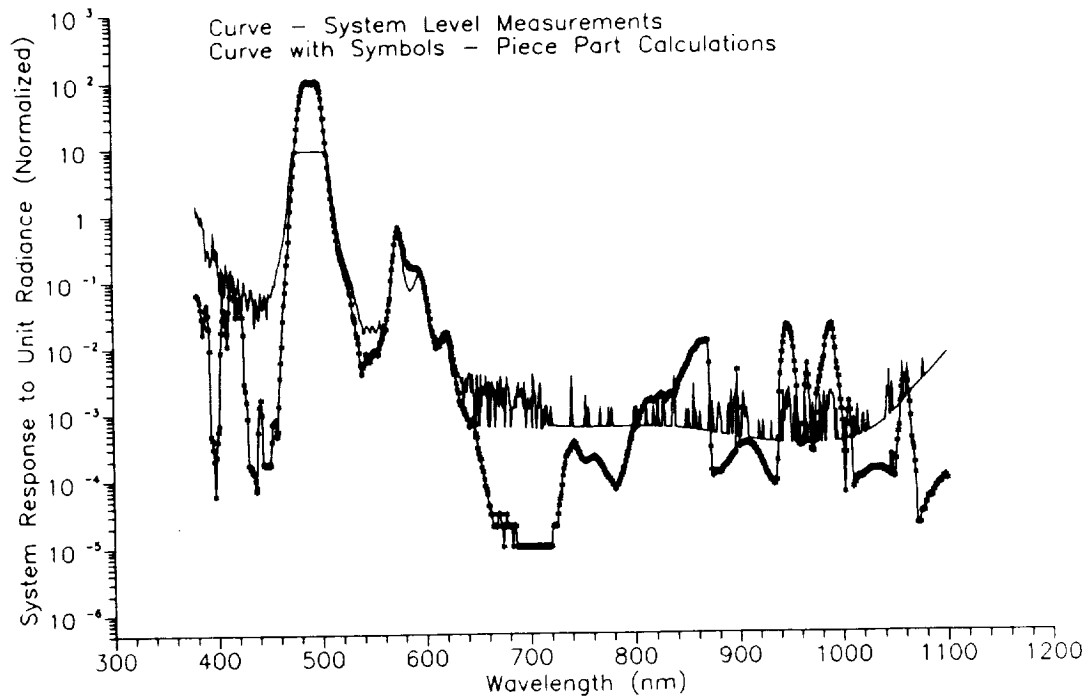


**Fig. 29.** Out-of-band measurements for the SeaWiFS bands. The curves show the response of the bands to a spectrally flat source as measured at the system level and as calculated from piece part measurements. The responses are normalized to 100%. The top panel shows Band 3 (490 nm). The bottom panel shows Band 4 (510 nm).

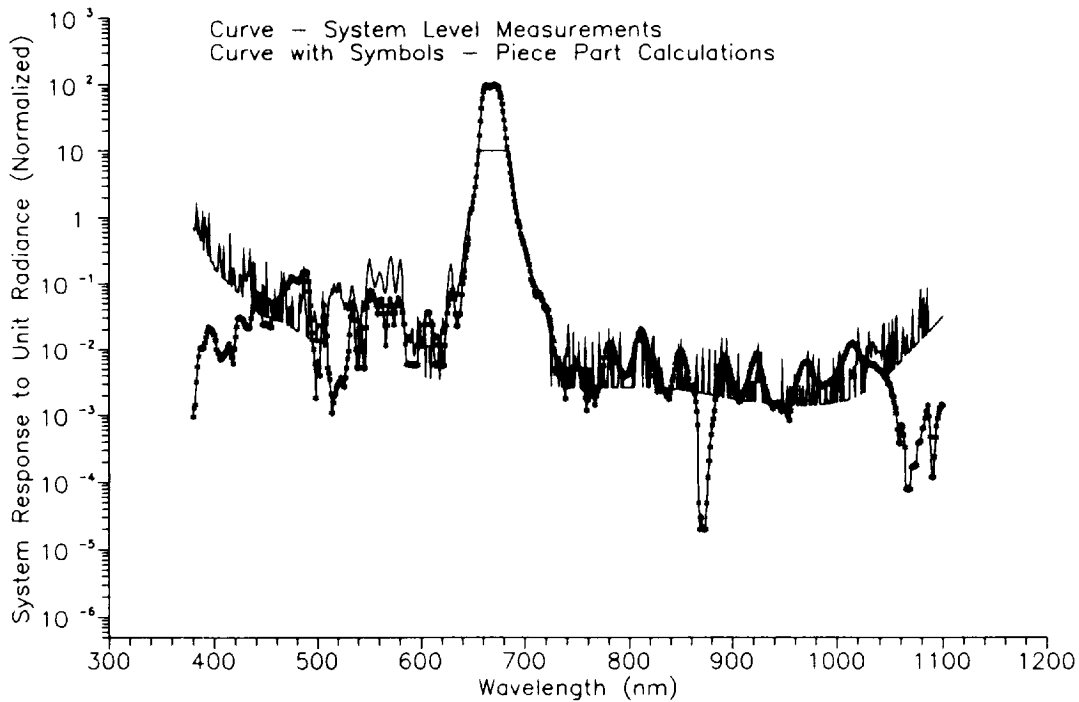
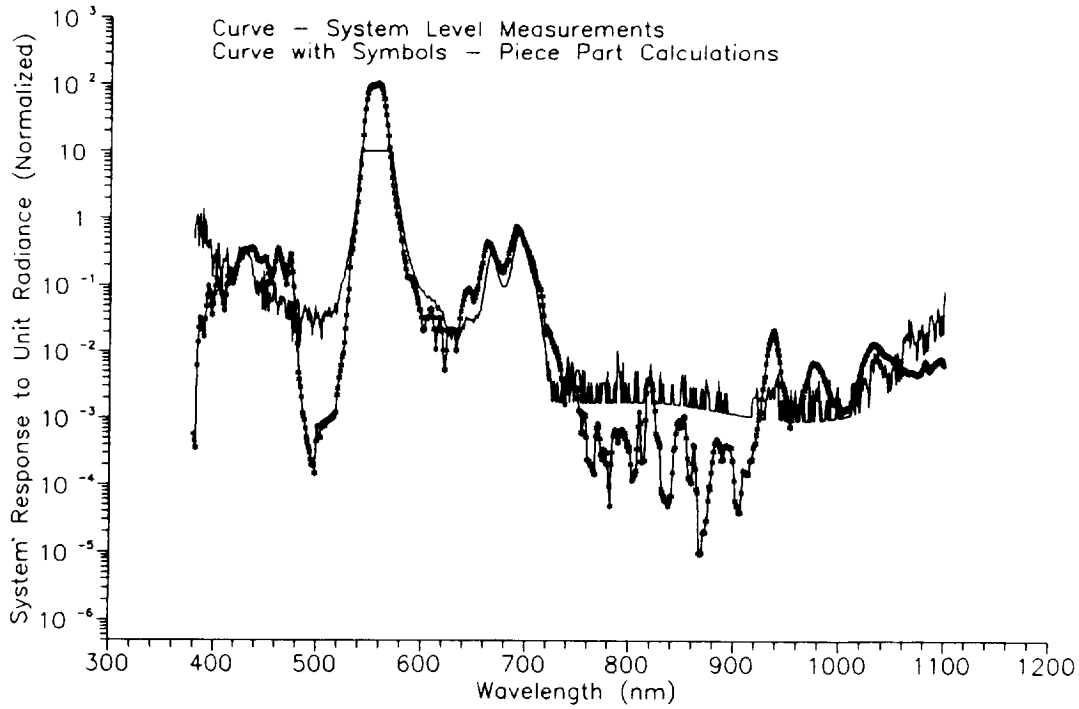


**Fig. 30.** Out-of-band measurements for the SeaWiFS bands. The curves show the response of the bands to a spectrally flat source as measured at the system level and as calculated from piece part measurements. The responses are normalized to 100%. The top panel shows Band 5 (555 nm). The bottom panel shows Band 6 (670 nm).

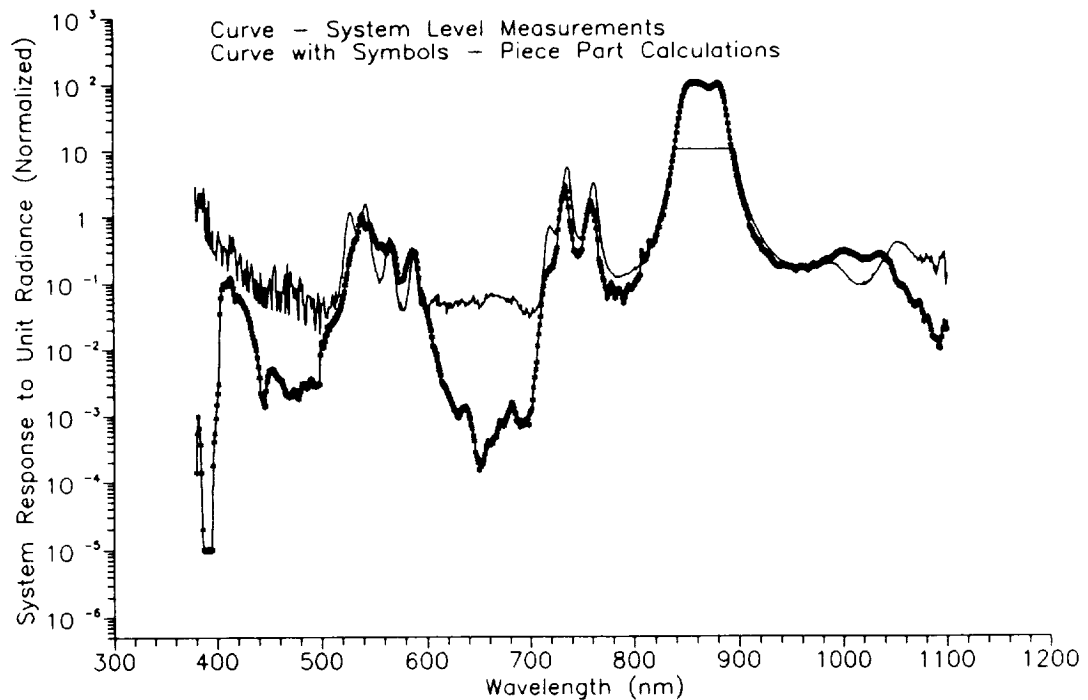
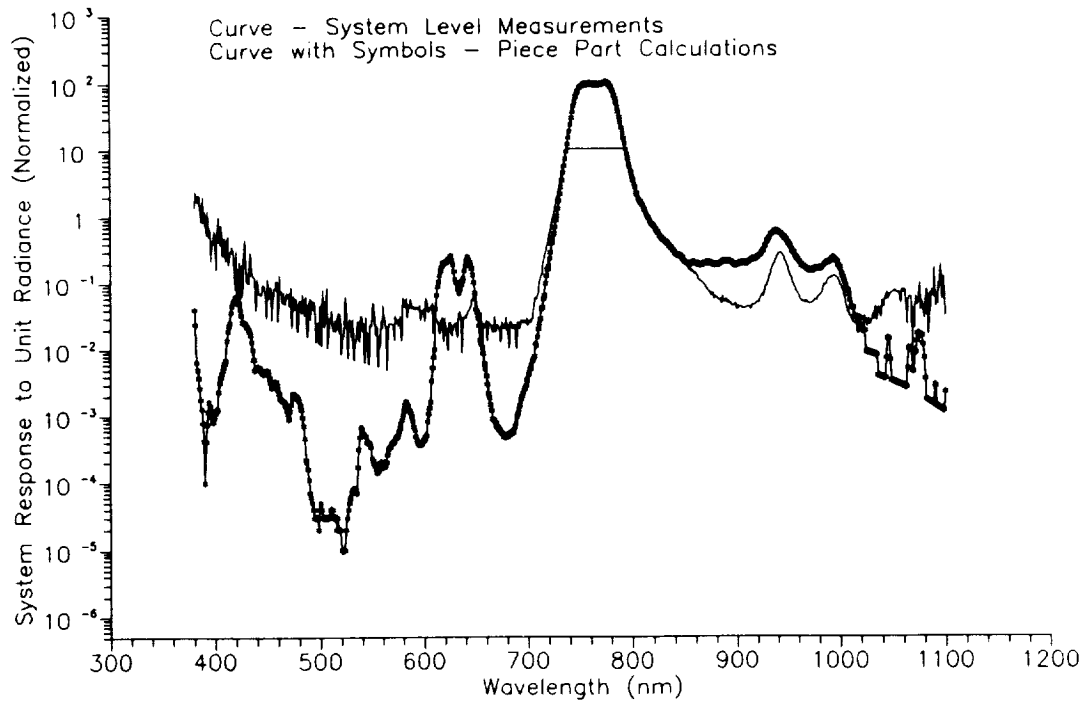


**Fig. 31.** Out-of-band measurements for the SeaWiFS bands. The curves show the response of the bands to a spectrally flat source as measured at the system level and as calculated from piece part measurements. The responses are normalized to 100%. The top panel shows Band 7 (765 nm). The bottom panel shows Band 8 (865 nm).

system measurements, the lock-in amplifier was set to saturate at about 10% of the full-scale output for each band. The lower limit for the system level measurements, for instance, the output from 600–1,100 nm in Fig. 28 (bottom), has been set at one count in these figures. Where the actual output of the lock-in amplifier was zero or negative in the measurements, they have been set to one count in this presentation. One count sets the resolution limit for the system level measurements.

Above the resolution limit for the system level measurements, there are structures in the piece part results that are not seen in the output from the lock-in amplifier. In general, these differences are at levels that are four to five orders of magnitude below the peak transmission of the bands. Again, the differences in the two sets of measurements are sufficiently small that the system level results verify the piece part results.

## 11. BAND EDGE WAVELENGTHS

The band edge measurements are given for the wavelengths at which the instrument response equals half that at the peak. The extended band edges give the points at which the output is 1% of the peak. The results (Table 13) come from the data sets that make up the sets of figures in this memorandum. The results from the piece part calculations are given for three source spectral shapes which are a spectrally flat source, a 5,900 K blackbody, and a 2,850 K blackbody.

Table 13 includes the band edge calculations for the piece part measurement of each interference filter, plus the values from the system level measurements. For the system level measurements, the spectral shape of the monochromator light source has been removed. Thus, the system level measurements are equivalent to the measurement of piece part values using a spectrally flat light source. Since the data in the measurement sets are tabulated at one nanometer intervals, the values in Table 13 have been obtained by linear interpolation.

## 12. OUT-OF-BAND RESPONSE

The values in Table 14 are based on the measurements shown in Figs. 21–24. The locations of the upper and lower extended band edges come from Table 13. All of the values in Table 14 come from the piece part calculations for the SeaWiFS bands as illuminated by a 5,900 K blackbody. This is the arrangement set forth in the SeaWiFS performance specifications (Barnes et al. 1994).

Figures 21–24 give the response of the instrument in picoamperes per nanometer. Table 14 gives the following sums of these responses over three wavelength ranges: from 380 nm to the lower extended band edge; from the lower to the upper extended band edge; and from the upper extended band edge to 1,150 nm. The SeaWiFS specifications require that out-of-band responses be no more than 5% of

the response between the extended band edges. The instrument is within these specifications for all eight bands.

## 13. SUMMARY

There are aspects to the SeaWiFS calibration equations that are specific to the spacecraft instrument. For example, there are small differences in the output of SeaWiFS from side to side of the half angle mirror. Most ground based instruments do not scan in the same manner as SeaWiFS. In addition, SeaWiFS uses bilinear gains to allow high sensitivity measurements of ocean-leaving radiances and low sensitivity measurements of radiances from clouds, which are much brighter than the ocean (Section 3.0).

There are, however, many calibration factors that are common to SeaWiFS and to other radiometers. The application of these factors to the SeaWiFS calibration equations has been presented both for users of the data set from the satellite instrument and for researchers making ground-based radiance measurements in support of SeaWiFS. Ground based radiometric measurements must account for many of these calibration factors.

In particular, there has been a detailed discussion of the spectral responses of the eight SeaWiFS bands. The discussions have been developed to show the integrated spectral responses within SeaWiFS as functions of the shape of the radiant source measured by the instrument (Section 9.10). These out-of-band responses of the bands contribute to the laboratory calibration of SeaWiFS. For the instrument's calibration coefficients presented here, the out-of-band response for the SBRC integrating sphere has been replaced with the out-of-band response for a source with the spectral distribution identical to the solar flux (Sections 7.2 and 7.3). Such spectral considerations may also be important for experimenters making ground based radiance measurements in support of SeaWiFS.

### ACKNOWLEDGEMENTS

The authors and editors wish to acknowledge the editorial assistance of Barbara A. Leroux, who worked on this document during her participation in the NASA/Goddard Prince George's County Teacher Intern Program.

### GLOSSARY

AD	Analog-to-Digital
ADC	Analog-to-Digital Converter
CZCS	Coastal Zone Color Scanner
IFOV	Instantaneous Field-Of-View
NASA	National Aeronautics and Space Administration
NIST	National Institute of Standards and Technology
OSC	Orbital Sciences Corporation
SBRC	Santa Barbara Research Center
SeaWiFS	Sea-viewing Wide Field-of-view Sensor
SNR	Signal-to-Noise Ratio

## SeaWiFS Prelaunch Radiometric Calibration and Spectral Characterization

**Table 13.** Band edges (half maximum wavelengths) and extended band edges (1% wavelengths) for SeaWiFS bands 1–4. The center wavelength is calculated from the upper and lower band edges. Results are given for three light sources: spectrally flat, 5,900 K blackbody, and 2,850 K blackbody. Results are also given for the interference filter only, and for the system level measurement using the monochromator as a light source.

Band	Nominal Band Edges [nm]	Lower Extended Band Edge [nm]	Lower Band Edge [nm]	Center Wavelength [nm]	Upper Band Edge [nm]	Upper Extended Band Edge [nm]	Source
1	402–422	394.9	403.1	413.2	423.3	433.4	Spectrally Flat
		395.1	403.3	413.3	423.4	433.6	5,900 K
		395.9	404.5	414.1	423.7	434.8	2,850 K
		393.6	402.4	412.6	422.7	432.3	Filter Only†
		393.8	402.3	413.0	423.7	433.8	System Level§
2	433–453	424.0	434.1	443.9	453.7	463.7	Spectrally Flat
		424.1	434.2	444.0	453.8	463.7	5,900 K
		424.8	435.1	444.6	454.1	464.3	2,850 K
		423.3	433.5	443.5	453.5	464.6	Filter Only†
		422.3	433.6	444.1	454.6	463.8	System Level§
3	480–500	470.7	480.8	491.1	501.4	511.8	Spectrally Flat
		470.7	480.8	491.1	501.4	511.8	5,900 K
		471.3	481.5	491.6	501.6	512.3	2,850 K
		470.1	480.5	490.8	501.2	511.3	Filter Only†
		468.1	479.1	490.1	501.1	511.7	System Level§
4	500–520	488.1	498.9	510.1	521.3	530.7	Spectrally Flat
		488.1	498.9	510.1	521.2	530.7	5,900 K
		488.9	499.4	510.5	521.5	531.1	2,850 K
		487.8	498.7	509.9	521.0	532.9	Filter Only†
		487.2	498.6	510.3	522.0	530.9	System Level§
5	545–565	536.4	545.5	554.6	563.8	577.3	Spectrally Flat
		536.3	545.4	554.6	563.8	577.2	5,900 K
		536.9	545.8	554.9	563.9	577.9	2,850 K
		536.6	545.5	554.6	563.8	577.1	Filter Only†
		535.3	544.6	554.2	563.9	577.0	System Level§
6	660–680	646.8	658.3	668.2	678.2	692.7	Spectrally Flat
		646.7	658.3	668.2	678.1	692.5	5,900 K
		646.9	658.5	668.4	678.3	692.9	2,850 K
		646.8	658.4	668.3	678.2	692.8	Filter Only†
		646.2	658.8	668.8	678.8	692.2	System Level§
7	745–785	728.0	744.7	764.9	785.0	814.5	Spectrally Flat
		727.6	744.6	764.6	784.6	812.9	5,900 K
		728.4	745.1	765.1	785.1	815.6	2,850 K
		725.1	744.3	765.0	785.7	814.2	Filter Only†
		†	743.3	763.8	784.2	†	System Level§
8	845–885	826.7	845.7	866.4	887.0	908.2	Spectrally Flat
		826.4	845.5	866.1	886.7	907.5	5,900 K
		826.8	845.7	866.5	887.2	908.4	2,850 K
		826.5	845.6	866.2	886.9	908.0	Filter Only†
		†	845.6	866.4	887.2	†	System Level§

† Calculated from measurements of the narrowband interference filter only.

§ Calculated from system level measurements using a monochromator as the light source.

‡ Outside of the range of the system level measurements.

**Table 14.** Calculated out-of-band responses for the eight SeaWiFS bands. The instrument responses are given as the output of the photodiode in picoamperes. The 5,900 K radiances in the calculations are normalized to the expected saturation radiance for each band at the nominal center wavelength for each band. The upper and lower extended band edges come from Tables 7 and 8. These results are calculated over the wavelength range from 380 nm to 1150 nm.

Band	Lower Out-of-Band Response [pA]	Lower Extended Band Edge [nm]	In-Band Response [pA]	Upper Extended Band Edge [nm]	Upper Out-of-Band Response [pA]	Out-of-Band Response [%]
1	3.38	395.2	2,175.35	433.6	11.77	0.70
2	9.59	424.1	3,418.80	463.7	1.56	0.33
3	6.48	470.7	4,301.14	511.7	28.08	0.80
4	17.32	488.1	4,586.23	530.7	8.96	0.58
5	39.14	536.6	3,631.84	577.2	46.14	2.35
6	12.66	646.7	2,071.19	692.2	7.84	0.99
7	10.17	727.3	2,818.97	813.4	29.58	1.41
8	66.36	826.4	2,191.97	907.5	15.43	3.73

TDI Time Delay and Integration

SYMBOLS

- $A_0$  Coefficient for linear term in scan modulation correction equation.
- $B_0$  Coefficient for power term in scan modulation correction equation.
- $C_1$  Measured value for the flight diffuser on a given scan line, in counts.
- $C_2$  Measured value of the flight diffuser for the scan line immediately sequential to the first scan line used to measure the flight diffuser, i.e.,  $S_1$ , in counts.
- $C_{dark}$  Instrument dark restore value, in counts.
- $C_{out}$  Instrument output, in counts.
- $C_{temp}$  Temperature sensor output, in counts, represented by an 8 bit digital word in the SeaStar telemetry.
- $ds$  Detector configuration datum.
- $G_1$  Gain setting 1.
- $G_2$  Gain setting 2.
- $G_3$  Gain setting 3.
- $G_4$  Gain setting 4.
- $gs$  Gain selection datum.
- $ICS$  Current from the current source diode.
  - $K_1$  Primary instrument sensitivity factor.
  - $K_2$  Gain factor.
  - $K_3$  Temperature dependence of detector output.
  - $K_4$  Scan modulation correction factor.
  - $K_5$  Spacecraft analog to digital conversion factor.
  - $K_6$  Analog-to-digital offset in spacecraft conversion.
  - $K_7$  Current from the diode at 20°C.
- $L(\lambda)$  Radiance.
- $L_{nadir}$  Measured radiance at nadir.
  - $LS_1$  Measured radiance for mirror side 1.
  - $LS_2$  Measured radiance for mirror side 2.
- $L_{scan}$  Measured radiance at any pixel in a scan.
  - $Pxl$  Pixel number, i.e., the numerical designation of a pixel in a scan line.
- $R_1$  Multiplier for mirror side 1.
- $R_2$  Multiplier for mirror side 2.
- $R_E$  Effective resistance for the thermistor-resistor pair.
- $R_T$  Resistance of the thermistor.
- $T$  Measured temperature of the focal plane assembly.
- $TC$  Approximate focal plane temperature.
- $T_{ref}$  Reference temperature for the temperature dependence (20° C).
- $V_T$  Focal plane temperature sensor voltage output.

REFERENCES

Allen, C.W., 1973: *Astrophysical Quantities, 3rd Edition*. Athlone Press London, 310 pp.

Barnes, R.A., and A.W. Holmes, 1993: Overview of the SeaWiFS Ocean Sensor. *SPIE*, **1,939**, 224-232.

Barnes, R.A., W.L. Barnes, W.E. Esaias, and C.L. McClain, 1994: Prelaunch Acceptance Report for the SeaWiFS Radiometer. *NASA Tech. Memo. 104566, Vol. 22*, S.B. Hooker, E.R. Firestone, and J.G. Acker, Eds., NASA Goddard Space Flight Center, Greenbelt, Maryland, 32 pp.

Biggar, S F., P.N. Slater, K.J. Thome, A.W. Holmes, and R.A. Barnes, 1993: Pre-flight solar-based calibration of SeaWiFS. *SPIE*, **1,939**, 233-242.

Cebula, R.P., H. Park, and D.F. Heath, 1988: Characterization of the Nimbus-7 SBUV radiometer for long-term monitoring of stratospheric ozone. *J. Atmos. Ocean. Technol.*, **5**, 215-227.

Evans, R.H., and H.R. Gordon, 1994: Coastal zone color scanner "system calibration": a retrospective examination. *J. Geophys. Res.*, **99**, 7,293-7,307.

Herman, J.R., R.D. Hudson, and G.N. Serafino, 1990: An analysis of the 8 year trend in ozone depletion from alternate models of SBUV instrument degradation. *J. Geophys. Res.*, **95**, 7,403-7,416.

## SeaWiFS Prelaunch Radiometric Calibration and Spectral Characterization

- Hooker, S.B., C.R. McClain, and A.W. Holmes, 1993: Ocean Color Imaging: CZCS to SeaWiFS, *Mar. Tech. Soc. J.*, **27**, 3-5.
- McClain, C.R., W.E. Esaias, W. Barnes, B. Guenther, D. Endres, S.B. Hooker, B.G. Mitchell, and R. Barnes, 1992: SeaWiFS Calibration and Validation Plan, *NASA Tech. Memo. 104566, Vol. 3*, S.B. Hooker and E.R. Firestone, Eds., NASA Goddard Space Flight Center, Greenbelt, Maryland, 41 pp.
- Mueller, J.L., 1993: The First SeaWiFS Intercalibration Round-Robin Experiment, SIRREX-1, July 1992. *NASA Tech. Memo. 104566, Vol. 14*, S.B. Hooker and E.R. Firestone, Eds., NASA Goddard Space Flight Center, Greenbelt, Maryland, 60 pp.
- Warneck, P., 1988: *Chemistry of the Natural Atmosphere*. Academic Press, 757 pp.
- Woodward, R.H., R. A. Barnes, C.R. McClain, W.E. Esaias, W.L. Barnes, and A.T. Mecherikunnel, 1993: Modelling of the SeaWiFS Solar and Lunar Observations, *NASA Tech. Memo. 104566, Vol. 10*, S.B. Hooker and E.R. Firestone, Eds., NASA Goddard Space Flight Center, Greenbelt, Maryland, 26 pp.
- Wyatt, C.L., 1978: *Radiometric Calibration: Theory and Methods*. Academic Press, 200 pp.

### THE SEAWIFS TECHNICAL REPORT SERIES

#### Vol. 1

Hooker, S.B., W.E. Esaias, G.C. Feldman, W.W. Gregg, and C.R. McClain, 1992: An Overview of SeaWiFS and Ocean Color. *NASA Tech. Memo. 104566, Vol. 1*, S.B. Hooker and E.R. Firestone, Eds., NASA Goddard Space Flight Center, Greenbelt, Maryland, 24 pp., plus color plates.

#### Vol. 2

Gregg, W.W., 1992: Analysis of Orbit Selection for SeaWiFS: Ascending vs. Descending Node. *NASA Tech. Memo. 104566, Vol. 2*, S.B. Hooker and E.R. Firestone, Eds., NASA Goddard Space Flight Center, Greenbelt, Maryland, 16 pp.

#### Vol. 3

McClain, C.R., W.E. Esaias, W. Barnes, B. Guenther, D. Endres, S. Hooker, G. Mitchell, and R. Barnes, 1992: Calibration and Validation Plan for SeaWiFS. *NASA Tech. Memo. 104566, Vol. 3*, S.B. Hooker and E.R. Firestone, Eds., NASA Goddard Space Flight Center, Greenbelt, Maryland, 41 pp.

#### Vol. 4

McClain, C.R., E. Yeh, and G. Fu, 1992: An Analysis of GAC Sampling Algorithms: A Case Study. *NASA Tech. Memo. 104566, Vol. 4*, S.B. Hooker and E.R. Firestone, Eds., NASA Goddard Space Flight Center, Greenbelt, Maryland, 22 pp., plus color plates.

#### Vol. 5

Mueller, J.L., and R.W. Austin, 1992: Ocean Optics Protocols for SeaWiFS Validation. *NASA Tech. Memo. 104566, Vol. 5*, S.B. Hooker and E.R. Firestone, Eds., NASA Goddard Space Flight Center, Greenbelt, Maryland, 43 pp.

#### Vol. 6

Firestone, E.R., and S.B. Hooker, 1992: SeaWiFS Technical Report Series Summary Index: Volumes 1-5. *NASA Tech. Memo. 104566, Vol. 6*, S.B. Hooker and E.R. Firestone, Eds., NASA Goddard Space Flight Center, Greenbelt, Maryland, 9 pp.

#### Vol. 7

Darzi, M., 1992: Cloud Screening for Polar Orbiting Visible and IR Satellite Sensors. *NASA Tech. Memo. 104566, Vol. 7*, S.B. Hooker and E.R. Firestone, Eds., NASA Goddard Space Flight Center, Greenbelt, Maryland, 7 pp.

#### Vol. 8

Hooker, S.B., W.E. Esaias, and L.A. Rexrode, 1993: Proceedings of the First SeaWiFS Science Team Meeting. *NASA Tech. Memo. 104566, Vol. 8*, S.B. Hooker and E.R. Firestone, Eds., NASA Goddard Space Flight Center, Greenbelt, Maryland, 61 pp.

#### Vol. 9

Gregg, W.W., F.C. Chen, A.L. Mezaache, J.D. Chen, J.A. Whiting, 1993: The Simulated SeaWiFS Data Set, Version 1. *NASA Tech. Memo. 104566, Vol. 9*, S.B. Hooker, E.R. Firestone, and A.W. Indest, Eds., NASA Goddard Space Flight Center, Greenbelt, Maryland, 17 pp.

#### Vol. 10

Woodward, R.H., R.A. Barnes, C.R. McClain, W.E. Esaias, W.L. Barnes, and A.T. Mecherikunnel, 1993: Modeling of the SeaWiFS Solar and Lunar Observations. *NASA Tech. Memo. 104566, Vol. 10*, S.B. Hooker and E.R. Firestone, Eds., NASA Goddard Space Flight Center, Greenbelt, Maryland, 26 pp.

#### Vol. 11

Patt, F.S., C.M. Hoisington, W.W. Gregg, and P.L. Coronado, 1993: Analysis of Selected Orbit Propagation Models for the SeaWiFS Mission. *NASA Tech. Memo. 104566, Vol. 11*, S.B. Hooker, E.R. Firestone, and A.W. Indest, Eds., NASA Goddard Space Flight Center, Greenbelt, Maryland, 16 pp.

#### Vol. 12

Firestone, E.R., and S.B. Hooker, 1993: SeaWiFS Technical Report Series Summary Index: Volumes 1-11. *NASA Tech. Memo. 104566, Vol. 12*, S.B. Hooker and E.R. Firestone, Eds., NASA Goddard Space Flight Center, Greenbelt, Maryland, 28 pp.

#### Vol. 13

McClain, C.R., K.R. Arrigo, J. Comiso, R. Fraser, M. Darzi, J.K. Firestone, B. Schieber, E-n. Yeh, and C.W. Sullivan, 1994: Case Studies for SeaWiFS Calibration and Validation, Part 1. *NASA Tech. Memo. 104566, Vol. 13*, S.B. Hooker and E.R. Firestone, Eds., NASA Goddard Space Flight Center, Greenbelt, Maryland, 52 pp., plus color plates.

Vol. 14

Mueller, J.L., 1993: The First SeaWiFS Intercalibration Round-Robin Experiment, SIRREX-1, July 1992. *NASA Tech. Memo. 104566, Vol. 14*, S.B. Hooker and E.R. Firestone, Eds., NASA Goddard Space Flight Center, Greenbelt, Maryland, 60 pp.

Vol. 15

Gregg, W.W., F.S. Patt, and R.H. Woodward, 1994: The Simulated SeaWiFS Data Set, Version 2. *NASA Tech. Memo. 104566, Vol. 15*, S.B. Hooker and E.R. Firestone, Eds., NASA Goddard Space Flight Center, Greenbelt, Maryland, 42 pp., plus color plates.

Vol. 16

Mueller, J.L., B.C. Johnson, C.L. Cromer, J.W. Cooper, J.T. McLean, S.B. Hooker, and T.L. Westphal, 1994: The Second SeaWiFS Intercalibration Round-Robin Experiment, SIRREX-2, June 1993. *NASA Tech. Memo. 104566, Vol. 16*, S.B. Hooker and E.R. Firestone, Eds., NASA Goddard Space Flight Center, Greenbelt, Maryland, 121 pp.

Vol. 17

Abbott, M.R., O.B. Brown, H.R. Gordon, K.L. Carder, R.E. Evans, F.E. Muller-Karger, and W.E. Esaias, 1994: Ocean Color in the 21st Century: A Strategy for a 20-Year Time Series. *NASA Tech. Memo. 104566, Vol. 17*, S.B. Hooker and E.R. Firestone, Eds., NASA Goddard Space Flight Center, Greenbelt, Maryland, 20 pp.

Vol. 18

Firestone, E.R., and S.B. Hooker, 1994: SeaWiFS Technical Report Series Summary Index: Volumes 1-17. *NASA Tech. Memo. 104566, Vol. 18*, S.B. Hooker and E.R. Firestone, Eds., NASA Goddard Space Flight Center, Greenbelt, Maryland, (in press).

Vol. 19

McClain, C.R., R.S. Fraser, J.T. McLean, M. Darzi, J.K. Firestone, F.S. Patt, B.D. Schieber, R.H. Woodward, E-n. Yeh, S. Mattoo, S.F. Biggar, P.N. Slater, K.J. Thome, A.W. Holmes, R.A. Barnes, and K.J. Voss, 1994: Case Studies for SeaWiFS Calibration and Validation, Part 2. *NASA Tech. Memo. 104566, Vol. 19*, S.B. Hooker, E.R. Firestone, and J.G. Acker, Eds., NASA Goddard Space Flight Center, Greenbelt, Maryland, 73 pp.

Vol. 20

Hooker, S.B., C.R. McClain, J.K. Firestone, T.L. Westphal, E-n. Yeh, and Y. Ge, 1994: The SeaWiFS Bio-Optical Archive and Storage System (SeaBASS), Part 1. *NASA Tech. Memo. 104566, Vol. 20*, S.B. Hooker and E.R. Firestone, Eds., NASA Goddard Space Flight Center, Greenbelt, Maryland, 40 pp.

Vol. 21

Acker, J.G., 1994: The Heritage of SeaWiFS: A Retrospective on the CZCS NIMBUS Experiment Team (NET) Program. *NASA Tech. Memo. 104566, Vol. 21*, S.B. Hooker and E.R. Firestone, Eds., NASA Goddard Space Flight Center, Greenbelt, Maryland, 43 pp.

Vol. 22

Barnes, R.A., W.L. Barnes, W.E. Esaias, and C.R. McClain, 1994: Prelaunch Acceptance Report for the SeaWiFS Radiometer. *NASA Tech. Memo. 104566, Vol. 22*, S.B. Hooker, E.R. Firestone, and J.G. Acker, Eds., NASA Goddard Space Flight Center, Greenbelt, Maryland, 32 pp.

Vol. 23

Barnes, R.A., A.W. Holmes, W.L. Barnes, W.E. Esaias, C.R. McClain, and T. Svitek, 1994: SeaWiFS Prelaunch Radiometric Calibration and Spectral Characterization. *NASA Tech. Memo. 104566, Vol. 23*, S.B. Hooker, E.R. Firestone, and J.G. Acker, Eds., NASA Goddard Space Flight Center, Greenbelt, Maryland, 55 pp.

# REPORT DOCUMENTATION PAGE

Form Approved  
OMB No. 0704-0188

Public reporting burden for this collection of information is estimated to average 1 hour per response, including the time for reviewing instructions, searching existing data sources, gathering and maintaining the data needed, and completing and reviewing the collection of information. Send comments regarding this burden estimate or any other aspect of this collection of information, including suggestions for reducing this burden, to Washington Headquarters Services, Directorate for Information Operations and Reports, 1215 Jefferson Davis Highway, Suite 1204, Arlington, VA 22202-4302, and to the Office of Management and Budget, Paperwork Reduction Project (0704-0188), Washington, DC 20503.

<b>1. AGENCY USE ONLY (Leave blank)</b>	<b>2. REPORT DATE</b> October 1994	<b>3. REPORT TYPE AND DATES COVERED</b> Technical Memorandum	
<b>4. TITLE AND SUBTITLE</b> SeaWiFS Technical Report Series Volume 23—SeaWiFS Prelaunch Radiometric Calibration and Spectral Characterization		<b>5. FUNDING NUMBERS</b>  Code 970.2	
<b>6. AUTHOR(S)</b> Robert A. Barnes, Alan W. Holmes, William L. Barnes, Wayne E. Esaias, Charles R. McClain, and Tomas Svitek Series Editors: Stanford B. Hooker and Elaine R. Firestone Technical Editor: James G. Acker		<b>8. PERFORMING ORGANIZATION REPORT NUMBER</b>  94B00144	
<b>7. PERFORMING ORGANIZATION NAME(S) AND ADDRESS(ES)</b>  Laboratory for Hydrospheric Processes Goddard Space Flight Center Greenbelt, Maryland 20771			
<b>9. SPONSORING/MONITORING AGENCY NAME(S) AND ADDRESS(ES)</b>  National Aeronautics and Space Administration Washington, D.C. 20546-0001		<b>10. SPONSORING/MONITORING AGENCY REPORT NUMBER</b>  TM-104566, Vol. 23	
<b>11. SUPPLEMENTARY NOTES</b> Robert A. Barnes: ManTech, Inc., Wallops Island, Virginia; Alan W. Holmes: Hughes Santa Barbara Research Center, Santa Barbara, California; Tomas Svitek: Orbital Sciences Corporation, Dulles, Virginia; Elaine R. Firestone: General Sciences Corporation, Laurel, Maryland; and James G. Acker: Hughes STX, Lanham, Maryland			
<b>12a. DISTRIBUTION/AVAILABILITY STATEMENT</b> Unclassified—Unlimited Subject Category 48 Report is available from the NASA Center for AeroSpace Information, 800 Elkridge Landing Road, Linthicum Heights, MD 21090-2934, (301) 621-0390.		<b>12b. DISTRIBUTION CODE</b>	
<b>13. ABSTRACT (Maximum 200 words)</b> Based on the operating characteristics of the Sea-viewing Wide Field-of-view Sensor (SeaWiFS), calibration equations have been developed that allow conversion of the counts from the radiometer into Earth-exiting radiances. These radiances are the geophysical properties the instrument has been designed to measure. SeaWiFS uses bilinear gains to allow high sensitivity measurements of ocean-leaving radiances and low sensitivity measurements of radiances from clouds, which are much brighter than the ocean. The calculation of these bilinear gains is central to the calibration equations. Several other factors within these equations are also included. Among these are the spectral responses of the eight SeaWiFS bands. A band's spectral response includes the ability of the band to isolate a portion of the electromagnetic spectrum and the amount of light that lies outside of that region. The latter is termed <i>out-of-band response</i> . In the calibration procedure, some of the counts from the instrument are produced by radiance in the out-of-band region. The number of those counts for each band is a function of the spectral shape of the source. For the SeaWiFS calibration equations, the out-of-band responses are converted from those for the laboratory source into those for a source with the spectral shape of solar flux. The solar flux, unlike the laboratory calibration, approximates the spectral shape of the Earth-exiting radiance from the oceans. This conversion modifies the results from the laboratory radiometric calibration by 1-4%, depending on the band. These and other factors in the SeaWiFS calibration equations are presented here, both for users of the SeaWiFS data set and for researchers making ground-based radiance measurements in support of SeaWiFS.			
<b>14. SUBJECT TERMS</b> SeaWiFS, Oceanography, Radiometer, Prelaunch Radiometric Calibration, Spectral Characterization, System Level Measurements		<b>15. NUMBER OF PAGES</b> 55	
<b>17. SECURITY CLASSIFICATION OF REPORT</b> Unclassified		<b>16. PRICE CODE</b>	
		<b>20. LIMITATION OF ABSTRACT</b>  Unlimited	
<b>18. SECURITY CLASSIFICATION OF THIS PAGE</b> Unclassified	<b>19. SECURITY CLASSIFICATION OF ABSTRACT</b> Unclassified		